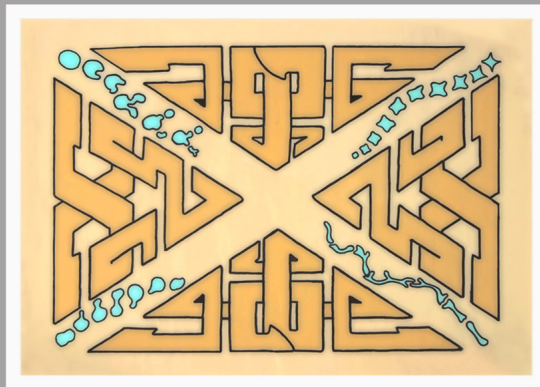


Engineering vascular development for tissue regeneration



Nicolas C. Rivron

Engineering vascular development for tissue regeneration

Nicolas C. Rivron

ENGINEERING VASCULAR DEVELOPMENT FOR TISSUE REGENERATION

Proefschrift

Ter verkrijging van
De grad van doctor aan de Universiteit Twente,
Op gezag van de rector magnificus,
Prof. Dr. H. Brinksma,
Volgens besluit van het College voor promoties,
In het openbaar te verdedigen
Op vrijdag 10 september 2010 om 15:00 uur

door

Nicolas Clemens Rivron
Geboren op 20 juni 1978
Te Antony, Frankrijk

Dit proefschrift is goedgekeurd door:
Prof. Dr. C.A. van Blitterswijk (promotor)
Dr. Ir. J. Rouwkema (assistant promotor)

Thesis committee members

Prof. Dr. Gerard. van der Steenhoven	University of Twente
Prof. Dr. Clemens A. van Blitterswijk	University of Twente
Prof. Dr. Yong Chen	Ecole Normale Superieure de Paris
Prof. Dr. Ir. Albert van den Berg	University of Twente
Prof. Dr. Niels Geijsen	Utrecht University, Harvard Stem Cell Institute
Prof. Dr. Ir. Dirk Grijpma	University of Twente
Dr. Marco Harmsen	University Medical Center of Groningen
Dr. Ir. Jeroen Rouwkema	University of Twente

Engineering vascular development for tissue regeneration

Nicolas C. Rivron

PhD thesis, University of Twente, The Netherlands

Copyright © N.C. Rivron, Enschede, The Netherland, 2010.

Neither this book nor its part may be reproduced without written permission of the author.

ISBN: 978-90-365-3075-0



Lonza

DSM



R&D
SYSTEMS®

The art cover was done by my brother, Charles Rivron and depicts tissue development on microfabricated templates.

The research in this thesis was carried out at the department of Tissue Regeneration, MIRA Institute and Faculty of Science and Technology, University of Twente, P.O. Box 217, 7500 AE Enschede, The Netherland

This research was financially supported by STW, the science and technology program of the Dutch Ministry of Research (Biomimetic capillary networks for tissue engineering scaffolds, project number TKG 6716)

Words underlined are defined in the glossary

To my family and Anne-Laure

Nous appellerons *Hollande*
Ce pays de contrebande
Entre la pluie et le vent
Comme un moment de césure
Dans la voix et la mesure
Entre l'après et l'avant

Louis Aragon

Le voyage de Hollande, 1965

Publications

Peer-reviewed papers

- 1: Rivron NC, Rouwkema J, Truckenmüller R, Karperien M, De Boer J, Van Blitterswijk CA. Tissue assembly and organization: developmental mechanisms in microfabricated tissues. *Biomaterials*. 2009 Oct;30(28):4851-8. Epub 2009 Jul 9.
- 2: Rouwkema J, Rivron NC, van Blitterswijk CA. Vascularization in tissue engineering. *Trends Biotechnology*. 2008 Aug;26(8):434-41. Epub 2008 Jun 26. Review.
- 3: Rivron NC, Liu J J, Rouwkema J, de Boer J, van Blitterswijk CA. Engineering vascularised tissues in vitro. *Eur Cell Mater*. 2008 Feb 21;15:27-40. Review.
- 4: Rivron NC, Raiss C, Rouwkema J, Liu J, Nandakumar A, Truckenmuller R, Sticht C, Gretz N, van Blitterswijk CA. Sonic hedgehog promotes *in vitro* vascular development and improves the *in vivo* formation of an engineered endochondral bone callus. Submitted.
- 5: Rivron NC, Vrij EJ, Rouwkema J, Truckenmüller R, Barradas A, Le Gac S, de Boer J, van den Berg A, van Blitterswijk CA. Microfabrication of self-organizing tissues. Submitted
- 6: Rivron NC, Vrij EJ, Truckenmüller R, Rouwkema J, Le Gac S, van den Berg A, van Blitterswijk CA. Endogenous tissue contractility spatially regulates angiogenesis. Submitted

Selected abstracts (non-exhaustive)

- 1: *EMBO* Conference Series on Morphogenesis and Dynamics of Multicellular Systems. Self-remodeling engineered tissues as templates for stereotyped Angiogenesis. Rivron NC et al. 2009. Oral presentation. Recipient of the travel award.
- 2: Harvard HST/Medical school - MIT NEBEC Conference. Microfabrication of shaped mm-scale tissues to study vascular development. Rivron NC et al. 2009. Oral presentation. Recipient of the travel award.
- 3: Gordon Conference on Vascular Cell Biology. Vascular development in microtissues using Hedgehog signaling. Rivron NC et al. 2008. Poster presentation.

4: TERMIS. Vascular development in microtissues using the hedgehog signalling. Rivron NC et al. 2008. Oral presentation.

5: TERMIS. Engineering vascularized microtissues for bone regeneration. Rivron NC et al. 2007. Oral presentation.

Book chapter

Cell and organ printing. Ringeisen, Bradley R.; Spargo, Barry J.; Wu, Peter K. (Eds.). Chapter 9: Emerging principles to rationally design tissues prone to self-organization, Rivron NC, Rouwkema J, Truckenmüller R, van Blitterswijk CA. 1st Edition., 2010, 300 p., Springer. ISBN: 978-90-481-9144-4

Patent

Rivron NC, Vrij EJ, Truckenmüller R, Rouwkema J, Le Gac S, van Blitterswijk CA. Self-assembling tissue modules. WO/2009/154466.

ENGINEERING VASCULAR DEVELOPMENT FOR TISSUE REGENERATION

CONTENTS	PAGE
Chapter 1- The vasculature in development and regeneration.	15
1- The vasculature	16
2- The vasculature in tissue diseases and regeneration	25
3- The coupling of the vascular and bone systems	27
4- Vascularization in the wound: role of endogenous tissue tension	32
5- The vasculature as a template for tissue regeneration	33
Chapter 2- Developmental mechanisms in microfabricated multicellular systems.	41
1- Microfabrication tools	43
2- How to orchestrate developmental mechanisms in vitro?	46
3- Bottom-up / modular approach	50
Aim of this thesis.	55
Chapter 3- Engineering a vascularized bone callus using Sonic Hedgehog.	57
<i>Keywords: prevascularization, endochondral ossification, bone callus, tissue engineering</i>	
Chapter 4- Microfabrication of self-remodeling tissues.	87
<i>Keywords: tissue microfabrication, bottom-up, geometry, remodeling</i>	
Chapter 5- Endogenous tissue contractility spatially regulates angiogenesis.	111
<i>Keywords: tissue model, vascular, pattern formation, self-organization, endogenous contractility</i>	
Chapter 6- Tissue complexity - or how I learned to stop worrying and love biology.	131
1- What did we learn from these experiments?	132
2- Pattern formation during vascular development	134
3- Investigating tissue morphogenesis using <i>in vitro</i> models	140
4- Is a formal approach to morphogenesis possible?	150
5- Appendix to the discussion	151
Glossary.	158
Summary.	160
Curriculum Vitae.	167
Acknowledgements.	168
Appendix.	172

Chapter 1

The vasculature in development and regeneration

This chapter is a global introduction to the vascular system and to its multiple roles during embryonic development and adult tissue regeneration. We will specifically focus on the important interactions between the vascular and the bone systems during skeletal development and regeneration and on the roles of the vasculature during wound healing.

The vasculature in development and regeneration

1- The vasculature

1-1 Introduction

Primitive, small animals such as the *Platyhelminthes* lack any circulatory system and exchanges rely strictly on absorption and diffusion. In the worm *Caenorhabditis elegans* and the fruitfly *Drosophila melanogaster*, oxygen passively diffuses respectively throughout a pump-less internal cavity and a tracheal airway to access all cells. In other larger species, which developed later in evolution, specialized tubular network arose, equipped with pumps, as active pipelines. Open circulatory systems (respiratory, digestive) are coupled with closed circulatory systems (vascular, lymphatic, nervous) and promote exchanges and distributions to distant cells, tissues and organs (1). The vascular system is the first functional organ in the developing vertebrate embryo and is critical for tissue development, homeostasis and regeneration.

The first blood vessels develop, both inside and outside the embryo, from mesenchymal progenitor cells which differentiate into endothelial cells and organize in small circular rings termed blood islands (vasculogenesis). These blood islands elongate, remodel and merge into an interconnected lattice termed the plexus by angiogenesis, meaning by endothelial sprouting, splitting, and fusion. Upon the first heart beat, the vascular plexus progressively expands and reorganizes into a highly stereotyped, hierarchical vascular network of larger vessels ramifying into smaller ones. This network is an adaptable life-support system irrigating almost every region of the body and providing exchanges of gas, metabolites, biological factors or cells (i.e. immunological cells, stem cells). The vasculature has the intrinsic plasticity to constantly and dynamically adapt to local requirements by enlargement, sprouting or regression.

During adult life, blood vessels are largely quiescent and stable. Their remodeling capacities are transiently reactivated upon reproduction, diseases and regeneration. During the cycling ovary and pregnancy, new blood vessels are formed to respectively prepare and

enhance exchanges in the niche receiving the embryo. During diseases, blood vessels are strongly affected and mediate the regression or progression of pathologies. As a classical example, solid cancer tumors can attract and induce the formation of new blood vessels to be nourished, grow to larger sizes and spread (metastasis). During wound healing and regeneration, blood vessels are disrupted and new blood vessels are formed early as a template for the growth of a new tissue.

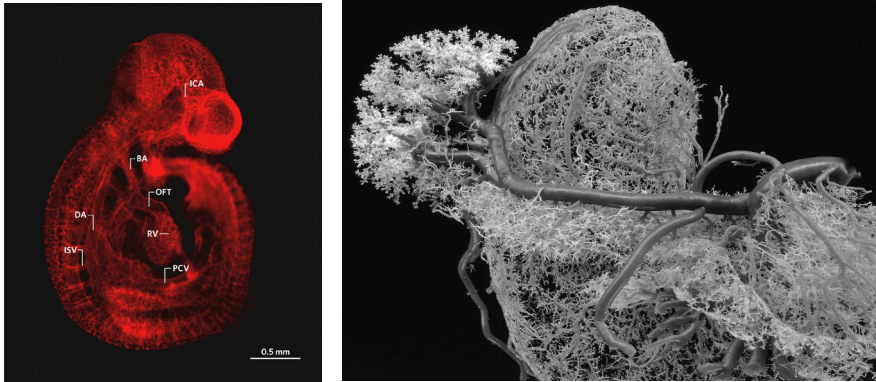


Figure 1: The vasculature during embryonic development and adult life. The vasculature is one of the first organ to develop in the embryo, to support life. The left picture shows the developing vasculature of a mouse embryo (day 9.5) labeled with CD31 (PECAM) immunofluorescence staining. BA, branchial arteries; DA, dorsal aorta; ICA, intercarotid artery; ISV, intersomitic vessels; OFT, outflow tract; PCV, posterior cardinal vein; RV, right ventricle. (Image courtesy of L. Davidson, Mouse Imaging Centre, Hospital for Sick Children, Toronto, Canada.). The right picture is a cast of the vasculature showing the complex hierarchical tree embedded in adult tissues.

1-2 The composition of blood vessels

The hierarchical vasculature is formed by bigger vessels (arteries, veins) connected through smaller vessels which are embedded in the tissues (capillaries). The smallest blood vessels (capillaries) are formed by endothelial cells, a basal lamina and pericytes. Larger blood vessels (arterioles, venules, arteries, veins) include several external layers of specialized cells.

The endothelium. The inner wall forming the lumen is always lined by a thin, single sheet of endothelial cells which makes the interface between the blood and the tissue. Endothelial cells form an interactive polarized epithelium connected through dynamic tight junctions

and cadherin molecules. Endothelial cells assume the functions of actively controlling the hemostatic balance, the vasomotor tone, regulating blood cell trafficking and the innate and adaptive immunity.

The basal lamina. The endothelium is separated from the surrounding outer layers by the basal lamina, a structural mesh of extra-cellular matrix proteins (i.e. laminin, collagen type IV) which serves as a substrate for endothelial cell migration, binds and regulates the distribution, activation, and presentation of pro- and antiangiogenic soluble factors (2). The basal lamina is a signal transducer acting through integrins which can either be pro- or antiangiogenic, often using different cleavage products of the same protein (3). Basal lamina is an important element regulating the remodeling of blood vessels.

Pericytes. In the finest branches of the vascular tree -the capillaries and sinusoids- the walls consist of nothing but endothelial cells and a basal lamina, together with a few scattered -but functionally important- cells termed pericytes. These are cells of the connective-tissue family, related to vascular smooth muscle cells and mesenchymal stem cells, that wrap themselves around the small vessels, are embedded in the basal lamina and form specific focal contacts with the endothelium. They are thought to stabilize the vessels, facilitate and integrate cell-cell communication. They often lie and bridge several endothelial cells and thus might coordinate their functions. Pericytes cover 10 to 50% of the endothelium depending on the organ. They may increase the barrier established by endothelial cells, function as sensors of hypoxia and hypoglycemia and regulate the vessels diameter to adapt to changes in the blood flow (4).

External elastic lamina and intima. The largest blood vessels have an external thick, tough wall of connective tissue including many layers of smooth muscle cells and extra-cellular matrix. Their amounts vary according to the vessel's diameter and function. These smooth muscle cells are thought to mainly modulate the vascular tone and contraction. They are separated from the basal lamina by a thin layer of mesenchymal cells and extracellular matrix termed the intima.

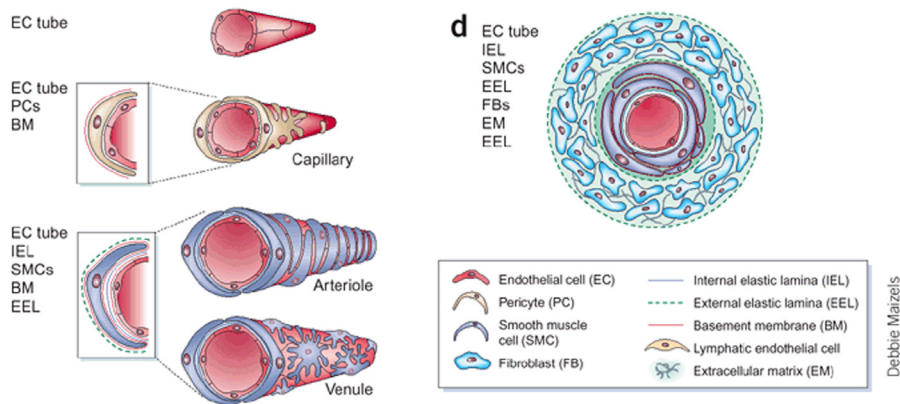


Figure 2: The composition of blood vessels. (a) Nascent vessels consist of a tube of endothelial cells (EC). These tubes mature into the specialized structures of capillaries, arteries and veins. (b) Capillaries, the most abundant blood vessels, consist of ECs surrounded by a basement membrane in which is embedded a sparsely distributed layer of pericytes. Because of their wall structure and large surface-area-to-volume ratio, these vessels form the main site of exchange of nutrients between blood and tissue. Depending upon the organ or tissue, the capillary endothelial layer is continuous as in muscle, fenestrated as in kidney or endocrine gland or discontinuous as in liver sinusoids. The endothelium of the blood-brain barrier or blood-retina barrier are further specialized to include tight junctions and are thus impermeable to various molecules. (c) Arterioles and venules have an increased coverage of mural cells compared with capillaries. Precapillary arterioles are completely invested with vascular smooth muscle cells (SMS) that form their own basement membrane, circumferentially, closely packed and tightly associated with the endothelium. Extravasation of macromolecules and cells from the blood stream typically occurs from postcapillary venules. (d) The walls of the larger blood vessels consist of an intima (EC), a media (SMC) and an adventitia of fibroblasts together with matrix and external lamina. SMC and elastic laminae contribute to the vessel tone. (Courtesy of Rakesh K. Jain. And Debbie Maizels)

1-3 The molecular regulation of vascular morphogenesis

The first in vitro culture of endothelial cells was accomplished in 1974 (5) and the first knockout mouse applied to angiogenesis in 1996 (6-7). Since then, genetic studies in human cell culture, mice, zebrafishes and tadpoles have provided extensive insights into the key cellular mechanisms and the molecular players which regulate the formation of a vascular network (see table 1 in the appendix for studies on knock-out

mice). Here, we will briefly describe the main molecular players of vascular development and homeostasis.

These molecules are orchestrating morphogenetic movements leading to migration, proliferation, assembly, hollowing or differentiation of the cells and matrix forming the blood vessels (figure 3). The highly vascular-specific signaling molecules include the vascular endothelial growth factors (VEGF)(8), the angiopoietins/Tie system (9), components of cell-cell junctions including Vascular Endothelial Cadherins (VE-Cad)(10) and mediators of cell-matrix interactions (integrins $\alpha V\beta 3$, $\alpha V\beta 5$)(11). More widely used signaling pathways including basic fibroblast growth factor (bFGF), platelet-derived growth factor (PDGF), transforming growth factor (TGF), ephrin, Notch and Hedgehog are also involved (12).

VEGF signaling is involved in the differentiation of progenitor cells, the survival and sprouting of endothelial cells and in the regulation of vascular permeability (13). The angiopoietin/Tie system regulates the survival of endothelial cells, the formation of vascular lumens, the stabilization and the permeability of the vessels through a cross-talk between endothelial cells and pericytes (9). The recruitment and stabilization of the mural cells (pericytes and smooth muscle cells) depend on PDGF-BB secreted by the endothelial cells and on PDGF receptors in the mural cells (12). The TGF signaling regulates the proliferation and migration of the endothelial cells and promotes the stabilization and maturation of the basal lamina (12). The signaling between adherence molecules (i.e. integrins) and extracellular molecules from the basal lamina (collagen type IV, laminin) regulates the apoptosis of endothelial cells and the formation of lumens (11). Figure 3 depicts the current knowledge on well-established genes and signaling pathways regulating the assembly of blood vessels.

Many of these signaling pathways are quiescent or have a low basal activity during adult tissue homeostasis and are reactivated in situations of neoangiogenesis (reproduction, disease, regeneration). The discovery of the key angiogenic genes and their corresponding biochemical factors opened up a new era of rational therapeutics for the prevention or the promotion of new blood-vessel growth.



Figure 3: Genetic and molecular players of vascular assembly. The progenitor endothelial cells differentiate in response to bFGF and VEGF and sprout to form cord-like structures. These structures form a lumen and attract pericytes through Ang/Tie signaling, PDGF and integrins/extra-cellular-matrices interactions. The vessel stabilization is achieved through Tgf signaling. This very schematic view of the molecular pathways in vessel maturation is described more in details in the table for signaling pathways, the table for cell-cell interaction and the table for cell-matrix interactions. (Courtesy of Karen K. Hirschi and Rakesh K. Jain)

1-4 The diversity in blood vessels' identity

Despite common components and features, blood vessels are highly diverse in their architectures. The blood vessels are organ-specific and present different phenotypical variations relative to their specific functions (14-15). ECs are typically flat but have a cuboidal phenotype in high endothelial venules (16). They are elongated and spindle shaped in arterioles; irregularly shaped in capillaries; large, elliptical, or irregularly shaped in postcapillary venules; and rounded in collecting venules (17). Endothelial cell thickness varies from less than 0.1 μm in capillaries and veins to 1 μm in the aorta (18). Capillaries are continuous and non-fenestrated in the skin, lung and heart, continuous and fenestrated in the endocrine gland and glomerulus and discontinuous and fenestrated in the liver sinusoid (14-15). This heterogeneity is related to specific functions including the regulation of leukocytes trafficking (16), permeability, transcytotic activity, endothelial regulation of vasomotor tone and innate and acquired immunity (14-15). A similar heterogeneity is found for pericyte coverage (4). The highest pericyte coverage around microvessels is found in the central nervous system (CNS) possibly to contribute to the formation of the blood– brain barrier (4). Their morphology may range from that of the typical CNS pericyte, a flattened, or elongated, stellate-shaped solitary cell with multiple cytoplasmic processes encircling the capillary endothelium and contacting a large abluminal vessel area, to that of a mesangial cell of the kidney glomerulus, rounded, compact and contacting a minimal abluminal vessel area, making only focal attachments to the basal lamina. These different phenotypes are related to molecular specificities: arterial endothelial cells, in the embryo at least, express the transmembrane protein ephrinB2, for example, while the venous arterial cells express the corresponding receptor protein, EphB4.

1-5 The stereotyped patterning of the vascular network

From an engineering point of view, the robustness and stereotyped properties (architecture, patterns, molecular profile) of the vascular network are intriguing (see figure 1 and 4): during embryonic development, blood vessels always arise, branch, connect at the same locations, sprout in the same directions and reproducibly form complex but stereotyped patterns. A range of cellular mechanisms are currently being discovered which partly reveal how patterns of the vascular sprouts are formed through

self-organization, guidance or templates. However, obviously much more remains to be elucidated to understand the formation of robust, stereotypical, complex networks at the system level.

At the tip of the sprouting vessel, leading the way, is an endothelial cell with distinctive characteristics. This tip cell has a pattern of gene expression different from that of the endothelial stalk cells following behind. Tip cells do not divide and form many long filopodia, resembling those of a neuronal growth cone (Figure 4). The stalk cells, meanwhile, divide and become hollowed out to form a lumen (Figure 4)(19). Here, we describe the well-studied established mechanisms of vascular patterning.

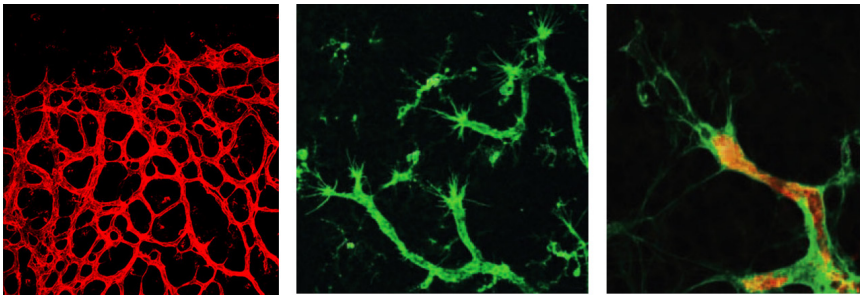


Figure 4: Vascular patterning. The patterning of blood vessels is illustrated by the formation of a simple wire mesh lattice termed “plexus” in the retina of a mouse which will progressively remodel in a hierarchical network (left). The sprouting of the blood vessels is done by the tip “leading” cell which explores its local environment using filopodias. This exploration allows for the capture of survival and differentiation signals whose gradient of concentration gives a direction (middle). The stalk “following” cells form a hollow tube termed “lumen” and proliferate (right). (Courtesy of Akiko Mammoto and Holger Gerhardt).

Long-range patterning- Long-range patterning is regulated by hypoxia (a lack of oxygen) in the target tissue which induces the stabilization of the Hypoxia-Inducible Factor (HIF1 α) by a regulation of the VHL gene coding for an E3 ubiquitin ligase subunit. HIF is an heterodimeric transcription factor that mediate the adaptation of many multicellular organisms to molecular oxygen. HIF1 α regulates the local production the of VEGF (20). A

gradient of this molecule is produced, possibly by graded production or diffusion, which orientate and attract new blood vessels. Upon irrigation of the tissue by new blood vessels, hypoxia decreases and so does the production of VEGF (19).

Initial sprouting- The initial outward movement of the nascent sprout from an existing vessel involves several mechanisms including lateral inhibition (Notch/Delta4) and local inhibitors produced along their own vessels (Tgf (21), Flt1 (22), cleavage products from the extracellular matrix). Delta 4 expression is fluctuating in endothelial cells and inhibits the production of the VEGF receptor in neighboring cells (paracrine lateral inhibition). Upon competition, one endothelial cell acquires the tip phenotype and sprouts toward the source of VEGF. Interestingly, this social interaction through Notch also regulates the trachea branching morphogenesis (23). Another lately discovered mechanism involves the production of angiogenic inhibitors by the vessel itself (Tgf, soluble VEGF receptor). Profiles of secretion of these inhibitors dictate the local sprouting of an endothelial cell away from the parent vessel. These interactions control which cells will be singled out to behave as tip cells, extending filopodia and crawling forward to create new vascular sprouts.

Tip guidance- Upon the initial outward movement away from the parent blood vessel, a range of receptor molecules which decorate the leading, tip cell, of the blood vessels, help in the guidance of the vessels along the tissue-scale gradient of soluble factors (semaphoring, netrins, slits, ephrins, robo...). Many of these guidance molecules are also involved in the guidance of nerves, which often grow in parallel with blood vessels.

Concomitantly to these well-assessed patterning mechanisms, we propose in this thesis that endogenous tissue contractility might also be regulating the formation of vascular patterns (see chapter 5).

These established mechanisms of pattern formation partly explain the organism-level organization of the vasculature. We will give, in chapter 6, a more integrated and detailed view of the range of possible mechanisms of vascular morphogenesis and patterning.

2- The vasculature in tissue diseases and regeneration

2-1 The vascular system is involved in a wide range of diseases

The ubiquity of the vascular system and its role in connecting tissues and organs makes it a main actor relaying and relating physiological and pathological phenomenon. It is thus not surprising that a lot of disease are related to the vascular system. Besides directly related diseases such as artherosclerosis, an ever growing list is connected to a deregulation of the vascular network (excessive or insufficient angiogenesis).

The most-studied conditions in which angiogenesis is excessive are malignant, ocular and inflammatory disorders whereas, ischaemic heart diseases or preeclampsia are related to insufficient angiogenic switch causing EC dysfunction, vessels malformation, regression, or preventing revascularization, healing and regeneration. Many additional processes are affected, such as obesity, asthma, diabetes, cirrhosis, multiple sclerosis, endometriosis, AIDS, bacterial infections, genetic diseases (i.e. von Hippel–Lindau (VHL) syndrome) and autoimmune diseases. Angiogenesis has been implicated in more than 70 disorders so far (1, 13, 24-25)(see table 2 in the appendix).

In this section we will first describe the ubiquitous role of the vascular system during homeostasis and regeneration. We will then focus on two specific examples describing the role of the vascular system during bone regeneration and wound healing. Finally, we will propose a general framework depicting the vascular bed as a template for tissue regeneration.

2-2 Role for the vascular system in tissue homeostasis and regeneration.

The vascular system has important interactions with the local microenvironment which are not limited to gas and nutrient exchanges. The vascular bed provides inductive signals and regulates organ development and pattern formation (26). Conversely, the vasculature responds to cues from the parenchyma that bestow upon its tissue-specific functions (26). Such interactions are critical during embryonic development but also appear to be important during the adult life and present opportunities for therapeutic strategies. Numerous examples including heart development, hematopoiesis, neural tissue, illustrate the importance of a cross-talk between the vascular bed and the

surrounding tissue during development and diseases (See the excellent review of K. Red-Horse (26)). Here we will first present the human mesenchymal stem cells which are aligning capillaries in the bone-marrow and are used in this thesis to built tissues and support the formation of vascular networks in vitro. We will then focus on the specific roles of the vasculature (i) during the development and the regeneration of the bone organ and during (ii) wound healing.

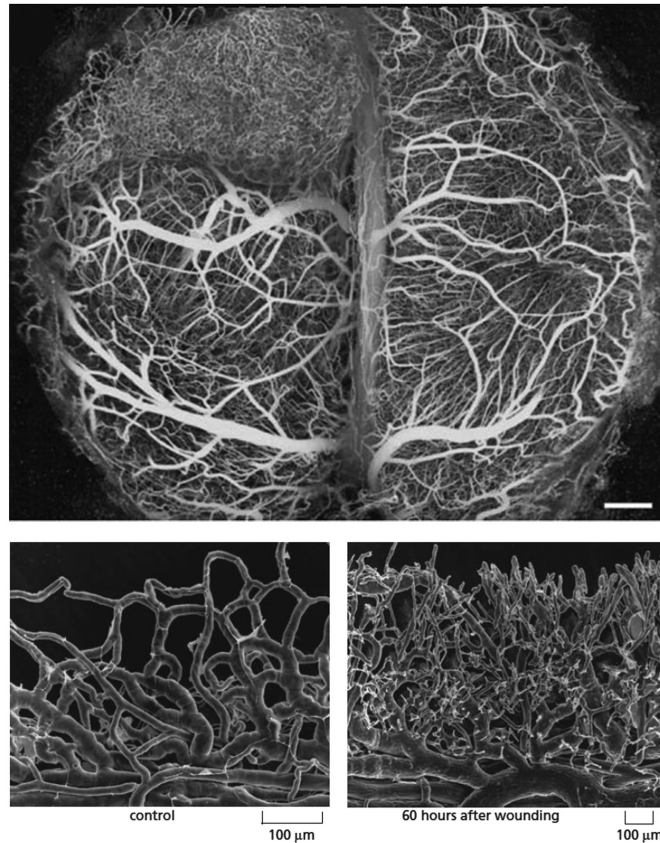


Figure 5: The vasculature in diseases and regeneration. The vasculature, due to its ubiquity and its role in transport, is an important regulator and mediator of diseases and regeneration. The top picture is the vasculature of a brain including a highly vascularized cancer tumor (top left). The bottom pictures are the vasculature surrounding the margin of a cornea in reaction to a wound. Sixty hours after wounding, many new capillaries have begun to sprout toward the site of injury. Their oriented outgrowth reflects a chemotactic response of the EC to an angiogenic factor released by the wound (Courtesy of Peter C. Burger).

3- The coupling of the vascular and bone systems

3-1 Vascular and bone development

Bone is a highly vascularized tissue which develops through two independent mechanisms. The first, termed Intramembranous ossification (IO), involves the direct differentiation of mesenchymal progenitors into osteoblasts, the bone forming cells. This mechanism is involved in the formation of flat bones of the skull. The second mechanism, termed endochondral ossification (EO) is responsible for the development of most other bones including long bones and the axial skeleton. EO occurs through a series of successive stages of remodeling of a cartilage template. Mesenchymal progenitors first condense and differentiate into chondrocytes to form an avascular template. The template undergoes sequential phases of proliferation, differentiation, hypertrophy and death. At the molecular level, Indian hedgehog (Ihh) and the Parathyroid hormone-related protein (PTHrP) signaling are crucial in regulating the proliferation and the onset of chondrocyte hypertrophy by forming a negative feedback loop in which Ihh signaling controls PTHrP expression (27). Ihh also regulates osteoblast differentiation (28). BMP signaling is currently thought to be a complementary signal maintaining chondrocytes proliferation and modulating the expression of Ihh (29). Tgf signaling is possibly modulating the Hh-PTHrP regulatory loop (30). During the hypertrophic stage, the chondrocytes activate the Hh signaling, produce collagen type X, the blood vessel-attracting molecule VEGF and Matrix metalloproteinase (MMP13, MMP9) enzymes which remodel the matrix and participate in the formation of the “bony collar” by recruited or differentiating bone forming cells (31). (31). Hedgehog signaling also contributes to the vascularization of the hypertrophic cartilage (32). The invasion of the blood vessels correlates with the replacement of the hypertrophic cartilage template by bone. Blood vessels are thought to deliver the bone forming cells (osteoblasts, osteoclasts) and the cells which will seed the hematopoietic niche. The process of angiogenesis and bone development are coupled both spatially and temporally.

3-1-1 VEGF signaling in skeletal development

The close interaction between angiogenesis and osteogenesis was first demonstrated by surgically disrupting the blood supply to the bone(33). The resulting bone had impaired density, tensile strength and modulus of elasticity. The effect

of was later confirmed and described in the growth plate of rabbits and rat (34-35). With the rise of molecular biology, VEGF was identified as a key regulator of this interplay. The inactivation of the VEGF released by chondrocytes through the systemic administration of a soluble receptor chimeric protein (Flt-(1-3)-IgG) to mice resulted in a strong impairment of blood vessel recruitment, trabecular bone formation and an expansion of the hypertrophic chondrocyte zone. The recruitment of the MMP9 expressing cells and matrix resorption was also impaired (31). Consistent with the possibility that VEGF diffuses away from the chondrocytes to attract blood vessels, mice expressing only the soluble isoform of VEGF (VEGF120) but not expressing the matrix-binding isoforms (VEGF164 and VEGF188) had delayed invasion of the blood vessels (36). Besides its chemotactic effect, VEGF directly acts on chondrocytes and osteoblasts and on the recruitment of osteoclasts (37). The VEGF receptors VEGFR1 and VEGFR2 are expressed in endothelial cells, hypertrophic chondrocytes and in osteoblasts (38). VEGF is produced by chondrocytes, particularly in their later stage of terminal differentiation, which increases their survival (39). Concomitantly, *in vitro* culture shows that osteoblasts, osteoprogenitors and human Mesenchymal Stem Cells (hMSC) produce important amounts of VEGF which induces numerous paracrine effect including survival, proliferation of endothelial cells in co-culture, migration of osteoblasts (40-41), differentiation (42-43) and the upregulation of early osteoblastic markers *cbfa1/runx2* and alkaline phosphatase (ALP) (42, 44-48). VEGF production in osteoblasts is regulated through a variety of signals including prostaglandins E1 and E2, bone morphogenetic proteins (BMPs), insulin-like growth factor 1 (IGF1), transforming growth factor beta (TGF β), endothelin-1 and vitamin D3 (49). Interestingly, the co-culture of endothelial cells and osteoblasts or hMSC support the *in vitro* formation of a primitive vascular network (50-51). These multiple effects might explain the close proximity of osteoclasts and blood capillaries *in vivo*, to regulate the hematopoietic stem cell niches (52) and emphasize the role of VEGF during skeletogenesis (49).

3-1-2 HIF signaling in skeletal development

HIF transcription factors are a driving force during bone development directly regulating VEGF but also modulating other critical mediators of EO (53). HIF1 α is a transcriptional regulator of VEGF which suggested a role during bone development (20). Indeed, mice overexpressing HIF1 α by disrupting VHL have in-

creased bone formation while mice with a disrupted HIF1a have reduced bone formation (54). In these mice, the amount of bone in the axial skeleton was directly proportional to the amount of skeletal vasculature. VEGF production and endothelial sprouting behavior was modulated in these mice. Interestingly, the role of HIF1a on bone development is not limited to the regulation of VEGF. Mice deficient for HIF1a strictly in their osteoblasts (OC-Cre mice) had normal flat bones of the skull, which resulted from IO (53) but mice deficient for HIF1a in their early mesenchymal cells (dermo1-Cre mice) had profound defects in both IO and EO including a complete failure of chondrocytes hypertrophy and defective osteoblast differentiation (decreased Osterix, RunX2) (53). Indeed, Osterix is a direct target of HIF-1 (53). Thus HIF-1 affects the angiogenic process and the differentiation of mesenchymal progenitors during EO. A second HIF transcription factor termed HIF-2a, was lately described as a central activator of Collagen type X, MMP13 and VEGFA genes during EO thus regulating the three central steps of chondrocytes hypertrophy, cartilage matrix degradation and vascular invasion (55). HIF transcription factors are probably upstream regulators coordinating numerous events of EO.

3-2 Vascular and bone regeneration

3-2-1 Bone-marrow derived mesenchymal stem cells as a reservoir for regeneration.

Adult bone marrow hosts both the hematopoietic and mesenchymal stem cell niches. The first one is thought to align the inner cavities of bone (endosteal hematopoietic stem cell niche) and the blood vessels (vascular hematopoietic progenitor niche) while the second one is suspected to be a subpopulation of pericytes (sinusoidal wall niche)(56-57). Both niches might partially overlap and might not be restricted to the bone marrow. Recent findings suggest that the adult hMSC niche can react to emergency signals transported through the blood following a trauma, migrate through the endothelium into the blood stream toward the site of trauma and contribute to neovascularization (58-59). Thus capillary-aligning hMSC could form a natural reservoir participating in the maintenance of tissue homeostasis regeneration and repair (60).

This pool of stem cells opened several perspectives in regenerative medicine. First, this population can be isolated, expanded and differentiated in vitro and is thus of great interest to form engineered tissues in vitro as implants to repair or replace portions of or whole

tissues. This is the Tissue Engineering approach (61). Second, this population of stem cells can be manipulated *in vivo* to leave its niche on demand, home to a target site, stimulate and enhance the body's own self-healing capacity or promote a specific artificial function (i.e. the vascularization of an artificial implanted device). This is the regenerative approach (62).

The hMSC populating the adult bone marrow were used in this thesis for tissue engineering applications (63). They are easy to isolate, culture, have high potential for *in vitro* expansion, immunosuppression properties, can differentiate *in vitro* in osteoblasts, chondrocytes, adipocytes and participate *in vivo* in ectopic bone formation. It is still controversial whether they can form other mesodermal or non-mesodermal tissues including an endothelium, neural and skeletal muscle tissue (64).

3-2-2 Mechanisms of bone regeneration

Fracture repair during adult life recapitulates many aspects of the developmental program of intramembranous and endochondral ossification (65-66). However, major differences specific to bone regeneration include the inflammatory activity, the formation of an hematoma, the necrotic tissue, the formation of a fibrin extra cellular matrix and the mechanical environment. Following the trauma, inflammatory factors contribute to the normal process of formation of the granulation tissue, digestion of the necrotic tissue, infectious agents and resorption of bone debris by neutrophils and macrophages. The disruption of the vasculature leads to the formation of an hematoma, a granulation tissue at the end of the bones through the recruitment of fibroblasts. The new vasculature forms by angiogenesis (sprouting from pre-existing vessels) splitting and probably by directed translocation of the vasculature (67). The growth factors, cytokines (68) embedded into the wound and the tensile endogenous forces generated by the wound (67) are critical to neovascularization.

Bone repair occurs by different specific mechanisms primarily dependent on the biophysical environment. (i) Primary bone repair occurs by direct contact repair in small cracks without interfragmentary space and with rigid stability. The repair process is mediated by intraosseous Haversian system osteoblasts and osteoclasts, without a cartilage phase. Osteoblasts directly synthesize lamellar bone parallel to the longitudinal axis of the bone and no remodelling of the repair bone is needed. (ii) Direct bone repair occurs in an envi-

ronment of interfragmentary space > 0.1 mm with rigid stability. The process is mediated without a cartilage phase by marrow derived vessels and hMSC. Bone is initially synthesized perpendicular to the long axis of the bone and then remodeled along the long axis. (iii) Endochondral bone repair occurs in large defects with inter-fragmentary spaces and mechanical instability. The repair process involve the formation of a transient vascularized callus to stabilize the fracture site. The granulation tissue formed at the edge of the broken bone gradually remodels into a fibrocartilagenous tissue while new bone is formed by intramembranous ossification, starting at the periosteum, to envelop the wounded site. The resulting tissue, termed the callus, undergoes progressive endochondral ossification in a progression from hypertrophic cartilage to woven bone and lamellar bone similar to the embryonic bone development (69-70). Besides their classical role, inflammatory factors also play a critical role during the endochondral ossification process of fracture healing by mediating angiogenesis (angiopoietins and VEGF signaling), chondrogenic apoptosis, the endochondral tissue remodeling by osteoclasts and the recruitment of osteoblasts progenitors (71-72). Bone repair must also be considered in relation to the regions of bone where repair is occurring. This illustrates how tissue regeneration recapitulates some aspects of but is not limited to the developmental program.

3-2-3 Hedgehog signaling in bone regeneration

As previously described, Hh proteins act as archetypical morphogens regulating multiple processes during embryonic skeletal development (73) but remain relatively silent in adult homeostasis (73). However, recent studies demonstrated its post-natal reactivation during several types of cancers (reviewed in (74)) and tissue regeneration processes (75-81). Hh genes (Sonic Hedgehog (Shh), Indian Hedgehog and Desert Hedgehog) have pleiotropic effects during both vascular (76, 82) and bone regeneration (81, 83-86). Shh is essential for the neovascularization of adult ischemic skeletal muscle (75, 77), myocardial tissue (79-80) and wound (78, 87). Hh is also highly reactivated upon bone fracture in adults in the callus undergoing EO (81, 86) and ectopic bone formation can be induced in mice by transplantation of Shh-transfected fibroblasts cells (88). These findings open possibilities for the use of Shh as a morphogen in clinical settings of bone regeneration. In chapter 3. we describe the possibility that Sonic Hedgehog can be used for bone regeneration.

4- Vascularization in the wound: role of endogenous tissue tension

Upon tissue injury, disrupted vessels irrigate the wounded site, platelets form a clot and immune cells such as neutrophils and macrophages infiltrate the wound site to digest necrotic tissue, remove cellular debris and infectious agents (89). 2-3 days after the injury, surrounding fibroblasts invade the site, secrete a fibrin matrix to fill the wound and form, along with the clotted blood, a granulation tissue (day 4-5). Later, in response to tensile stress, fibronectin and macrophage-derived growth factors (i.e. TGF β 1, (90)), fibroblasts differentiate into highly contractile myofibroblasts that express α -smooth muscle actin (91). Interconnected by gap junctions, myofibroblasts secrete extracellular matrix components and at the same time contract the wound (92) by transmitting tension across intracellular actin stress fibers connected to the extracellular matrix (93). The formation of new blood vessels is thought to be dependent on the endogenous forces generated by the myofibroblasts (94). New blood vessels are formed by sprouting of the surrounding capillaries and, in a lesser extent, by recruitment of cells through the circulatory system (58). Concomitantly, it has been proposed that tissue tension generated by activated fibroblasts or myofibroblasts during wound contraction mediates and directs the mechanical translocation of the vasculature. These mechanical forces pull vessels from the preexisting vascular bed as vascular loops with functional circulation which expands as an integral part of the growing granulation tissue through vessel enlargement and elongation (67). This example of the wound healing depicts an important role for the endogenous tissue forces in regulating vascular development. Interestingly, solid tumors are dependent on the recruitment of blood vessels, are secreting a fibrin matrix (95) and have an elevated endogenous tension (96). In the chapter 5, we use a microfabricated tissue model to investigate the possibility that endogenous tissue tension act as a tissue-scale morphogenetic regulator of the angiogenic microenvironment and angiogenesis.

5- The vasculature as a template for tissue regeneration

The vasculature is, along with the lymphatic and the nervous system, embedded into almost every tissues and organs. It is a critical template for the exchange of gas, nutrients, cells or molecules and a regulator of tissue development and patterning. Its disruption and disorganization is a hallmark of injuries and diseases and it plays a central role during regeneration and healing. As such, we propose in this thesis to view the vasculature as a template to promote and guide tissue regeneration.

“By viewing the process of angiogenesis as an organizing principle in biology, intriguing insights into the molecular mechanisms of seemingly unrelated phenomena might be gained”

Judah Folkman

1. Carmeliet P (2005) Angiogenesis in life, disease and medicine. (Translated from eng) *Nature* 438(7070):932-936 (in eng).
2. Gerhardt H & Betsholtz C (2003) Endothelial-pericyte interactions in angiogenesis. (Translated from eng) *Cell Tissue Res* 314(1):15-23 (in eng).
3. Nyberg P, Xie L, & Kalluri R (2005) Endogenous inhibitors of angiogenesis. (Translated from eng) *Cancer Res* 65(10):3967-3979 (in eng).
4. Armulik A, Abramsson A, & Betsholtz C (2005) Endothelial/pericyte interactions. (Translated from eng) *Circ Res* 97(6):512-523 (in eng).
5. Gimbrone MA, Jr., Cotran RS, & Folkman J (1974) Human vascular endothelial cells in culture. Growth and DNA synthesis. (Translated from eng) *J Cell Biol* 60(3):673-684 (in eng).
6. Carmeliet P, et al. (1996) Abnormal blood vessel development and lethality in embryos lacking a single VEGF allele. (Translated from eng) *Nature* 380(6573):435-439 (in eng).
7. Ferrara N, et al. (1996) Heterozygous embryonic lethality induced by targeted inactivation of the VEGF gene. (Translated from eng) *Nature* 380(6573):439-442 (in eng).
8. Ferrara N, Gerber HP, & LeCouter J (2003) The biology of VEGF and its receptors. (Translated from eng) *Nat Med* 9(6):669-676 (in eng).
9. Thomas M & Augustin HG (2009) The role of the Angiopoietins in vascular morphogenesis. (Translated from eng) *Angiogenesis* 12(2):125-137 (in eng).
10. Dejana E, Tournier-Lasserre E, & Weinstein BM (2009) The control of vascular integrity by endothelial cell junctions: molecular basis and pathological implications. (Translated from eng) *Dev Cell* 16(2):209-221 (in eng).
11. Silva R, D'Amico G, Hodivala-Dilke KM, & Reynolds LE (2008) Integrins: the keys to unlocking angiogenesis. (Translated from eng) *Arterioscler Thromb Vasc Biol* 28(10):1703-1713 (in eng).
12. Hirschi KK, Skalak TC, Peirce SM, & Little CD (2002) Vascular assembly in natural and engineered tissues. (Translated from eng) *Ann N Y Acad Sci* 961:223-242 (in eng).
13. Ferrara N & Kerbel RS (2005) Angiogenesis as a therapeutic target. (Translated from eng) *Nature* 438(7070):967-974 (in eng).
14. Aird WC (2007) Phenotypic heterogeneity of the endothelium: II. Representative vascular beds. (Translated from eng) *Circ Res* 100(2):174-190 (in eng).
15. Aird WC (2007) Phenotypic heterogeneity of the endothelium: I. Structure, function, and mechanisms. (Translated from eng) *Circ Res* 100(2):158-173 (in eng).
16. Miyasaka M & Tanaka T (2004) Lymphocyte trafficking across high endothelial venules: dogmas and enigmas. (Translated from eng) *Nat Rev Immunol* 4(5):360-370 (in eng).
17. Hirata A, Baluk P, Fujiwara T, & McDonald DM (1995) Location of focal silver staining at endothelial gaps in inflamed venules examined by scanning electron microscopy. (Translated from eng) *Am J Physiol* 269(3 Pt 1):L403-418 (in eng).
18. Florey (1966) The endothelial cell. (Translated from eng) *Br Med J* 2(5512):487-490 (in eng).
19. Gerhardt H, et al. (2003) VEGF guides angiogenic sprouting utilizing endothelial tip cell filopodia. (Translated from eng) *J Cell Biol* 161(6):1163-1177 (in eng).
20. Shweiki D, Itin A, Soffer D, & Keshet E (1992) Vascular endothelial growth factor induced by hypoxia may mediate hypoxia-initiated angiogenesis. (Translated from eng) *Nature* 359(6398):843-845 (in eng).
21. Nelson CM, Vanduijn MM, Inman JL, Fletcher DA, & Bissell MJ (2006) Tissue geometry determines sites of mammary branching morphogenesis in organotypic cultures. (Translated from eng) *Science* 314(5797):298-300 (in eng).
22. Chappell JC, Taylor SM, Ferrara N, & Bautch VL (2009) Local guidance of emerging vessel sprouts requires soluble Flt-1. (Translated from eng) *Dev Cell* 17(3):377-386 (in eng).
23. Ghabrial AS & Krasnow MA (2006) Social interactions among epithelial cells during tracheal branching morphogenesis. (Translated from eng) *Nature* 441(7094):746-749 (in eng).
24. Carmeliet P (2004) Manipulating angiogenesis in medicine. (Translated from eng) *J Intern Med* 255(5):538-561 (in eng).
25. Gariano RF & Gardner TW (2005) Retinal angiogenesis in development and disease. (Translated from eng) *Nature* 438(7070):960-966 (in eng).

26. Red-Horse K, Crawford Y, Shojaei F, & Ferrara N (2007) Endothelium-microenvironment interactions in the developing embryo and in the adult. (Translated from eng) *Dev Cell* 12(2):181-194 (in eng).
27. Mak KK, Kronenberg HM, Chuang PT, Mackem S, & Yang Y (2008) Indian hedgehog signals independently of PTHrP to promote chondrocyte hypertrophy. (Translated from eng) *Development* 135(11):1947-1956 (in eng).
28. Long F, et al. (2004) Ihh signaling is directly required for the osteoblast lineage in the endochondral skeleton. (Translated from eng) *Development* 131(6):1309-1318 (in eng).
29. Minina E, et al. (2001) BMP and Ihh/PTHrP signaling interact to coordinate chondrocyte proliferation and differentiation. (Translated from eng) *Development* 128(22):4523-4534 (in eng).
30. Alvarez J, et al. (2002) TGFbeta2 mediates the effects of hedgehog on hypertrophic differentiation and PTHrP expression. (Translated from eng) *Development* 129(8):1913-1924 (in eng).
31. Gerber HP, et al. (1999) VEGF couples hypertrophic cartilage remodeling, ossification and angiogenesis during endochondral bone formation. (Translated from eng) *Nat Med* 5(6):623-628 (in eng).
32. Joeng KS & Long F (2009) The Gli2 transcriptional activator is a crucial effector for Ihh signaling in osteoblast development and cartilage vascularization. (Translated from eng) *Development* 136(24):4177-4185 (in eng).
33. Coolbaugh CC (1952) Effects of reduced blood supply on bone. (Translated from eng) *Am J Physiol* 169(1):26-33 (in eng).
34. Trueta J & Trias A (1961) The vascular contribution to osteogenesis. IV. The effect of pressure upon the epiphyseal cartilage of the rabbit. (Translated from eng) *J Bone Joint Surg Br* 43-B:800-813 (in eng).
35. Trueta J & Amato VP (1960) The vascular contribution to osteogenesis. III. Changes in the growth cartilage caused by experimentally induced ischaemia. (Translated from eng) *J Bone Joint Surg Br* 42-B:571-587 (in eng).
36. Zelzer E, et al. (2002) Skeletal defects in VEGF(120/120) mice reveal multiple roles for VEGF in skeletogenesis. (Translated from eng) *Development* 129(8):1893-1904 (in eng).
37. Shapiro F (2008) Bone development and its relation to fracture repair. The role of mesenchymal osteoblasts and surface osteoblasts. (Translated from eng) *Eur Cell Mater* 15:53-76 (in eng).
38. Deckers MM, et al. (2000) Expression of vascular endothelial growth factors and their receptors during osteoblast differentiation. (Translated from eng) *Endocrinology* 141(5):1667-1674 (in eng).
39. Zelzer E, et al. (2004) VEGFA is necessary for chondrocyte survival during bone development. (Translated from eng) *Development* 131(9):2161-2171 (in eng).
40. Fiedler J, Leucht F, Waltenberger J, Dehio C, & Brenner RE (2005) VEGF-A and PlGF-1 stimulate chemotactic migration of human mesenchymal progenitor cells. (Translated from eng) *Biochem Biophys Res Commun* 334(2):561-568 (in eng).
41. Mayr-Wohlfart U, et al. (2002) Vascular endothelial growth factor stimulates chemotactic migration of primary human osteoblasts. (Translated from eng) *Bone* 30(3):472-477 (in eng).
42. Clarkin CE, Emery RJ, Pitsillides AA, & Wheeler-Jones CP (2008) Evaluation of VEGF-mediated signaling in primary human cells reveals a paracrine action for VEGF in osteoblast-mediated cross-talk to endothelial cells. (Translated from eng) *J Cell Physiol* 214(2):537-544 (in eng).
43. Mayer H, et al. (2005) Vascular endothelial growth factor (VEGF-A) expression in human mesenchymal stem cells: autocrine and paracrine role on osteoblastic and endothelial differentiation. (Translated from eng) *J Cell Biochem* 95(4):827-839 (in eng).
44. Wang DS, Miura M, Demura H, & Sato K (1997) Anabolic effects of 1,25-dihydroxyvitamin D3 on osteoblasts are enhanced by vascular endothelial growth factor produced by osteoblasts and by growth factors produced by endothelial cells. (Translated from eng) *Endocrinology* 138(7):2953-2962 (in eng).
45. Villars F, Bordenave L, Bareille R, & Amedee J (2000) Effect of human endothelial cells on human bone marrow stromal cell phenotype: role of VEGF? (Translated from eng) *J Cell Biochem* 79(4):672-685 (in eng).
46. Guillotin B, Bareille R, Bourget C, Bordenave L, & Amedee J (2008) Interaction between human umbilical vein endothelial cells and human osteoprogenitors triggers pleiotropic effect that may sup-

- port osteoblastic function. (Translated from eng) Bone 42(6):1080-1091 (in eng).
47. Grellier M, et al. (2009) Role of vascular endothelial growth factor in the communication between human osteoprogenitors and endothelial cells. (Translated from eng) J Cell Biochem 106(3):390-398 (in eng).
48. Villars F, et al. (2002) Effect of HUVEC on human osteoprogenitor cell differentiation needs heterotypic gap junction communication. (Translated from eng) Am J Physiol Cell Physiol 282(4):C775-785 (in eng).
49. Zelzer E & Olsen BR (2005) Multiple roles of vascular endothelial growth factor (VEGF) in skeletal development, growth, and repair. (Translated from eng) Curr Top Dev Biol 65:169-187 (in eng).
50. Rouwkema J, de Boer J, & Van Blitterswijk CA (2006) Endothelial cells assemble into a 3-dimensional prevascular network in a bone tissue engineering construct. (Translated from eng) Tissue Eng 12(9):2685-2693 (in eng).
51. Hofmann A, et al. (2008) The effect of human osteoblasts on proliferation and neo-vessel formation of human umbilical vein endothelial cells in a long-term 3D co-culture on polyurethane scaffolds. (Translated from eng) Biomaterials 29(31):4217-4226 (in eng).
52. Il-Hoan O & Kyung-Rim K (2010) Multiple Niches for Hematopoietic Stem Cell Regulations. (Translated from Eng) Stem Cells (in Eng).
53. Wan C, et al. (2010) Role of HIF-1alpha in skeletal development. (Translated from eng) Ann N Y Acad Sci 1192(1):322-326 (in eng).
54. Wang Y, et al. (2007) The hypoxia-inducible factor alpha pathway couples angiogenesis to osteogenesis during skeletal development. (Translated from eng) J Clin Invest 117(6):1616-1626 (in eng).
55. Saito T, et al. (2010) Transcriptional regulation of endochondral ossification by HIF-2alpha during skeletal growth and osteoarthritis development. (Translated from eng) Nat Med 16(6):678-686 (in eng).
56. Sacchetti B, et al. (2007) Self-renewing osteoprogenitors in bone marrow sinusoids can organize a hematopoietic microenvironment. (Translated from eng) Cell 131(2):324-336 (in eng).
57. Maes C, Kobayashi T, & Kronenberg HM (2007) A novel transgenic mouse model to study the osteoblast lineage in vivo. (Translated from eng) Ann N Y Acad Sci 1116:149-164 (in eng).
58. Asahara T & Isner JM (2002) Endothelial progenitor cells for vascular regeneration. (Translated from eng) J Hematother Stem Cell Res 11(2):171-178 (in eng).
59. Rafii S, Lyden D, Benezra R, Hattori K, & Heissig B (2002) Vascular and haematopoietic stem cells: novel targets for anti-angiogenesis therapy? (Translated from eng) Nat Rev Cancer 2(11):826-835 (in eng).
60. Bianco P, Robey PG, & Simmons PJ (2008) Mesenchymal stem cells: revisiting history, concepts, and assays. (Translated from eng) Cell Stem Cell 2(4):313-319 (in eng).
61. Langer R & Vacanti JP (1993) Tissue engineering. (Translated from eng) Science 260(5110):920-926 (in eng).
62. Daar AS & Greenwood HL (2007) A proposed definition of regenerative medicine. (Translated from eng) J Tissue Eng Regen Med 1(3):179-184 (in eng).
63. da Silva Meirelles L, Caplan AI, & Nardi NB (2008) In search of the in vivo identity of mesenchymal stem cells. (Translated from eng) Stem Cells 26(9):2287-2299 (in eng).
64. Bianco P, Riminucci M, Gronthos S, & Robey PG (2001) Bone marrow stromal stem cells: nature, biology, and potential applications. (Translated from eng) Stem Cells 19(3):180-192 (in eng).
65. Gerstenfeld LC, Cullinane DM, Barnes GL, Graves DT, & Einhorn TA (2003) Fracture healing as a post-natal developmental process: molecular, spatial, and temporal aspects of its regulation. (Translated from eng) J Cell Biochem 88(5):873-884 (in eng).
66. Carano RA & Filvaroff EH (2003) Angiogenesis and bone repair. (Translated from eng) Drug Discov Today 8(21):980-989 (in eng).
67. Kilarski WW, Samolov B, Petersson L, Kvanta A, & Gerwins P (2009) Biomechanical regulation of blood vessel growth during tissue vascularization. (Translated from eng) Nat Med 15(6):657-664 (in eng).
68. Barnes GL, Kostenuik PJ, Gerstenfeld LC, & Einhorn TA (1999) Growth factor regulation of fracture repair. (Translated from eng) J Bone Miner Res 14(11):1805-1815 (in eng).

69. Street J, et al. (2002) Vascular endothelial growth factor stimulates bone repair by promoting angiogenesis and bone turnover. (Translated from eng) *Proc Natl Acad Sci U S A* 99(15):9656-9661 (in eng).
70. Le AX, Miclau T, Hu D, & Helms JA (2001) Molecular aspects of healing in stabilized and non-stabilized fractures. (Translated from eng) *J Orthop Res* 19(1):78-84 (in eng).
71. Gerstenfeld LC, et al. (2001) Impaired intramembranous bone formation during bone repair in the absence of tumor necrosis factor-alpha signaling. (Translated from eng) *Cells Tissues Organs* 169(3):285-294 (in eng).
72. Lehmann W, et al. (2005) Tumor necrosis factor alpha (TNF-alpha) coordinately regulates the expression of specific matrix metalloproteinases (MMPS) and angiogenic factors during fracture healing. (Translated from eng) *Bone* 36(2):300-310 (in eng).
73. McMahon AP, Ingham PW, & Tabin CJ (2003) Developmental roles and clinical significance of hedgehog signaling. (Translated from eng) *Curr Top Dev Biol* 53:1-114 (in eng).
74. Ruiz i Altaba A, Sanchez P, & Dahmane N (2002) Gli and hedgehog in cancer: tumours, embryos and stem cells. (Translated from eng) *Nat Rev Cancer* 2(5):361-372 (in eng).
75. Straface G, et al. (2008) Sonic Hedgehog Regulates Angiogenesis and Myogenesis During Post-Natal Skeletal Muscle Regeneration. (Translated from Eng) *J Cell Mol Med* (in Eng).
76. Pola R, et al. (2001) The morphogen Sonic hedgehog is an indirect angiogenic agent upregulating two families of angiogenic growth factors. (Translated from eng) *Nat Med* 7(6):706-711 (in eng).
77. Pola R, et al. (2003) Postnatal recapitulation of embryonic hedgehog pathway in response to skeletal muscle ischemia. (Translated from eng) *Circulation* 108(4):479-485 (in eng).
78. Le H, et al. (2008) Hedgehog signaling is essential for normal wound healing. (Translated from eng) *Wound Repair Regen* 16(6):768-773 (in eng).
79. Kusano KF, et al. (2005) Sonic hedgehog myocardial gene therapy: tissue repair through transient reconstitution of embryonic signaling. (Translated from eng) *Nat Med* 11(11):1197-1204 (in eng).
80. Kusano KF, et al. (2004) Sonic hedgehog induces arteriogenesis in diabetic vasa nervorum and restores function in diabetic neuropathy. (Translated from eng) *Arterioscler Thromb Vasc Biol* 24(11):2102-2107 (in eng).
81. Murakami S & Noda M (2000) Expression of Indian hedgehog during fracture healing in adult rat femora. (Translated from eng) *Calcif Tissue Int* 66(4):272-276 (in eng).
82. Vokes SA, et al. (2004) Hedgehog signaling is essential for endothelial tube formation during vasculogenesis. (Translated from eng) *Development* 131(17):4371-4380 (in eng).
83. Zhou Z, et al. (2000) Impaired endochondral ossification and angiogenesis in mice deficient in membrane-type matrix metalloproteinase I. (Translated from eng) *Proc Natl Acad Sci U S A* 97(8):4052-4057 (in eng).
84. Vu TH, et al. (1998) MMP-9/gelatinase B is a key regulator of growth plate angiogenesis and apoptosis of hypertrophic chondrocytes. (Translated from eng) *Cell* 93(3):411-422 (in eng).
85. St-Jacques B, Hammerschmidt M, & McMahon AP (1999) Indian hedgehog signaling regulates proliferation and differentiation of chondrocytes and is essential for bone formation. (Translated from eng) *Genes Dev* 13(16):2072-2086 (in eng).
86. Emans PJ, et al. (2007) A novel in vivo model to study endochondral bone formation; HIF-1alpha activation and BMP expression. (Translated from eng) *Bone* 40(2):409-418 (in eng).
87. Asai J, et al. (2006) Topical sonic hedgehog gene therapy accelerates wound healing in diabetes by enhancing endothelial progenitor cell-mediated microvascular remodeling. (Translated from eng) *Circulation* 113(20):2413-2424 (in eng).
88. Kinto N, et al. (1997) Fibroblasts expressing Sonic hedgehog induce osteoblast differentiation and ectopic bone formation. (Translated from eng) *FEBS Lett* 404(2-3):319-323 (in eng).
89. Singer AJ & Clark RA (1999) Cutaneous wound healing. (Translated from eng) *N Engl J Med* 341(10):738-746 (in eng).
90. Serini G, et al. (1998) The fibronectin domain ED-A is crucial for myofibroblastic phenotype induction by transforming growth factor-beta1. (Translated from eng) *J Cell Biol* 142(3):873-881 (in eng).
91. Majno G, Gabbiani G, Hirschel BJ, Ryan GB, & Statkov PR (1971) Contraction of granulation tis-

Chapter 1

- sue in vitro: similarity to smooth muscle. (Translated from eng) *Science* 173(996):548-550 (in eng).
92. Gabbiani G, Hirschel BJ, Ryan GB, Statkov PR, & Majno G (1972) Granulation tissue as a contractile organ. A study of structure and function. (Translated from eng) *J Exp Med* 135(4):719-734 (in eng).
93. Tomasek JJ, Gabbiani G, Hinz B, Chaponnier C, & Brown RA (2002) Myofibroblasts and mechano-regulation of connective tissue remodelling. (Translated from eng) *Nat Rev Mol Cell Biol* 3(5):349-363 (in eng).
94. Korff T & Augustin HG (1999) Tensional forces in fibrillar extracellular matrices control directional capillary sprouting. (Translated from eng) *J Cell Sci* 112 (Pt 19):3249-3258 (in eng).
95. Dvorak HF (1986) Tumors: wounds that do not heal. Similarities between tumor stroma generation and wound healing. (Translated from eng) *N Engl J Med* 315(26):1650-1659 (in eng).
96. Paszek MJ, et al. (2005) Tensional homeostasis and the malignant phenotype. (Translated from eng) *Cancer Cell* 8(3):241-254 (in eng).

Chapter 2

Developmental mechanisms in microfabricated multicellular systems

In this chapter, we discuss the possibility to use microfabrication techniques to assemble multicellular constructs to recapitulate and investigate some aspects of tissue development. We will first briefly discuss the current state-of-the-art in microfabrication techniques to pattern multicellular constructs. We will then describe seminal proof-of-concept studies using microfabricated multicellular constructs to recapitulate and study the emergence of tissue organization and patterns.

Developmental mechanisms in microfabricated multicellular systems *

As described in the preceding section, in the context of vascular development, advances in genomics, proteomics and molecular biology provided increasing knowledge of molecular components and interactions. These interactions are context-dependent, dynamically orchestrated and integrated at different scales to contribute to tissue organization, architectures and functions. However, in spite of our knowledge of the actors and of their context-dependent behaviors, we are still missing the theatre to reproduce the scene *in vitro*. We speculate microfabricated multicellular systems might help.

Microfabricated platforms are tools which allow for the fabrication of primitive multicellular constructs to investigate the mechanisms driving multicellular organization. They provide an intermediate complexity in the chain of models ranging from simple 2D culture to complex living metazoans (i.e. *Caenorhabditis elegans*, *Drosophila melanogaster*, zebrafish, mouse). To develop such models, one must form primitive multicellular patterns or architectures with the minimum level of complexity necessary for autonomous organization to emerge. These experimental set-up potentially allow for a higher throughput and content, more precise and systematic variations in the design, manipulations, perturbation and monitoring, in defined environment.

In this text we will focus on (i) approaches and technologies to assemble cells into a defined *metastable* constructs, (ii) on 6 seminal studies describing emergent behaviors of multicellular organization suggesting primitive rules to control and predict differentiation and morphogenesis related mechanisms, (iii) possibilities to scale-up models and implants of relevant size using a *bottom-up* or *modular* approach.

* Parts of this chapter were published as a Leading Opinion paper in the journal *Biomaterials* and as a chapter in the book "Cell and organ printing" edited by Peter Wu, Bradley R. Ringeisen and Barry J. Spargo ; Springer New York.

1- Microfabrication tools

Recapitulating tissue development in vitro, using multicellular constructs is not new to biologists: they are culturing aggregates of cells inside a drop of liquid hanging from a surface since 1907 [1]. Such system has been used to grow tumor models [2] or embryoid bodies [3] and to study tissue development of liver [4], cartilage [5], retina [6] or pancreas [7]. However, more powerful technologies are emerging enabling more reproducible and precise experimental set ups. Those technologies, including micro-fabrication, contribute to forming simple primitive architectures prone to remodelling and organization.

The fabrication methods of forming patterned multicellular systems are multiple and varied. Here, we present several examples we consider important for biological applications. To be widely applicable these techniques must remain low in cost and experimentally convenient for routine use in biology laboratories.

1-1 Patterning cells on two dimensional substrates using soft lithography. This set of related techniques uses elastomeric (“soft”) stamps to pattern proteins and cells on 2D substrates. This set includes microcontact printing, microfluidic channels, laminar flow and the use of stencils to form patterns of alkanethiols and proteins on gold-coated and glass substrates. The rest of the surface is treated with a non-adherent coating (i.e. tri(ethylene glycol)-terminated alkanethiol or ethylene oxide and propylene oxide “pluronic”). Extra cellular matrix ECM components (i.e. fibronectin) are absorbed only on the stamped regions thus promoting the spatially restricted attachment of cells [8-10]. This method was mostly used to confine single cells into a restricted space (“islands”) or to study their migration on large patterned substrates. These single cell studies correlated spreading and internal mechanical stress through Rho, Rac signaling and focal adhesions to diverse cellular functions such as proliferation, apoptosis [11], protein synthesis [9], directional motility [12], directional lamellipodia extension [13] and lineage differentiation [14-16]. Three seminal studies used this method to look at multicellular organization of endothelial cells [8, 17] and the function of hepatocytes [10] as described in the following section.

1-3 Encapsulation of cells into free-standing micro-molded blocks of hydrogel. Microscale hydrogel blocks are formed by replica molding or extrusion of a collagen type I hydrogel encapsulating cells in a process that is similar to cookie fabrication. Casting can be done

on micropatterned elastomeric templates (i.e. PDMS) immersed in F127 pluronic to prevent cell adhesion [21-23]. Extrusion can be done through the lumen of an ethylene oxide gas-sterilized PE tube [24]. Cells can be randomly suspended inside the bioactive hydrogel and encapsulated upon gelation. These 3D blocks can be used to form building blocks that can later be assembled into macroscale constructs [21, 24]. One seminal study used this method to look at the differentiation of hMSC [23] as described in the following section.

1-2 Dynamic organization of cells into photopolymerizable hydrogel using dielectrophoretic forces. A range of molding techniques allows to process polymer at the melting phase and form micro-scale structures. An adaptation of these techniques termed Substrate Modification and Replication by Thermoforming (SMART) processes polymer in the thermoelastic state [18-19]. The SMART technique presents the advantage that it allows a pre-process of the unformed, flat membrane which will then be deformed into a 3D structure. For example, before thermoforming, the flat membrane can be patterned with nanoscale structures or coated with a photopatterned layer of poly(L-lysine) (PLL) and hyaluronic acid (VAHyal) to gain spatial control over cell adhesion [20].

1-3 Patterning of cells onto thermoresponsive polymers. Thermoresponsive polymers (i.e. poly(N-isopropylacrylamide) [26] or n-butyl methacrylate [27]) can be grafted on cell culture substrates. Cells cultured on these substrates form a confluent layer which can be released from the substrate by lowering the temperature and releasing the grafted polymer. The resulting sheets of cells can further be manipulated and stacked to form three dimensional stratified tissues [28]. Techniques were developed to form patterns of cells using previously described micro-contact printing [29] and the grafting of two different thermoresponsive polymers by electron beam polymerization [27].

1-4 Encapsulation of cells into geometric wells/compartments replicated in a hydrogel. Patterns of wells/compartments can be replicated inside layers of hydrogels spread on a surface, using polymer templates coated with (i.e. PDMS, SU-8) [30]. Cells are seeded in the wells and covered by an additional layer of hydrogel to close the compartment. This technique proved useful to increase the throughput of a DNA damage assay using agarose, a bioinert hydrogel [31] and the throughput of an epithelial culture “acinus” model using Matrigel® [32]. One seminal study used this method to study the branching morphogenesis

of the mammary epithelial tubule using a microstructured collagen type I extra-cellular-matrix [33] as described in the following section.

1-5 Sequential aggregation of cells in agarose templates. Bioinert hydrogels (i.e. agarose) can be imprinted using templates (i.e. PDMS, stainless steel) to form wells/compartments. Cells can be seeded in these non-adherent compartments and spontaneously aggregate into cell clusters. Cell clusters can further be used as building blocks and aggregated into macroscale geometric tissues [34-35]. This 3D model allows for the formation of geometric, free-standing and biomaterial-free tissues and was used in the chapters 4 and 5 of this thesis.

2- How to orchestrate developmental mechanisms *in vitro*?

During development, homeostasis and regeneration, tissues and organs undergo precisely coordinated changes in cellular behavior and progressive remodeling through different stages of organization. These techniques produce a *meta-stable* multicellular construct prone to remodeling over time according to biological and physical principles (i.e. migration of the cells, shrinkage of the hydrogel): Shapes and patterns are not inevitably translated to the final tissue. Properties must be given “by design” to promote progressive remodeling and organization toward the final architecture. Clearly, understanding, predicting and controlling the self-organization of multicellular constructs would benefit to understanding morphogenesis and tremendously improve tissue micro-fabrication. The first properties “by design” being investigated are the geometric form and dimensions of the multicellular systems. Here we describe current attempts to understand the importance of forms/geometries in the initial multicellular architecture and describe the observed subsequent organization of the microenvironment and cellular behaviors.

Here we present 6 seminal studies showing the possibilities of microfabricated multicellular systems which range of scientific and technical investigations from developmental models to screening platforms for the pharmacological industry.

In a **first study** by Laura E. Dike, endothelial cells were seeded on lines of fibronectin of 10 and 30 micrometers wide. Unpatterned substrate and small islands for single cell culture (squares with sides > 10 micrometers) were used as controls. Fibronectin lines of 10 micrometers induced the alignment and tubulogenesis of endothelial cells when controls and lines of 30 micrometers wide did not. Interestingly, this correlated with a regulation of the cell cycle: endothelial cells cultured on unpatterned substrates proliferated (40% at 72 hours), endothelial cells cultured on small islands had limited proliferation (>2%). Lines of 30 micrometers induced an intermediate proliferation rate (20%) and lines of 10 micrometers limited the proliferation (>2%). The apoptotic program was only induced on small islands (10 micrometers). Concomitantly, a reorganization of the CD31 membrane marker and of the fibronectin into a central fibril was only observed in the lumen-forming 10 micrometers lines. This study suggests that the remodeling and decrease in the area of cell-substrate adhesion modulate the balance between growth and apoptosis and

triggers a differentiation program (tubulogenesis) possibly through integrin clustering and cytoskeletal tension. Although largely descriptive, this study is the first one showing that the microenvironment (spatial restriction and geometry) prevails upon chemical signals (growth factors, integrin binding) on dictating the activation of the cellular and multicellular program of tubulogenesis [17].

In a **second study** using multicellular patterns on 2D substrates, Celeste M. Nelson showed that the geometric form of a multicellular sheet of endothelial cells dictates the formation of heterogeneous patterns of mechanical stress. This effect was specifically important in the corners and periphery of cellular sheets as shown using (i) a computational model by using the finite-element method to simulate a sheet of cells contracting against a matrix-coated substratum, (ii) direct measurement using an elastomeric force sensor array and (iii) pharmacological and genetic disturbance of the Rho signaling and of VE-cadherin intercellular adhesion. This internal patterns of mechanical stress emerged spontaneously and correlated with patterns of cellular proliferation. This study shows a clear relation between geometry and local proliferation and suggest a role of local mechanical forces. From the experimental point-of-view, it introduce for the first time the combination of microfabricated multicellular systems, genetic and pharmacological and computational approaches to investigate the emergence of patterned behavior in multicellular systems [8].

In a **third study** using elastomeric stencils, Salman R. Khetani patterned islands of collagen and multicellular sheets of hepatocytes. The rest of the substrate was seeded with 3T3-J2 fibroblasts. The dimensions of the island diameter were optimized to improve liver-specific functions as compared to unorganized cultures, the supporting role of 3T3-J2 fibroblast was confirmed (as previously described in a classical feeder-layer culture). Functional and phenotypic characterization of the hepatocytes were supported for several weeks. (i.e. rates of albumin secretion and urea synthesis, Activities of phase I (CYP450) and phase II (conjugation) enzymes and related to a gene expression profile. Utility of microscale liver cultures for screening of hepatotoxicity and drug interactions was assessed using a panel of compounds and classical markers (i.e. hepatotoxins by TC50, Mitochond-

drial toxicity was evaluated using the MTT assay). This study is the first one showing the utility (throughput) of microscale culture for screening of hepatotoxic drugs and interactions as compared to current systems (classical cell culture or explanted liver slices).

In a **fourth study**, Sami A. Ruiz repeated the experiment of Celeste M. Nelson (second study), replacing endothelial cells by hMSC. Using the same experimental set up, he confirms the previously described role of mechanical forces in regulating differentiation of single hMSC [15] and shows the emergence of differentiation patterns in multicellular sheets of hMSC. Similar to the work of Celeste M. Nelson, he shows that peripheries of circular sheets of hMSC differentiate preferentially toward the osteogenic lineage whereas the central part of the sheets of hMSC differentiate preferentially toward the adipogenic lineage. More interestingly, he translates this finding to hMSC encapsulated into 3D, free-standing micro-molded blocks of collagen type I and shows a similar pattern of differentiation. Cells in the periphery of the blocks differentiated preferentially into the osteogenic lineage whereas cells in the core of the blocks differentiated preferentially into adipocytes. This preferential differentiation was strongly impaired when adding pharmacological inhibitors of the Rho, myosin II and actin elements (Blebistatin and Y27632, similar to **chapter 5**). This is the first study showing emergent patterns of differentiation in 3D, free-standing microfabricated multicellular systems.

In a **fifth study**, Dirk R. Albrecht describes an optimization study of chondrocytes production of sulfated glycosaminoglycans using a patterning method of dielectrophoretic forces. Cellular clusters of different sizes (1, 5, 10, 18 cells/cluster) produced different amount of sulfated glycosaminoglycans per cell: the non-clustered cultures produced the most matrix and the amount of matrix produced decreased up to 30% when the size of the cluster increased. This optimization study demonstrate that the patterning of chondrocytes into clusters decreased the efficiency of the system to produce sulfated glycosaminoglycans [25]: microfabricated multicellular systems do not necessarily improve the biological response. However, this decrease might be due to a damage of the cell function following the exposure to the electric field.

In a **sixth study**, Celeste M. Nelson studies the role of geometry in the initiating the sprouting of the branching mammary gland. She used a molding method to form microscale cavities into the surface of type I collagen gels with an elastomeric stamp (PDMS). Mouse mammary epithelial cells were seeded in these cavities and covered by a layer of collagen type I. The cavity mimics the initial epithelial sac which transform into the mammary tree during puberty. The form of the cavity in itself dictated different Epithelial Growth Factor-induced branching sites with preferential sprouting in the cavity corners. Interestingly, those branching sites matched with computer simulated and experimental profiles of secretion of autocrine inhibitory factors including TGF β . The spatial arrangement of different geometric cavities proved that one cavity filled with cells could inhibit sprouting in a neighboring cavity. This strongly suggests that tissue geometry conditions the formation of local microenvironments (here, local gradients of soluble inhibitors of cellular sprouting) and subsequent morphogenesis processes [36]. This study is the first one describing a physiologically relevant mechanism and precise quantitative data to understand of how spatial positioning of the initial sprout is determined in the mammary epithelial tubule rudiment. This mechanism was later confirmed to modulate *in vivo* the initial sprouting during angiogenesis [37].

These results demonstrate the role of microfabricated multicellular systems as tools to investigate developmental mechanisms or as screening platforms. These tools allow for high reproducibility, throughput/content, precise quantifications and can be combined with live microscopy (i.e. reporter assays) and easy manipulation (i.e. microfluidic, microsurgery). These 6 initial studies pinpoint the importance of the architecture (geometry and size) of the initial cellular construct in creating local microenvironment (local gradients of factors or local mechanical stresses) resulting in specific biological function or morphogenesis related processes. They opened opportunities to understand the mechanisms by which the physical environment of multicellular systems dynamically feeds-back to regulate changes of patterns of cellular states and behavior and genetic programs. These studies suggest that tissue morphogenesis, differentiation and maintenance result from the intricate interplay between genetic material and cellular processes orchestrated by strong feed-back mechanisms resulting from the physical environment.

3- Bottom-up / modular approach

From a tissue engineering point-of-view, microfabricated tissues can be used to form implants. Tissues are often a combination of small repeating units assembled over several scales. Cortical bone and skeletal muscle are characterized by fascicles of repeating longitudinal units, respectively osteons and muscle fibers (100-500 micrometers diameter). Subsequently, it was proposed to build tissues by assembling blocks mimicking those units in a *bottom-up* or *modular* approach [24, 34, 38]. This approach facilitates the fabrication of architectures using complementary shapes and opens possibility for scaling-up and an automated production. It uses cellular aggregates [34] or micromolded gel encapsulated cells [24]. Architectures were achieved by complementary shapes and spatial arrangement [24, 38, 42-44], self assembly using microfluidic chip [45] or liquid-liquid interface [46]. Blocks can fuse [33, 34], be cross-linked [47] and develop coordinated functionalities [35, 36]. Examples of constructs resulting from a *bottom-up* approach include neural tubes [34], collagen rods encapsulating hepatocytes and covered by endothelial cells [24] or beating cardiac sheets generated by stacking cell-sheets [48-49].

1. Harrison, R., Observations on the living developing nerve fiber. *Anat. Rec.*, 1907. 116-28.
2. Inch, W.R., J.A. McCredie, and R.M. Sutherland, Growth of nodular carcinomas in rodents compared with multi-cell spheroids in tissue culture. *Growth*, 1970. 34(3): p. 271-82.
3. Itskovitz-Eldor, J., et al., Differentiation of human embryonic stem cells into embryoid bodies compromising the three embryonic germ layers. *Mol Med*, 2000. 6(2): p. 88-95.
4. Tong, J.Z., et al., Long-term culture of adult rat hepatocyte spheroids. *Exp Cell Res*, 1992. 200(2): p. 326-32.
5. Denker, A.E., S.B. Nicoll, and R.S. Tuan, Formation of cartilage-like spheroids by micromass cultures of murine C3H10T1/2 cells upon treatment with transforming growth factor-beta 1. *Differentiation*, 1995. 59(1): p. 25-34.
6. Rothermel, A., et al., Pigmented epithelium induces complete retinal reconstitution from dispersed embryonic chick retinae in reaggregation culture. *Proc Biol Sci*, 1997. 264(1386): p. 1293-302.
7. Lehnert, L., et al., Hollow-spheres: a new model for analyses of differentiation of pancreatic duct epithelial cells. *Ann N Y Acad Sci*, 1999. 880: p. 83-93.
8. Nelson, C.M., et al., Emergent patterns of growth controlled by multicellular form and mechanics. *Proc Natl Acad Sci U S A*, 2005. 102(33): p. 11594-9.
9. Singhvi, R., et al., Engineering cell shape and function. *Science*, 1994. 264(5159): p. 696-8.
10. Khetani, S.R. and S.N. Bhatia, Microscale culture of human liver cells for drug development. *Nat Biotechnol*, 2008. 26(1): p. 120-6.
11. Chen, C.S., et al., Geometric control of cell life and death. *Science*, 1997. 276(5317): p. 1425-8.
12. Xia, N., et al., Directional control of cell motility through focal adhesion positioning and spatial control of Rac activation. *FASEB J*, 2008. 22(6): p. 1649-59.
13. Parker, K.K., et al., Directional control of lamellipodia extension by constraining cell shape and orienting cell tractional forces. *FASEB J*, 2002. 16(10): p. 1195-204.
14. Engler, A.J., et al., Matrix elasticity directs stem cell lineage specification. *Cell*, 2006. 126(4): p. 677-89.
15. McBeath, R., et al., Cell shape, cytoskeletal tension, and RhoA regulate stem cell lineage commitment. *Dev Cell*, 2004. 6(4): p. 483-95.
16. Gao, L., R. McBeath, and C.S. Chen, Stem cell shape regulates a chondrogenic versus myogenic fate through Rac1 and N-cadherin. *Stem Cells*, 2010. 28(3): p. 564-72.
17. Dike, L.E., et al., Geometric control of switching between growth, apoptosis, and differentiation during angiogenesis using micropatterned substrates. *In Vitro Cell Dev Biol Anim*, 1999. 35(8): p. 441-8.
18. Giselbrecht, S., et al., 3D tissue culture substrates produced by microthermoforming of pre-processed polymer films. *Biomed Microdevices*, 2006. 8(3): p. 191-9.
19. Truckenmuller, R., et al., Flexible fluidic microchips based on thermoformed and locally modified thin polymer films. *Lab Chip*, 2008. 8(9): p. 1570-9.
20. Richter, C., et al., Spatially controlled cell adhesion on three-dimensional substrates. *Biomed Microdevices*, 2010.
21. McGuigan, A.P., et al., Cell encapsulation in sub-mm sized gel modules using replica molding. *PLoS One*, 2008. 3(5): p. e2258.
22. McGuigan, A.P., B. Leung, and M.V. Sefton, Fabrication of cell-containing gel modules to assemble modular tissue-engineered constructs [corrected]. *Nat Protoc*, 2006. 1(6): p. 2963-9.
23. Ruiz, S.A. and C.S. Chen, Emergence of patterned stem cell differentiation within multicellular structures. *Stem Cells*, 2008. 26(11): p. 2921-7.
24. McGuigan, A.P. and M.V. Sefton, Vascularized organoid engineered by modular assembly enables blood perfusion. *Proc Natl Acad Sci U S A*, 2006. 103(31): p. 11461-6.
25. Albrecht, D.R., et al., Probing the role of multicellular organization in three-dimensional micro-environments. *Nat Methods*, 2006. 3(5): p. 369-75.
26. Kwon, O.H., et al., Rapid cell sheet detachment from poly(N-isopropylacrylamide)-grafted porous cell culture membranes. *J Biomed Mater Res*, 2000. 50(1): p. 82-9.
27. Tsuda, Y., et al., The use of patterned dual thermoresponsive surfaces for the collective recovery as co-cultured cell sheets. *Biomaterials*, 2005. 26(14): p. 1885-93.

28. Asakawa, N., et al., Pre-vascularization of in vitro three-dimensional tissues created by cell sheet engineering. *Biomaterials*, 2010. 31(14): p. 3903-9.
29. Elloumi Hannachi, I., et al., Fabrication of transferable micropatterned-co-cultured cell sheets with microcontact printing. *Biomaterials*, 2009. 30(29): p. 5427-32.
30. Tang, M.D., A.P. Golden, and J. Tien, Molding of three-dimensional microstructures of gels. *J Am Chem Soc*, 2003. 125(43): p. 12988-9.
31. Wood, D.K., et al., Single cell trapping and DNA damage analysis using microwell arrays. *Proc Natl Acad Sci U S A*, 2010. 107(22): p. 10008-13.
32. Sodunke, T.R., et al., Micropatterns of Matrigel for three-dimensional epithelial cultures. *Biomaterials*, 2007. 28(27): p. 4006-16.
33. Nelson, C.M., J.L. Inman, and M.J. Bissell, Three-dimensional lithographically defined organotypic tissue arrays for quantitative analysis of morphogenesis and neoplastic progression. *Nat Protoc*, 2008. 3(4): p. 674-8.
34. Kelm, J.M., et al., Design of custom-shaped vascularized tissues using microtissue spheroids as minimal building units. *Tissue Eng*, 2006. 12(8): p. 2151-60.
35. Rago, A.P., D.M. Dean, and J.R. Morgan, Controlling cell position in complex heterotypic 3D microtissues by tissue fusion. *Biotechnol Bioeng*, 2009. 102(4): p. 1231-41.
36. Nelson, C.M., et al., Tissue geometry determines sites of mammary branching morphogenesis in organotypic cultures. *Science*, 2006. 314(5797): p. 298-300.
37. Chappell, J.C., et al., Local guidance of emerging vessel sprouts requires soluble Flt-1. *Dev Cell*, 2009. 17(3): p. 377-86.
38. Jakab, K., et al., Engineering biological structures of prescribed shape using self-assembling multicellular systems. *Proc Natl Acad Sci U S A*, 2004. 101(9): p. 2864-9.
39. Martin, I., et al., Computer-based technique for cell aggregation analysis and cell aggregation in in vitro chondrogenesis. *Cytometry*, 1997. 28(2): p. 141-6.
40. Kelm, Microscale tissue engineering using gravity-enforced cell assembly. *Trends in biotechnology*, 2004.
41. Layer, P.G., et al., Of layers and spheres: the reaggregate approach in tissue engineering. *Trends Neurosci*, 2002. 25(3): p. 131-4.
42. Tsuda, Y., et al., Cellular control of tissue architectures using a three-dimensional tissue fabrication technique. *Biomaterials*, 2007. 28(33): p. 4939-4946.
43. Jakab, Three-dimensional tissue constructs built by bioprinting. *Biorheology*, 2006.
44. Wan, A.C., et al., Encapsulation of biologics in self-assembled fibers as biostructural units for tissue engineering. *J Biomed Mater Res A*, 2004. 71(4): p. 586-95.
45. Bruzewicz, D.A., A.P. McGuigan, and G.M. Whitesides, Fabrication of a modular tissue construct in a microfluidic chip. *Lab Chip*, 2008. 8(5): p. 663-71.
46. Du, Y., et al., Directed assembly of cell-laden microgels for fabrication of 3D tissue constructs. *Proc Natl Acad Sci U S A*, 2008. 105(28): p. 9522-7.
47. Du, Y., et al., Directed assembly of cell-laden microgels for fabrication of 3D tissue constructs. *Proc Natl Acad Sci U S A*, 2008.
48. Shimizu, T., et al., Long-term survival and growth of pulsatile myocardial tissue grafts engineered by the layering of cardiomyocyte sheets. *Tissue Eng*, 2006. 12(3): p. 499-507.
49. Shimizu, T., et al., Cell sheet engineering for myocardial tissue reconstruction. *Biomaterials*, 2003. 24(13): p. 2309-16.

Aim of this thesis

This thesis aims at recapitulating vascular morphogenesis *in vitro* for tissue regeneration. We speculate that the *in vitro* development of vascularized tissues will contribute to and improve the processes of tissue regeneration.

In **chapter 3**, we postulated that an engineered tissue including a vascular network *in vitro* could mimic and improve the process of endochondral bone regeneration.

In **chapter 4**, we develop a technique of sequential aggregation to form geometric, free-standing tissues using microfabricated templates.

In **chapter 5**, we postulated that microfabricated multicellular systems with the freedom to autonomously deform their shapes will recapitulate some mechanisms of vascular pattern formation.

More generally, we postulate that the *in vitro* development of engineered vasculatures can contribute to both therapeutic and fundamental studies in regenerative medicine through (i) the pre-vascularization of grafts and (ii) the microfabrication of tissues as integrated models to investigate basic principles of vascular morphogenesis, differentiation or maintenance.

Chapter 3

Engineering a vascularized bone callus using Sonic Hedgehog

N.C. Rivron¹, C. Raiss¹, J. Rouwkema², J. Liu¹, A. Nandakumar¹, R. Truckenmuller¹,
C. Sticht³, N. Gretz³, C.A. van Blitterswijk¹

- 1- Department of Tissue Regeneration, MIRA Institute for Biomedical Technology and Technical Medicine, 7500AE, University of Twente, Enschede, The Netherlands.
- 2- Department of Biomechanical Engineering, MIRA Institute for Biomedical Technology and Technical Medicine, 7500AE, University of Twente, Enschede, The Netherlands.
- 3- Medical Research Center, 68267, University Hospital Mannheim, Mannheim, Germany

Large bone defects regenerate via a highly vascularized callus formed by a combination of intramembranous and endochondral ossification. During regeneration, Hedgehog (Hh) proteins regulate both the vascularization and endochondral bone formation. Here, we used Sonic Hedgehog (Shh) to engineer a vascularized tissue, using human mesenchymal stem cells and human umbilical vein endothelial cells, which remodeled *in vivo* similarly to a regenerating callus, into a bone organ. We found *in vitro* that endogenous Hh activity regulates angiogenesis and that exogenous Shh further induced the development of vascular lumens, the regulation of their size, distribution and the expression of collagen type X. This *in vitro* development was essential to consistently and robustly improve bone osteoids formation upon implantation. The bone formed *in vivo* through a combination of external intramembranous and internal endochondral ossification and matured into a bone organ including bone, blood vessels and bone marrow cavities with apparent hematopoiesis. We demonstrate the *in vitro* development of a vascularized tissue which efficiently recapitulates, ectopically, some critical aspects of the regenerative process of endochondral bone repair.

Introduction

Large bone defects with inter-fragmentary spaces and mobility regenerate via a highly vascularized callus which stabilizes the fracture site and progressively remodels into a bone organ (1). The callus is composed of a shell, originating from the periosteum and bone fragments, formed by intramembranous ossification (IO) and a core vascularized fibrocartilagenous tissue, originating from the granulation tissue, which undergoes local endochondral ossification (EO) (1). The callus formation and remodeling is critically dependent on the hedgehog (Hh) signaling pathway (2) and on angiogenesis (3). Its vascularization is quantitatively important and persists until the normal medullar, periosteal and osseous blood supply is reestablished (4).

Efficient clinical applications of grafts for bone regeneration are currently limited by a lack of vascularization and subsequent necrosis (5). We previously demonstrated that a vasculature can be formed inside a graft, rapidly anastomose with the host vasculature upon implantation and improve graft perfusion and survival (6). Such engineered vasculature must rapidly develop and become perfused upon implantation to prevent capillaries regression (7), form functional, long-lasting blood vessels (6) and contribute to tissue formation.

Hedgehog (Hh) proteins act as archetypical morphogens regulating multiple processes during embryonic development. They remain relatively silent during homeostasis but are reactivated during adult tissue regeneration processes (2, 8-11). Among the 3 human Hh genes (Sonic, Indian and Desert Hedgehog), Sonic Hedgehog (Shh) is the most expressed, is a functional substitute to Indian Hedgehog (12) and has pleiotropic effects during both vascular and bone regeneration. Shh is essential for endothelial tube formation during vascular development (13), neovascularization upon adult disease or trauma (9, 11, 14-15) and wound healing (10, 16). Hh signaling is an essential regulator of cartilage (17), osteoblast development (18) and is reactivated during fracture healing in the regenerating callus (2, 19).

Here, we reasoned that Shh can be used to promote the *in vitro* development of a vascularized tissue for bone regeneration. We found that endogenous Hh activity regulates the assembly of primitive vascular structures in a co-culture of human mesenchymal stem cells (hMSC) and human umbilical vein endothelial cells (huvEC). *In vitro* stimulation using Shh induced the tubulogenesis of the engineered vasculature and regulated the production

of collagen type X, two critical regulators of EO. Upon implantation, the grafts showed improved perfusion and a robust increase in the formation of woven bone osteoids through both IO and EO. The woven bone remodeled into mature bone with apparent trabecular structure and bone-marrow cavities. Our data demonstrate the *in vitro* development of a vascularized tissue which recapitulates, *in vivo*, critical aspects of endochondral bone regeneration (1).

Results

Endogenous Hedgehog signaling regulates lumen formation in an engineered vasculature. The co-culture of hMSC (92%) and hucEC (8%) supports the formation of a primitive three dimensional vascular network which forms few lumens (as previously optimized (20-21)) (Fig. 1a). We previously demonstrated that this primitive network is not mature enough to become rapidly functional upon implantation (20-21). Consistent with a role of Hh during vascular tube formation (13), we found that, in this co-culture, a specific pharmacological inhibition of the canonical Hh signaling pathway using cyclopamine (5 μ M), a Smo modulator (22) (day 0 to 12), led to a significant 2-fold decrease in the formation of lumens ($p=0.002$, fig. 1b, c). A partial inhibition from day 4 to 12 was sufficient ($p=0.001$) but not from day 8 to 12 which suggests a later role for Hh in the development of lumens (Fig. 1c). A genetic screen (day 12) revealed that cyclopamine stimulation significantly regulated 303 genes among which 52 are directly linked to hedgehog signaling or angiogenesis (Figs. 1d, e, S1). Cyclopamine regulated two Hh inhibitors (GAS1 and RAB23, fig. 1d) and the two Hh target signaling pathways Wnt and Tgf (Fig. S1). Consistent with the current knowledge on vascular lumen formation (23), expression of laminins (alpha 1, 3, 4, 5, beta 2), integrins (alpha 2, 7, beta 5) were regulated (Fig. 1e) along with axon guidance molecules (ephrin alpha 1, beta 1, 2, semaphorins 3G, 5A, 6A, 6D) and cytoskeletal elements (Fig. S1). These results demonstrate a role for endogenous Hh activity, in this co-culture, regulating the formation of vascular lumens.

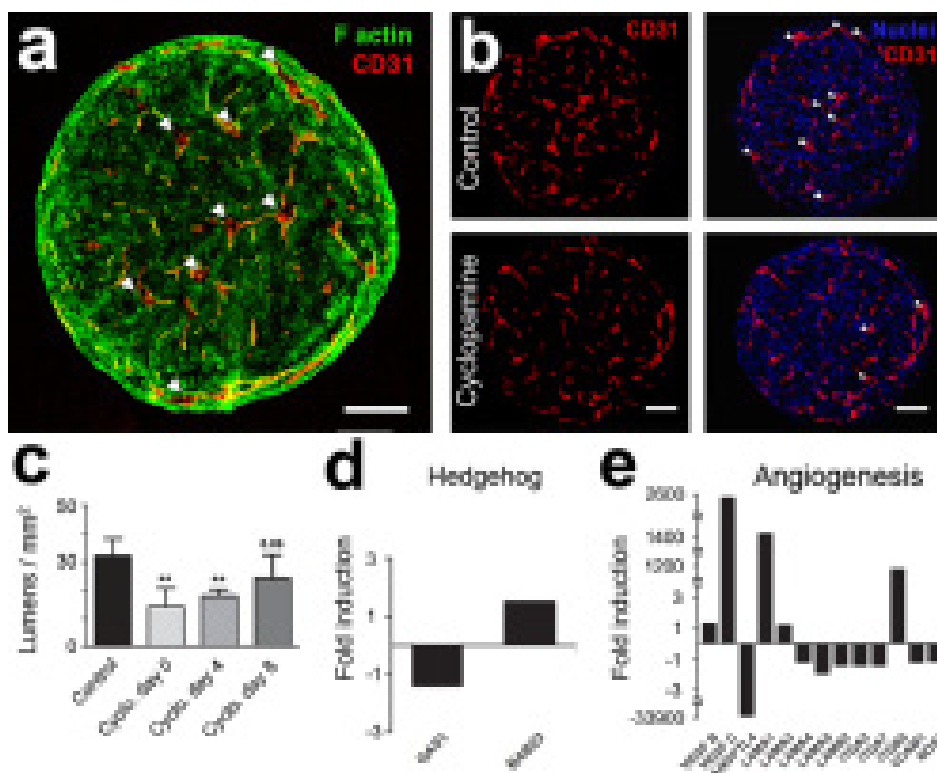


Figure 1: Endogenous Hh activity regulates the formation of lumens.

Multicellular aggregates of hMSC (92%) and huVEC (8%) assembled *in vitro* and formed a primitive 3D vascular network which formed few lumens (day 12, lumens are indicated by arrow heads) (a). A specific pharmacological inhibition of the Hh pathway from day 0 and from day 4 using cyclopamine (5 μ M) inhibited the process of lumen formation (b, c). n=4 sections x 4 samples. Genome-wide genetic screen on cyclopamine treated-multicellular aggregates revealed the up-regulation of two main inhibitors of the canonical Hh pathway (GAS1, RAB23) (d) and the regulation of angiogenic molecules (e). Laminins and integrins are of special relevance to lumen formation (e). All presented genes are significantly regulated compared to vehicle-treated multicellular aggregates. Errors bars are S.D. Scale bars are 100 μ m.

Stimulation of lumen formation by exogenous Sonic Hedgehog. We tested the potential for exogenous Shh administration to improve vascular lumen formation. A dose response in the physiological range (0.5 – 30 nM) (24) revealed a classical morphogen response inducing different effects at different concentrations (Fig. 2a). 0.5 nM Shh induced a significant decrease in the number of lumens (3.25 lumens/mm², 13 lumens/

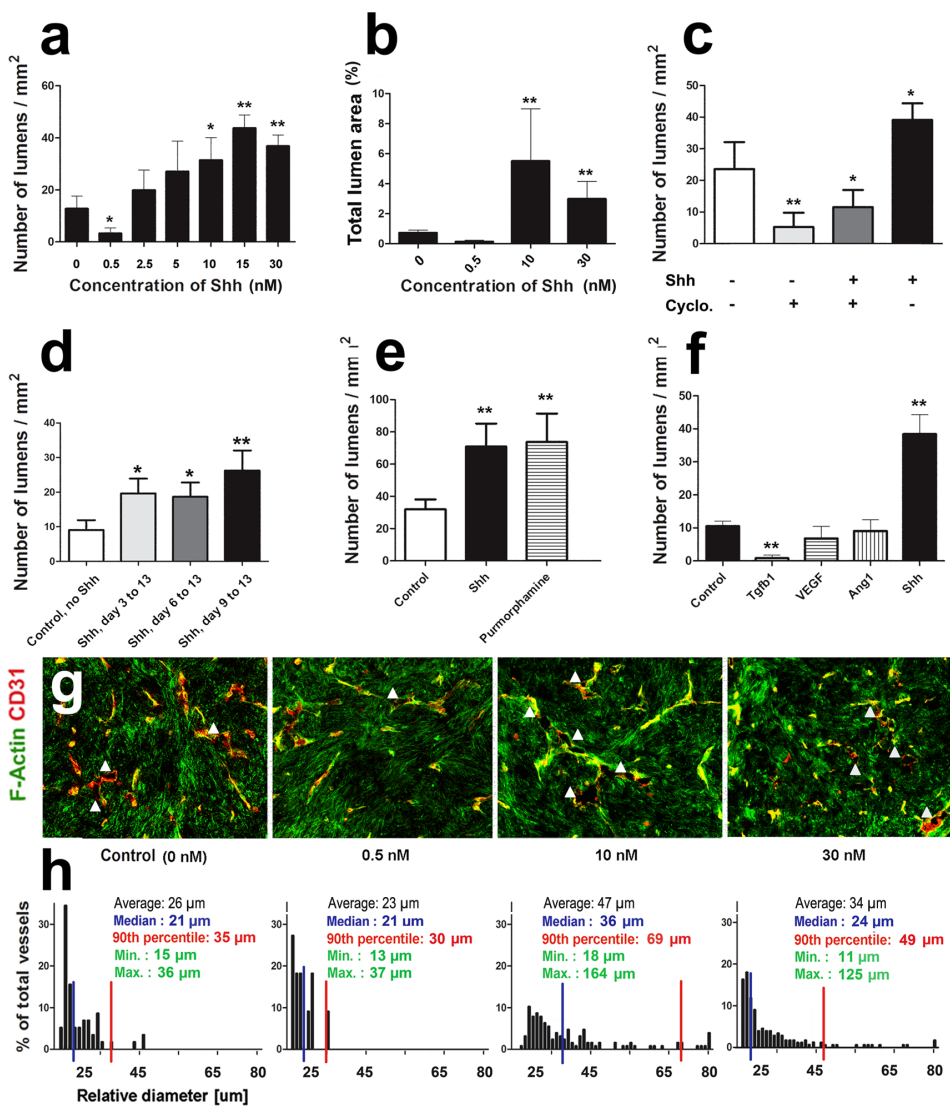
mm² in the control, $p < 0.05$) while concentrations above 15 nM induced a significant increase in lumen formation up to 3.4 fold (44 lumens/mm², $p < 0.01$) (Fig. 2a). This resulted in an opening of the vascular structures up to 5.5% of the tissue area (10 nM; 0.73% at 0 nM and 0.13% at 0.5 nM) (Fig. 2b). This effect was further inhibited by cyclopamine (10 μ M, $p < 0.05$) (Fig. 2c). A later stimulation (day 9 to 12) was sufficient and correlated with the previous observation suggesting a later development of lumens (Fig. 2d). The total vessel length area (total CD31+ area, mm²/mm²) was unchanged upon Shh stimulation (Fig. S2a). Furthermore, the proliferation of huVEC in serum-free medium on 2D plastic decreased upon Shh stimulation (Fig. S2b). Thus, the increase in vascular lumens formation is not caused by an increase in endothelial cell number and Shh drives the morphological process of lumen formation independently of cell proliferation. Similar regulation of lumen formation was found when using purmorphamine (day 8) (Fig. 2e), a known pharmacological activator of Hh pathway which shunts the Ptc receptor, thus directly unleashing Smo inhibition (25). We compared the effect induced by Shh to classical anti-angiogenic and angiogenic factors (Fig. 2f). Tgf β 1 (10 ng/ml), a known inhibitor of endothelial cell proliferation and motility (26), dramatically decreased lumen formation (tgf β 1: 0.8 lumen/mm², control: 10.5 lumens/mm², $p < 0.05$) whereas VEGF and Ang1 did not affect lumen formation. These findings correlate with previous observations that vascular networks formed in multicellular aggregates are not responsive to VEGF (27). The Shh-induced lumen formation was reproduced using a commercially available hMSC population (Lonza, group Ltd.) (Fig. S3). These results show that exogenous Shh acts as a typical morphogen modulating vascular lumen formation based on its concentration.

Modulation of the distribution profile of lumens by Sonic Hedgehog. To test the effect of exogenous Shh at the tissue level, we observed the distribution profiles of lumen areas and their relative diameters (Fig. 2g, h). The untreated group (control group) and the group treated with 0.5 nM Shh developed uniformly small lumens with an average diameter of 26 μ m (Table S1) and an exponential distribution reflecting the prevalence of capillaries (Control group: Median lumen diameter = 21 μ m, 90th percentile = 35 μ m, fig. 2g, h). In the group treated with 10 nM Shh, the distribution was normal, wider with an average lumen diameter of 47 μ m, significantly different from

the control group ($p < 0.0003$, table S1) and included lumens of middle and large diameter (10 nM Shh group: Median lumen diameter = 35 μm , 90th percentile = 69 μm). In contrast, the group treated with high Shh concentration (30nM) had an average lumen diameter of 34 μm , similar to the control ($p > 0.05$) with predominant small diameter lumens (30 nM Shh group: Median lumen diameter = 24 μm , 90th percentile = 49 μm , Table S1). Exogenous Shh can thus regulate the size and distribution profile of lumens based on its concentration. These results correlate with *in vivo* observations of Shh-induced neovascularization in ischemic hindlimb (8) and are consistent with the notion of morphogens.

Figure 2: Shh increases the in vitro maturation of the vascular network.

Multicellular aggregates treated with a physiological range of concentrations of Shh (0-30 nM) developed a typical morphogen response which either inhibited (0.5 nM) or upregulated (10-30 nM) the formation of vascular lumens (**a**). This resulted in a total lumen area covering up to 5.5% of the sections (**b**). The Shh-induced formation of lumens was further inhibited by cyclopamine (**c**). A later stimulation between day 9 and 12 was sufficient for lumen formation (**d**) and was replicated using purmorphamine, a known pharmacological regulator of the canonical Hh pathway (**e**). Classical direct effectors of the angiogenic cascade (tgf, VEGF, Ang1) did not up-regulate the formation of lumens (**f**). Different Shh concentrations affected the distribution of the size of the lumens with a wider, normal distribution observed at 10 nM (see also table S1). Vascular networks treated with 0, 0.5 and 30 nM Shh had an exponential distribution with prevalent small lumens (**g, h**). n=4 sections x 4 samples for each experiment. Errors bars are S.D.



Regulation of the expression of cartilage-related genes by Sonic Hedgehog.

Because Hh proteins can induce the differentiation of mesenchymal cells into osteo- chondro-progenitors (1, 28), we tested the possibility that Shh can regulate the expression of cartilage-related molecules. EO is mediated and characterized by the transient formation of a collagen type X matrix (29). Upon stimulation of the co-culture with Shh (10 nM, day 4 to 12), the analysis of mRNA levels using quantitative reverse transcriptase (RT)-PCR revealed that Shh significantly upregulated the expression of collagen type X by 21 fold ($p=0.04$, fig. 3a) while other chondrogenic markers remained statistically similar (Collagen I, collagen II, aggrecan, Sox9) (Fig. 3c). Cells produced Collagen type I and limited amount of collagen II as confirmed using Masson-Goldner and immunohistochemistry and no differences were observed upon stimulation with Shh (Fig. S4). Stimulation of the co-culture with Tgfb1 (10 ng/ml) led to the formation of a tissue with typical cartilage phenotype but to the concomitant disappearance of the CD31+ network (Fig. S4, S5). Comparison of Ptc expression at different time points showed an upregulation overtime, from day 4 to day 12. Shh treated samples only slightly upregulated Ptc (day 12, n.s.) which suggests either a transient stimulation by Shh or a partially Ptc independent activation.

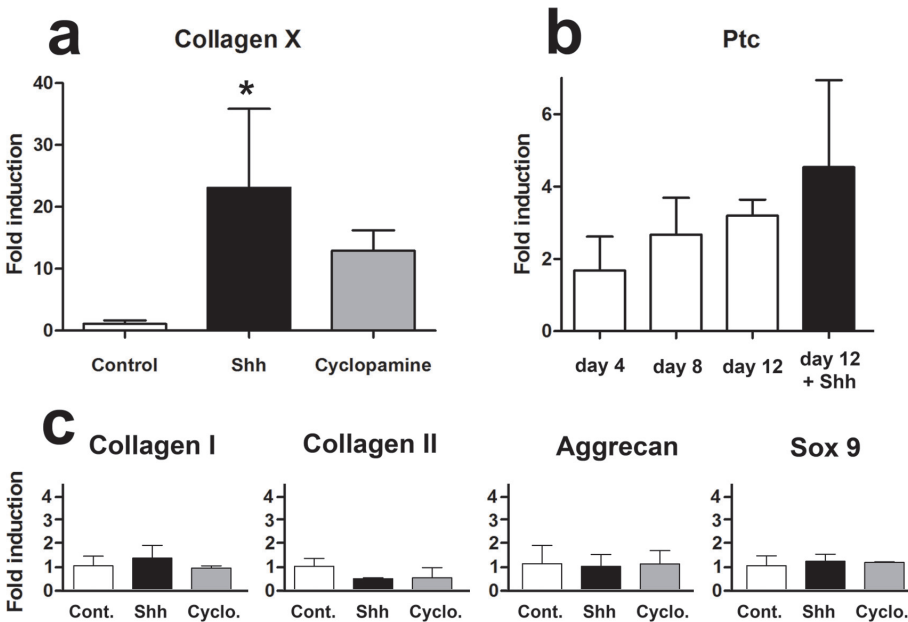


Figure 3: Shh regulates collagen type X expression

Quantitative RT-PCR for Collagen X, Ptc, collagen I, II, aggrecan, and sox 9 show that the co-culture of hMSC and huvEC responded to Shh by upregulating collagen type X (21 fold, $p = 0.04$) (a). Ptc showed a basal upregulation overtime and a non-significant upregulation by Shh (b). Expression of other cartilage related markers/molecules are not affected by Shh (c). $n=3$. Errors bars are S.D.

The engineered vasculature increases graft perfusion *in vivo*. To examine the potential of the engineered vasculature to improve bone formation, we implanted a tissue engineered graft composed of multicellular aggregates, osteoinductive ceramic granules (30) and collagen type I in the back of immunodeficient mice (31). 5 weeks after implantation, the human CD31+ lumens were perfused with erythrocytes (Fig. 4a) and with fluorescently labeled lectin injected in the tail vein of the mice (Fig. 4b). Upon quantification of the density of perfused lumens (number of perfused lumens / mm^2), vascularized grafts (huvEC, no Shh) were significantly more perfused compared to the control grafts with hMSC alone (no huvEC, no Shh) (23.6 and 9.5 perfused blood vessels/ mm^2 respectively, 5 cuts per sample, 5 mice, $p=0.014$, fig. 4c). Shh stimulation further increased the perfusion of vascularized grafts by 4-fold (41 perfused blood-vessels/ mm^2 , $p=0.02$, fig. 4c). The density of lumens formed *in vitro* strongly correlated with the density of lumens perfused *in vivo* (Fig. 2a and 4c). Thus, the stage of *in vitro* development of the vasculature regulates the subsequent perfusion and vascularization of the grafts. In vascularized grafts, blood vessels were derived for 60-63% from the mice (hCD31-) and for 37-40% from the implanted huvEC (hCD31+) (Fig. 4g). Part of the capillaries were found positive for the pericyte marker Smooth Muscle Actin (Fig. S7) which is consistent with the pericyte heterogeneity of the vascular bed (32).

The tissue engineered grafts recapitulate intramembranous and endochondral ossification. 5 weeks after implantation, grafts formed large osteoids of woven bone, mostly in the outer part of the grafts (Fig. 4g), characterized by a green Masson-Goldner staining and including red freshly secreted, unmineralized matrix (Fig. 4h). The woven bone was partly aligning the osteoinductive particles and could originate from the differentiation of implanted hMSC and from mesenchymal cells from adjacent, injured connective tissue (i.e. muscle) (1). A cartilage tissue with round cells in

large lacunae surrounded by proteoglycans (Alcian blue positive) aligned the inner part of the woven bone (Fig. 4d, e). Pericellular collagen type X extracellular matrix specific of hypertrophic cartilage formed in this cartilage (insert fig. 4e). The cartilage formation and hypertrophy in the inner bone-lining part of the graft was possibly driven by local hypoxia, IO in the outer part of the graft and enhanced by Shh stimulation. The cartilage was clearly aligning the newly formed bone osteoids as expected during the process of EO (Fig. 4j, k). During EO, the remodeling of the cartilage matrix necessitate its digestion by osteoclasts. We observed lines of Tartrate-resistant acid phosphatase (TRACP-) positive osteoclasts (bone-resorbing cells) at the bone-cartilage interface (insert fig. 4k). Osteoclasts were also observed around the osteoinductive particles as expected from local IO. Lamellar bone was observed using polarized light (Fig. S6). These results demonstrate that the grafts recapitulated both IO in the vicinity of the osteoinductive particles and EO on the inner part of the grafts with the intermediate production of hypertrophic cartilage, a collagen type X template, the digestion and remodeling of the cartilage by osteoclasts.

Shh-engineered vasculature increases the amount and consistency of bone formation *in vivo*. After 5 weeks *in vivo*, we quantified the amount of cartilage and osteoids formed. Interestingly, grafts stimulated with Shh (no huVEC) formed the largest amount of cartilage (25% of the graft area, fig. 4f). The amount of cartilage decreased in the vascularized grafts stimulated with Shh (with huVEC), an observation consistent with blood vessels regulating the remodeling from cartilage to bone tissue (1, 3) (Fig. 4f, 5 cuts per sample, 5 mice). We quantified the amount of osteoids (5 cuts per sample, 5 mice). Grafts without cells did not form any bone. The vascularized grafts stimulated with Shh was the only group which significantly increased osteoids formation as compared to the control grafts with hMSC alone (49.2% and 41.3% respectively, $p=0.0003$) (Fig. 4i, S7). The non-stimulated vascularized grafts (no Shh) formed 48.6% of osteoids with no statistical difference compared to the control ($p=0.2$, see table S2 for the detailed quantification and statistical analysis). The amount of osteoids were not statistically different between the 2 prevascularized groups ($p=0.8$), but the process was clearly more consistent with the more mature vasculature (with Shh) (Fig. 4i). The huVEC + Shh group always increased bone formation when the huVEC group inconsistently increased or decreased osteoids formation

(Fig. 4i). To assess for the robustness of the process, we quantified the consistency in the increase of osteoids as compared to hMSC alone (Fig. 4l). The variance in the increase for the Shh + huVEG group was significantly smaller from the Shh and the huVEG groups (F-Test, $p=0.0093$, $p=0.0026$ respectively). These results demonstrate that only Shh-stimulated vascularized grafts increase the robustness and the amount of woven bone. Less mature engineered vasculature fail to increase bone osteoids formation due to a lack of consistency.

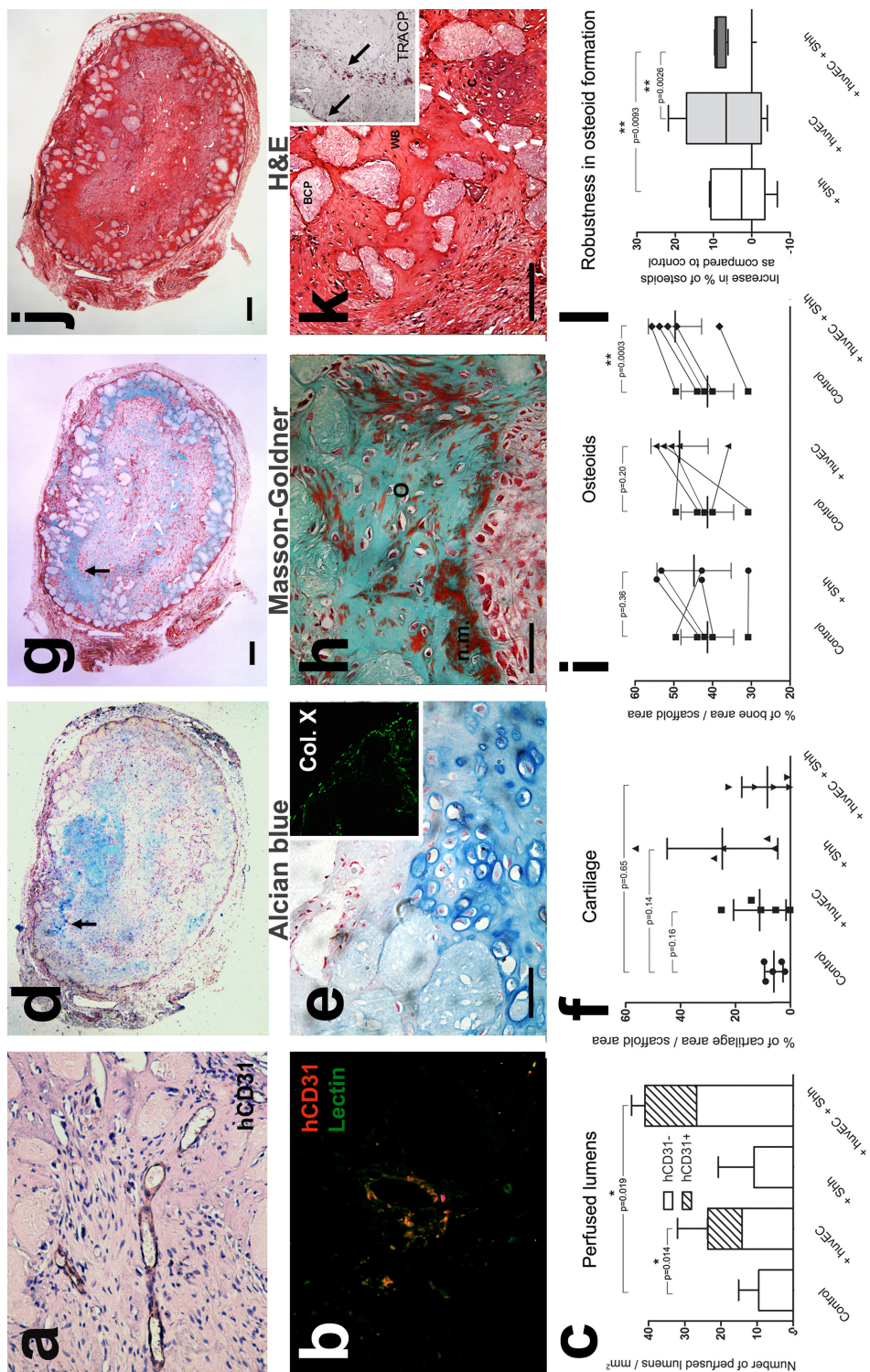


Figure 4: Shh engineered vasculature improves perfusion and osteoids formation *in vivo*.

Subcutaneous implantation of various grafts for 5 weeks in mice (n=5). The perfusion, cartilage and osteoids formation were assessed in grafts with hMSC, hMSC + huvEC, hMSC stimulated with Shh, and hMSC + huvEC stimulated with Shh. (a, b, c) Functional perfusion of the engineered vasculature. (a) Human CD31+ lumens included erythrocytes and (b) were perfused by fluorescently labeled lectin injected into the mouse tail vein. (c) In vitro development with Shh improved the perfusion of the vascularized grafts. In the vascularized grafts, 40-43% of the total perfused blood vessels were human (dashed area). (d-l) Skeletal tissue formation in the graft. (d-e) Grafts formed a cartilage tissue with typical morphology including round cells surrounded by Alcian blue positive extra cellular matrix. Part of the cartilage tissue was hypertrophic and included a collagen type X matrix (insert in e). (f) The non-vascularized grafts treated with Shh formed a large amount of cartilage tissue. (g, h) Large amounts of osteoids were formed at the periphery of the osteoinductive particles and at the border of the cartilage tissue (d, g, black arrows) as shown by green, Masson-Goldner staining. Osteoids included red, freshly secreted, non-mineralized matrix (h, o is osteoids, n.m. is non-mineralized matrix). (i) Only the vascularized grafts treated with Shh formed a significantly larger amount of osteoids as compared to the control. (j, k) Haematoxylin-Eosin staining showed cartilage aligning the newly formed woven bone (k, c is cartilage, wb is woven bone, dashed white line delimits cartilage-woven bone interface). Digestion and remodeling of the cartilage matrix was assessed by a TRACP-positive line of osteoclasts at the bone-cartilage interface (insert in k). (l) The robustness in osteoids formation was significantly higher in the vascularized grafts treated with Shh compared to the Shh and huvEC groups (F-Test, $p=0.0093$ and $p=0.0026$ respectively). (c, e, g) are sections from the same graft. (f, i) each dot represent one mouse implanted with the different conditions. Errors bars are S.D. . Scale bars are 500 μm (d, g, j) and 200 μm (e, h, k).

Maturation of the bone. After 7 weeks *in vivo*, a bone organ including bone, cartilage, fibrous tissue, bone-marrow and blood vessels was formed. Very little cartilage tissue (Fig. 5a, black arrow) was found and this cartilage was again aligning the newly formed bone (Fig. 5a, white arrow) suggesting the completion of the endochondral ossification of the cartilage. The bone was mineralized (stained for basic fuchsin), had bone lining surface osteoblasts synthesizing lamellar bone (Fig. 5b, black arrow) and blood vessels (Fig. 5b, white arrow). This ectopically formed bone was structurally similar to normal bones with regions of compact and interconnected trabecular structures (Fig. 5d). The process was robust (mature bone was observed in all grafts). We observed the formation of bone lacunae filled with bone marrow-like tissue including adipocytes- and

hematopoietic-like cells (Fig. 5c, black arrow, 4/6 mice), a process previously described as related to EO (33). This result demonstrate that the graft can recapitulate of some aspects of bone regeneration and contain elements which can initiate the formation of an ectopic bone marrow cavity. Large amount of mature bone was formed as compared to the current state-of-the-art in bone tissue engineering exploiting strictly intramembranous ossification. 24% (7 weeks) of the graft area was filled with mature bone as compared to <10% (6 weeks) for the current state-of-the-art in intramembranous bone tissue engineering strategy (34). We propose the combination of IO and EO as a powerful route to form clinically relevant amount of bone for the treatment of large defects.

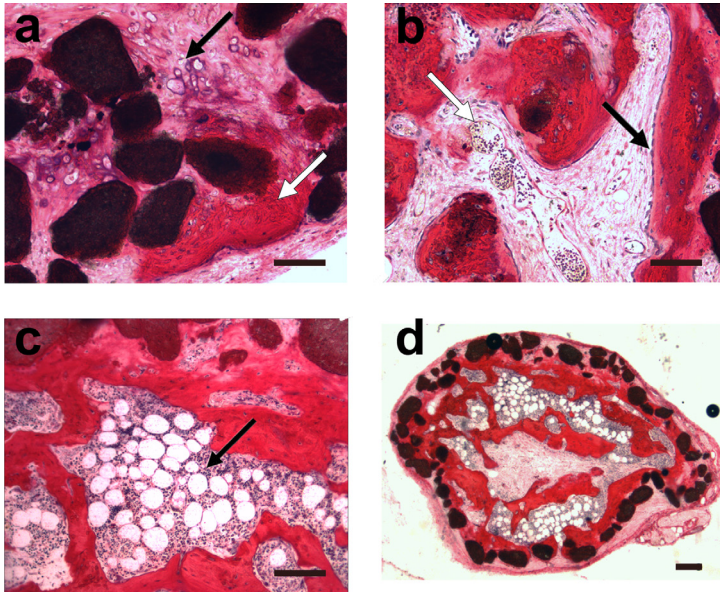


Figure 5: Graft maturation and formation of a bone organ

After 7 weeks of subcutaneous implantation, small amount of cartilage (a, black arrow) was aligning a large area of mature bone (a, white arrow and d). The mature bone stained for basic fuchsin, had bone lining cells (b, black arrow) and blood vessels (b, white arrow). Bone lacunae filled with bone marrow-like structures, adipocyte- and hematopoietic-like cells (c, black arrow) were observed. The amount of mature bone resulting from both intramembranous and endochondral ossification was large compared to current state-of-the-art in tissue engineering and clinically relevant to treat large defects (d). Errors bars are S.D. Scale bars are 200 μ m (a-c) and 500 μ m (d).

Discussion

Our results clearly show that Shh acts *in vitro* as a typical morphogen modulating vascular lumen formation and the distribution of lumens size. Based on its reactivation upon bone regeneration (1-2), we propose Shh may be critical to vascularize and regulate endochondral ossification during bone regeneration. The regulation of two Hh canonical inhibitors (GAS1 and RAB23) upon Hh inhibition using cyclopamine and the effect of the Smo activator Purmorphamine both argue for a regulation of lumen formation through the canonical pathway. Concomitantly, it was proposed that Hh proteins can directly regulate endothelial cell morphology through a non-canonical modulation of actin stress fibers (35) or indirectly modulate angiogenesis through the production of angiogenic molecules in interstitial mesenchymal cells (8). Besides angiogenesis, Hh proteins can regulate the differentiation of mesenchymal cells into osteo- chondro-progenitors (1, 28, 36). Here we show that Shh induces the production of collagen type X, a critical regulator of the process of EO. This combined regulation of angiogenesis and EO-specific extra-cellular matrix makes Shh a powerful factor for bone regeneration.

This study demonstrates the importance of *in vitro* vascular development to obtain lasting, functional blood vessels which can contribute to and improve tissue formation. The *in vitro* maturation of the vasculature (density of lumens formed, fig. 2a, b) strongly correlated with the *in vivo* perfusion of the grafts (density of lumen perfused, fig. 4c) which suggest that only mature vessels become functional upon implantation. Concomitantly, only the matured Shh-stimulated vasculature efficiently and robustly contributed to the increased formation of bone tissue. The necessity to implant a mature vasculature can result from the selection and maintenance of the perfused capillaries by the flow along with the rapid regression of the non-perfused capillaries (7, 37).

Besides its classical role of improving oxygen and nutrient exchanges, the vasculature plays a complex role during bone regeneration. Molecules including VEGF and Hypoxia-inducible factors (HIF1a, HIF2a), whose expressions are regulated by the vasculature, directly contribute to bone development. VEGF directly acts on chondrocytes survival (38) and osteoblast differentiation (39). HIF, a transcriptional regulator of VEGF, regulates chondrocytes hypertrophy and osteoblast differentiation independently of VEGF (40). Concomitantly, the vasculature recruits the osteoclasts, mesenchymal and hematopoietic progeni-

tors to the bone forming sites thus facilitating the replacement of the cartilage template into bone and seeding the hematopoietic niche (1). The coupling between the vasculature and bone development is critical to the process of endochondral ossification observed and is likely to critically contribute, along with graft survival, to the increased robustness and amount of bone formed.

Bone is one of the few organs that have the potential to fully repair itself, however, promoting the rapid regeneration of large defects is still challenging (41). Cell-based therapies currently exploit the intramembranous ossification process, rely on large amounts of filling biomaterial to stabilize the wound, are limited in size by the lack of vascularization (5, 42) and form limited amount of bone (41). Unlike previous studies demonstrating that implanted endothelial cells can contribute to angiogenesis (20, 43), this study demonstrates the *in vitro* development of a 3D vascularized tissue which contributes to formation of bone tissue through both intramembranous and endochondral ossification. This sequential formation of woven bone and lamellar bone through external intramembranous ossification and internal endochondral ossification is similar to the formation of the regenerating callus and can explain the large volume of bone formed as compared to seminal studies exploiting solely intramembranous ossification (34). The procedure is clinically relevant, using human adult stem cells in serum-free conditions. The use of alternative sources of endothelial cells was previously investigated by us (21). In further investigations, this protocol shall be tested in mechanically challenged orthotopic sites. We speculate this fibrocartilagenous graft will demonstrate improved compliance to stabilize the fracture, resist fracture deformation, motion and mechanical solicitations using less solid biomaterial.

We have demonstrated that vascularized tissue can develop *in vitro* using a morphogen naturally reactivated upon bone regeneration. The grafts recapitulated a combination of intramembranous and endochondral bone formation, a process similar to callus formation. The engineered vasculature contributed to and improved the graft perfusion and the formation of new bone tissue. Due to the pleiotropic role of the vasculature in the development and function of its surrounding tissue, we believe tissue formation in grafts will strongly benefit from the development of intrinsic vasculatures. These vascularized bone organs should be useful in many tissue engineering applications and also in more fundamental studies of bone organ development and regeneration.

Material and Methods

Bone marrow aspirates were obtained from donors with written informed consent and hMSCs were isolated and proliferated as described previously (34). Alternatively, hMSC were obtained from Lonza (Lonza, group Ltd.). Human umbilical vein endothelial cells (hUVECs) were purchased from Lonza (Lonza, group Ltd. Switzerland). Cells were routinely split at a 1:5 ratio and passage 3 or 4 were used for co-culture experiments. Co-culture of hMSC (92%) and hUVEC (8%) were previously optimized (20-21) and obtained by resuspending a total of 150,000 cells per spherical aggregate in 2 ml of differentiation medium and then seeded in a well of a Deepwell 96 well-plate (Nunc). The plate was then inverted to form a drop hanging from each well.

To evaluate the effect of prevascularization and Shh on ectopic bone formation by hMSCs and hUVEC, we used the following tissue engineering protocols. Spherical aggregates were pooled with osteoinductive biphasic calcium phosphate (BCP) ceramic granules of 100 μm prepared and sintered at 1,150°C as described previously (43) and incorporated in 300 μl of 2 mg/ml rat tail collagen (BD Bioscience). We implanted a total of 1,500,000 cells/graft. Grafts were subcutaneously implanted in 5 or 6 immune-deficient mice (Hsd-cpb:NMRI-nu; Harlan) for respectively 5 and 7 weeks. All experiments were approved by the local Animal Experimental Committee. The resulting tissues were evaluated through microarray, PCR and immunohistochemistry as described in the supplementary data. A detailed description of all material and methods is included in the SI Text.

Isolation and culture of hMSCs. Bone marrow aspirates were obtained from donors with written informed consent and hMSCs were isolated and proliferated as described previously (1). Alternatively, hMSC were obtained from Lonza ((Lonza, group Ltd.)(mentioned as “Cambrex” cells in the text). Briefly, aspirates were resuspended by using 20-gauge needles, plated at a density of 5×10^5 cells per square centimeter and cultured in hMSC proliferation medium containing α -MEM (Life Technologies), 10% FBS (Cambrex), 0.2 mM ascorbic acid (Asap; Life Technologies), 2mM L-glutamine (Life Technologies), 100 units/ml penicillin (Life Technologies), 10 $\mu\text{g/ml}$ streptomycin (Life Technologies), and 1 ng/ml basic FGF (Intrachemie). Cells were grown at 37°C in a humid atmosphere with 5% CO₂. Medium was refreshed twice a week, and cells were used for further subculturing

or cryopreservation. The co-culture differentiation medium was composed of Dulbecco's Modified Eagle's Medium, 10⁻⁷ M dexamethasone, 50 mg/ml ascorbate 2-phosphate, 40 mg/ml proline, 100 mg/ml pyruvate, and 50 mg/ml ITS 1 Premix (Becton–Dickinson, MA: 6.25 mg/ml insulin, 6.25 mg/ml transferrin, 6.25 ng/ml selenious acid, 1.25 mg/ml bovine serum albumin, 5.35 mg/ml linoleic acid).

Human umbilical vein endothelial cells. Human umbilical vein endothelial cells (hUVECs) were purchased from Lonza (Lonza, group Ltd. Switzerland). Cells were grown at 37°C in a humid atmosphere with 5% carbon dioxide (CO₂) in endothelial growth medium-2 (Lonza, group Ltd. Switzerland). Cells were routinely split at a 1:5 ratio. Cells from passage 3 or 4 were used for co-culture experiments.

Co-culture in a modified hanging drop system. Co-culture of hMSC (92%) and hUVEC (8%) were obtained by resuspending a total of 150,000 cells per spherical aggregate in 2 ml of differentiation medium and then seeded in a well of a Deepwell 96 well-plate (Nunc). A meniscus was formed by slightly overfilling the wells. The plate was then inverted to form a drop hanging from each well. Cells accumulated by gravity at the tip of the hanging drop (air-liquid interface) and cells formed a spherical aggregate within 48 hours. Plates were placed inverted, using plastic spacers, on a lid and cultured at 37°C in a humid atmosphere with 5% CO₂. Pictures of spherical aggregates were taken using an inverted microscope. Medium was changed every third day by inverting the plate and transferring the spherical aggregates to a new plate.

Gene Expression Analysis by RT-PCR and Microarray. The effect of cyclopamine on expression of Hedgehog, angiogenesis and axon guidance marker genes was analyzed by seeding a co-culture of 92% hMSCs and 8% hUVEC (150,000 cells in total) in Deepwell 96 well-plates (adapted hanging-drop method) supplemented or not in cyclopamine, for 12 days. Medium was changed every third day by transferring the spherical aggregate to a new plate. Three pools of 12 aggregates each were formed for each condition and RNA was isolated by using an RNeasy mini kit (Qiagen). To study the genome-wide effect of cyclopamine, gene expression profiling was performed using arrays of HumanU133_2-type from

Affymetrix. Biotinylated antisense cRNA was then prepared according to the Affymetrix standard labelling protocol. Afterwards, the hybridization on the chip was performed on a GeneChip Hybridization oven 640, then dyed in the GeneChip Fluidics Station 450 and thereafter scanned with a GeneChip Scanner 3000. All of the equipment used were from the Affymetrix-Company (Affymetrix, High Wycombe, UK). A Custom CDF Version 12 with Entrez based gene definitions was used to annotate the arrays (2). The raw fluorescence intensity values were normalized applying quantile normalization. Differential gene expression was analysed based on ANOVA using a commercial software package SAS JMP7 Genomics, version 4, from SAS (SAS Institute, Cary, NC, USA). A false positive rate of $\alpha=0.05$ with FDR correction was taken as the level of significance. Represented genes in Fig. 1d, e are all significantly regulated ($n=3$) and the values are log2-converted fold-changes.

The effect of Shh on gene expression was analyzed by seeding a co-culture of 92% hMSCs and 8% huVEC (150,000 cells in total) in Deepwell 96 well-plates supplemented or not with Sonic Hedgehog, from day 4 to 12. Medium was changed every third day by transferring the spherical aggregate to a new plate. RNA was isolated by using an RNeasy mini kit (Qiagen), and qPCR was performed by using SYBR green (Invitrogen) and established primers (SABioscience) on a MyiQ2 detection system (Biorad). Data were analyzed using the Biorad software, using the fit point method by setting the noise band to the exponential phase of the reaction to exclude background fluorescence. Expression of chondrogenic marker genes was calculated relative to GAPDH levels by the comparative CT method.

Histological analysis. After harvesting, spherical aggregates were frozen in Cryomatrix at -60°C . Sections ($7\text{ }\mu\text{m}$) were cut with a cryotome. Sections were fixed in cold acetone for 5 min and air-dried, rehydrated for 10 min, after which they were incubated for 30 min with 10% FBS in PBS to block nonspecific background staining. Sections were incubated with mouse anti-human CD31 (Dako) (dilution 1/20) or Phalloidin-Alexa fluor 488 conjugated antibody (Invitrogen) (dilution 1/30) for 1 h. Sections were washed in PBS and subsequently incubated with the secondary antibody (Alexa Fluor 494 antibody, Invitrogen). Samples were counterstained with Dapi (Sigma). Tissue explants (5 weeks) were fixed in paraformaldehyde, decalcified overnight in 0.1mM EDTA and embedded in paraffin. Sections ($6\text{ }\mu\text{m}$) were cut with a microtome. Masson-Goldner (Merck Chemicals) and TRACP (Takara)

staining kits were used according to the manufacturer's instructions. CD31 (dilution 1/80) and SMA (1/80) (Dako) were incubated for 1 hour and subsequently incubated with the secondary antibody (horseradish peroxidase conjugated goat-anti-mouse immunoglobulin antibody, Dako) for 45 min. Slides were developed with diaminobenzidine (Dako) as substrate and were weakly counterstained with hematoxylin (Sigma). Tissue explants (7 weeks) were directly embedded in methyl methacrylate (Sigma) for sectioning. Approximately 10 μm -thick, undecalcified sections were processed on a histological diamond saw (Leica saw microtome cutting system). The sections were stained with basic fuchsin and methylene blue to visualize new bone formation. The newly formed mineralized bone stains red with basic fuchsin, all other cellular tissues stain light blue with methylene blue, and the ceramic material remains black and unstained by both the dyes. Histological sections were qualitatively analyzed using a light microscope (Leica), and quantitative histomorphometry was performed using high-resolution digital photographs (300 dpi) of the middle section out of three total sections from each implant. Before histomorphometrical analysis, bone was pseudocolored using Photoshop CS2 (Adobe Systems) and normalized to the total surface area of the implant.

In Vivo Evaluation Studies. To evaluate the effect of prevascularization and Shh on ectopic bone formation by hMSCs and huVEC, we used the following tissue engineering protocols. Spherical aggregates were pooled with biphasic calcium phosphate (BCP) ceramic granules of 100 μm prepared as described previously (3) and incorporated in 300 μl of 2 mg/ml rat tail collagen (BD Bioscience). We implanted a total of 1,500,000 cells/implant. Implant were subcutaneously implanted in immune-deficient mice for 5 or 7 weeks. In the two in vivo experiment, 5 and 6 nude male mice (Hsd-cpb:NMRI-nu; Harlan) were respectively used. Animals were anesthetized by inhalation of isoflurane. Four s.c. pockets were made, and each pocket was supplied with one implant (all 4 conditions in each mouse). The incisions were closed with avicryl 5-0 suture and the implants were left for 5 or 7 weeks. All experiments were approved by the local Animal Experimental Committee. After 5-7 weeks, the mice were euthanized by using CO₂ and samples were explanted, fixed in paraformaldehyde (Merck) in 0.14M cacodylic acid (Fluka) buffer (pH 7.3), dehydrated, and either decalcified and embedded in paraffin (5 weeks) or directly embedded in methyl

methacrylate (Sigma) for sectioning. Histological staining and analysis was performed as described above.

Statistical analysis. Statistical analysis for in vitro experiments were performed (exception made for RT-PCR and microarray, see above) using 4 biological samples and 4 cuts per biological sample. Differences between conditions were measured using a 2 tailed-distribution, two-sample equal variance Student's t-test and were considered as significantly different for a p value below 0.05 (*) or 0.01 (**). Statistical analysis for in vivo experiments were performed using 6 mice and 3 cuts per mouse. Since each mouse was implanted with the 4 different conditions, differences between conditions were measured using a 2 tailed-distribution, paired Student's t-Test and were considered as significantly different for a p value below 0.05 (*).

Technical references from the material and methods

1. Siddappa R, et al. (2008) cAMP/PKA pathway activation in human mesenchymal stem cells in vitro results in robust bone formation in vivo. (Translated from eng) *Proc Natl Acad Sci U S A* 105(20):7281-7286 (in eng).
2. Sandberg R & Larsson O (2007) Improved precision and accuracy for microarrays using updated probe set definitions. (Translated from eng) *BMC Bioinformatics* 8:48 (in eng).
3. Yuan H, van Blitterswijk CA, de Groot K, & de Bruijn JD (2006) Cross-species comparison of ectopic bone formation in biphasic calcium phosphate (BCP) and hydroxyapatite (HA) scaffolds. (Translated from eng) *Tissue Eng* 12(6):1607-1615 (in eng).

Supplementary Information

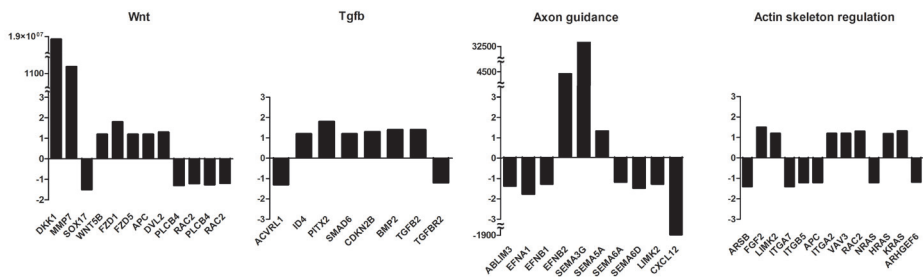


Fig. S1: Regulation of specific pathways upon treatment with cyclopamine. Upon treatment with cyclopamine (5 μ M), the two Hh target signaling pathways, Tgb and Wnt are regulated. Actin skeleton elements which are crucial for adequate lumen formation and axon guidance molecules which are crucial for the of tip endothelial cells guidance are also regulated. All presented genes are significantly regulated compared to vehicle-treated multicellular aggregates.

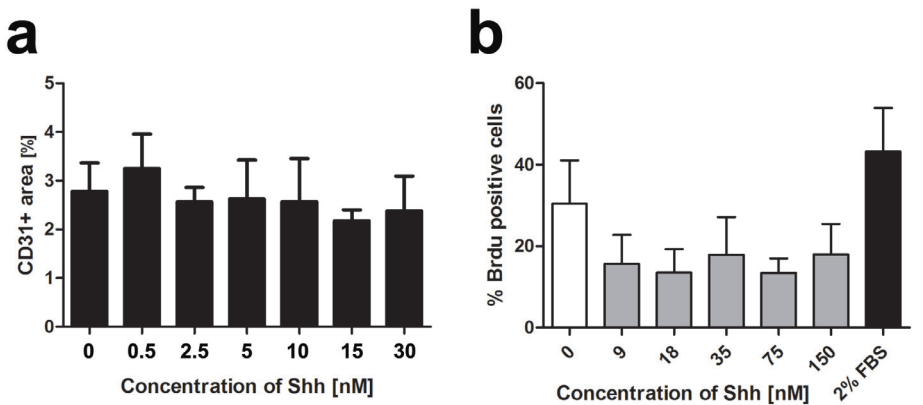


Fig. S2: Effect of Shh on proliferation of endothelial cells. Upon treatment with Shh, the total CD31+ area in the multicellular aggregates were measured as a percentage of the total section area (4 samples, 4 sections per sample). The total CD31+ area was found statistically similar ($p>0.05$) (a). Stimulation of huvEC in serum-free medium, on plastic led to a decrease in proliferation. All concentrations of Shh led to a significant decrease in huvEC concentration compare to the control (0 nM). Error bars are standard deviations between 4 samples.

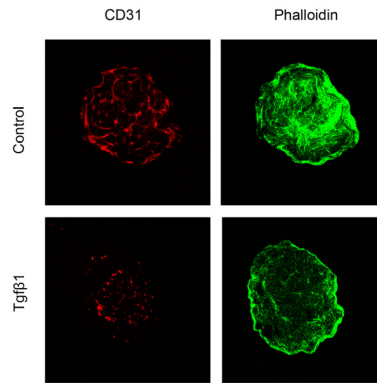


Fig. S5: Tgf β 1 prevent the development of a CD31+ network. The stimulation of the co-culture with Tgf β 1 prevented the formation of the CD31+ vascular network as compared to the control (medium without Tgf β 1) thus preventing the use of this cartilage matrix initiator for prevascularized bone engineering.

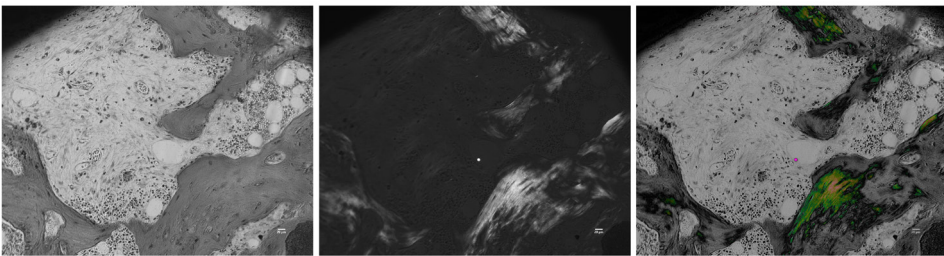


Fig. S6: Lamellar bone. The newly formed bone tissue consisted of lamellar bone as revealed using polarized light. Scale bars are 20 μ m.

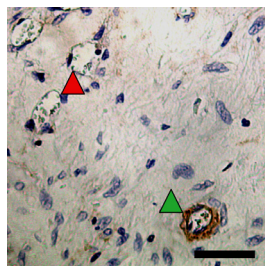


Fig. S7: Pericyte coverage. The blood vessels were found partly Smooth muscle actin (SMA) positive after 5 weeks of implantation which is consistent with the heterogeneity of the capillary bed. The green triangle shows a SMA+ blood vessel when the red triangle shows SMA- blood vessels. Scale bar is 50 μ m.

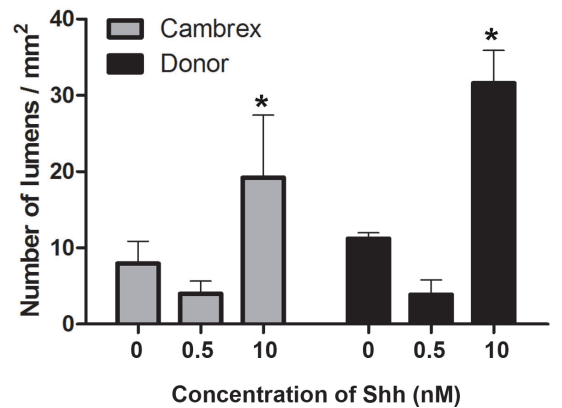


Fig. S3: Shh induced lumen formation for 2 types of hMSC. Protocols for the isolation of hMSC are heterogeneous and can lead to different populations with specific characteristics. Here we show the response of hMSC commercially available (Cambrex, Lonza Ltd) and isolated by our laboratory according to previously described procedures (1). The response to 0.5 and 10 nM was found similar, as previously described (fig. 2a)

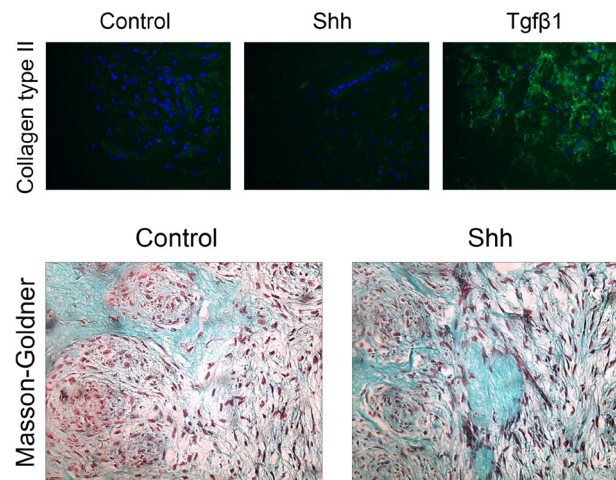


Fig. S4: Collagen type II and goldner staining in the co-culture. Immunofluorescent staining for collagen type II and Masson-Goldner staining reveal a limited expression of the collagen type II in the control co-culture and in the Shh stimulated co-culture as compared to co-culture stimulated with Tgfβ1. Masson-Goldner reveals the production of a collagen type I matrix.

Concentration of Shh (nM)	Lumen area (μm^2) Median	Lumen area (μm^2) 90 th percentile	Lumen area (μm^2) Average	Relative diameter (μm)	T-Test on lumen area with respect to 0 nM
0	336	988	544	26	-
0.5	331	697	411	23	0.31
10	987	3714	1756	47	0.00025
30	454	1856	887	34	0.052

Table S1: Shh modulates the distribution profile of the lumens

Different Shh concentrations induced different lumen profiles as described in fig. 2g, h). Here we present the complete results and statistical analysis. The Student T-test was performed on the lumen area of each group with respect to the control group (0 nM) using a two tail distribution and unpaired groups. Relative diameters are calculated based on the area of the lumen as followed. Relative diameter (μm) = $\sqrt{(\text{lumen area}/\pi)}$.

Osteoids formation (% of graft area)	M1	M2	M3	M4	M5	Average	SD	T-Test
hMSC	40.1	42.2	44	49.5	30.9	41.3	6.8	-
hMSC + huvEC	36	54.6	50.7	48.6	52.7	48.6	7.3	0.1980
hMSC + Shh	42.8	53.2	54.4	42.8	30.8	44.8	9.6	0.3572
hMSC + huvEC + Shh	49.2	51.6	53.7	55.7	38.2	49.2	6.9	0.0003

Table S2: Quantification and statistical differences of the different implants after 5 weeks *in vivo*.

The average percentage of osteoids was measured using 5 different cuts for each implant and is presented in this table. 5 mice were implanted, each with the 4 different types of implants: hMSC alone, hMSC and huvEC co-culture, hMSC stimulated with Shh (10 nM), hMSC and huvEC co-culture stimulated with Shh (10 nM). The Student T-test was performed as compared to the control group with hMSC alone using a two tail distribution and paired groups. SD is the standard deviation.

1. Shapiro F (2008) Bone development and its relation to fracture repair. The role of mesenchymal osteoblasts and surface osteoblasts. (Translated from eng) *Eur Cell Mater* 15:53-76 (in eng).
2. Murakami S & Noda M (2000) Expression of Indian hedgehog during fracture healing in adult rat femora. (Translated from eng) *Calcif Tissue Int* 66(4):272-276 (in eng).
3. Hausman MR, Schaffler MB, & Majeska RJ (2001) Prevention of fracture healing in rats by an inhibitor of angiogenesis. (Translated from eng) *Bone* 29(6):560-564 (in eng).
4. Glowacki J (1998) Angiogenesis in fracture repair. (Translated from eng) *Clin Orthop Relat Res* (355 Suppl):S82-89 (in eng).
5. Rivron NC, Liu JJ, Rouwkema J, de Boer J, & van Blitterswijk CA (2008) Engineering vascularised tissues in vitro. (Translated from eng) *Eur Cell Mater* 15:27-40 (in eng).
6. Levenberg S, *et al.* (2005) Engineering vascularized skeletal muscle tissue. (Translated from eng) *Nat Biotechnol* 23(7):879-884 (in eng).
7. Koike N, *et al.* (2004) Tissue engineering: creation of long-lasting blood vessels. (Translated from eng) *Nature* 428(6979):138-139 (in eng).
8. Pola R, *et al.* (2001) The morphogen Sonic hedgehog is an indirect angiogenic agent upregulating two families of angiogenic growth factors. (Translated from eng) *Nat Med* 7(6):706-711 (in eng).
9. Pola R, *et al.* (2003) Postnatal recapitulation of embryonic hedgehog pathway in response to skeletal muscle ischemia. (Translated from eng) *Circulation* 108(4):479-485 (in eng).
10. Le H, *et al.* (2008) Hedgehog signaling is essential for normal wound healing. (Translated from eng) *Wound Repair Regen* 16(6):768-773 (in eng).
11. Kusano KF, *et al.* (2005) Sonic hedgehog myocardial gene therapy: tissue repair through transient reconstitution of embryonic signaling. (Translated from eng) *Nat Med* 11(11):1197-1204 (in eng).
12. Mak KK, Kronenberg HM, Chuang PT, Mackem S, & Yang Y (2008) Indian hedgehog signals independently of PTHrP to promote chondrocyte hypertrophy. (Translated from eng) *Development* 135(11):1947-1956 (in eng).
13. Vokes SA, *et al.* (2004) Hedgehog signaling is essential for endothelial tube formation during vasculogenesis. (Translated from eng) *Development* 131(17):4371-4380 (in eng).
14. Straface G, *et al.* (2008) Sonic Hedgehog Regulates Angiogenesis and Myogenesis During Post-Natal Skeletal Muscle Regeneration. (Translated from Eng) *J Cell Mol Med* (in Eng).
15. Kusano KF, *et al.* (2004) Sonic hedgehog induces arteriogenesis in diabetic vasa nervorum and restores function in diabetic neuropathy. (Translated from eng) *Arterioscler Thromb Vasc Biol* 24(11):2102-2107 (in eng).
16. Asai J, *et al.* (2006) Topical sonic hedgehog gene therapy accelerates wound healing in diabetes by enhancing endothelial progenitor cell-mediated microvascular remodeling. (Translated from eng) *Circulation* 113(20):2413-2424 (in eng).
17. Karp SJ, *et al.* (2000) Indian hedgehog coordinates endochondral bone growth and morphogenesis via parathyroid hormone related-protein-dependent and -independent pathways. (Translated from eng) *Development* 127(3):543-548 (in eng).
18. Long F, *et al.* (2004) Ihh signaling is directly required for the osteoblast lineage in the endochondral skeleton. (Translated from eng) *Development* 131(6):1309-1318 (in eng).
19. Emans PJ, *et al.* (2007) A novel in vivo model to study endochondral bone formation; HIF-1alpha activation and BMP expression. (Translated from eng) *Bone* 40(2):409-418 (in eng).
20. Rouwkema J, de Boer J, & Van Blitterswijk CA (2006) Endothelial cells assemble into a 3-dimensional prevascular network in a bone tissue engineering construct. (Translated from eng) *Tissue Eng* 12(9):2685-2693 (in eng).
21. Rouwkema J, Westerweel PE, de Boer J, Verhaar MC, & van Blitterswijk CA (2009) The use of endothelial progenitor cells for prevascularized bone tissue engineering. (Translated from eng) *Tissue Eng Part A* 15(8):2015-2027 (in eng).
22. Taipale J, *et al.* (2000) Effects of oncogenic mutations in Smoothened and Patched can be reversed by cyclopamine. (Translated from eng) *Nature* 406(6799):1005-1009 (in eng).
23. Iruela-Arispe ML & Davis GE (2009) Cellular and molecular mechanisms of vascular lumen formation. (Translated from eng) *Dev Cell* 16(2):222-231 (in eng).
24. Dessaud E, *et al.* (2007) Interpretation of the sonic hedgehog morphogen gradient by a temporal

- adaptation mechanism. (Translated from eng) *Nature* 450(7170):717-720 (in eng).
25. Sinha S & Chen JK (2006) Purmorphamine activates the Hedgehog pathway by targeting Smoothened. (Translated from eng) *Nat Chem Biol* 2(1):29-30 (in eng).
 26. Muller G, Behrens J, Nussbaumer U, Bohlen P, & Birchmeier W (1987) Inhibitory action of transforming growth factor beta on endothelial cells. (Translated from eng) *Proc Natl Acad Sci U S A* 84(16):5600-5604 (in eng).
 27. Korff T, Kimmina S, Martiny-Baron G, & Augustin HG (2001) Blood vessel maturation in a 3-dimensional spheroidal coculture model: direct contact with smooth muscle cells regulates endothelial cell quiescence and abrogates VEGF responsiveness. (Translated from eng) *FASEB J* 15(2):447-457 (in eng).
 28. St-Jacques B, Hammerschmidt M, & McMahon AP (1999) Indian hedgehog signaling regulates proliferation and differentiation of chondrocytes and is essential for bone formation. (Translated from eng) *Genes Dev* 13(16):2072-2086 (in eng).
 29. Shen G (2005) The role of type X collagen in facilitating and regulating endochondral ossification of articular cartilage. (Translated from eng) *Orthod Craniofac Res* 8(1):11-17 (in eng).
 30. Yuan H, *et al.* (1998) Osteoinduction by calcium phosphate biomaterials. (Translated from eng) *J Mater Sci Mater Med* 9(12):723-726 (in eng).
 31. Kratchmarova I, Blagoev B, Haack-Sorensen M, Kassem M, & Mann M (2005) Mechanism of divergent growth factor effects in mesenchymal stem cell differentiation. (Translated from eng) *Science* 308(5727):1472-1477 (in eng).
 32. Armulik A, Abramsson A, & Betsholtz C (2005) Endothelial/pericyte interactions. (Translated from eng) *Circ Res* 97(6):512-523 (in eng).
 33. Chan CK, *et al.* (2009) Endochondral ossification is required for haematopoietic stem-cell niche formation. (Translated from eng) *Nature* 457(7228):490-494 (in eng).
 34. Siddappa R, *et al.* (2008) cAMP/PKA pathway activation in human mesenchymal stem cells in vitro results in robust bone formation in vivo. (Translated from eng) *Proc Natl Acad Sci U S A* 105(20):7281-7286 (in eng).
 35. Chinchilla P, Xiao L, Kazanietz MG, Natalia AN, & Riobo GM (2010) Hedgehog proteins activate pro-angiogenic responses in endothelial cells through non-canonical signaling pathways. (Translated from eng) *Cell Cycle* 9(3):570-579 (in eng).
 36. Dohle E, *et al.* (2010) Sonic hedgehog promotes angiogenesis and osteogenesis in a coculture system consisting of primary osteoblasts and outgrowth endothelial cells. (Translated from eng) *Tissue Eng Part A* 16(4):1235-1237 (in eng).
 37. Jones EA, le Noble F, & Eichmann A (2006) What determines blood vessel structure? Genetic prespecification vs. hemodynamics. (Translated from eng) *Physiology (Bethesda)* 21:388-395 (in eng).
 38. Zelzer E, *et al.* (2004) VEGFA is necessary for chondrocyte survival during bone development. (Translated from eng) *Development* 131(9):2161-2171 (in eng).
 39. Villars F, *et al.* (2002) Effect of HUVEC on human osteoprogenitor cell differentiation needs heterotypic gap junction communication. (Translated from eng) *Am J Physiol Cell Physiol* 282(4):C775-785 (in eng).
 40. Wan C, *et al.* (2010) Role of HIF-1alpha in skeletal development. (Translated from eng) *Ann N Y Acad Sci* 1192(1):322-326 (in eng).
 41. Meijer GJ, de Bruijn JD, Koole R, & van Blitterswijk CA (2007) Cell-based bone tissue engineering. (Translated from eng) *PLoS Med* 4(2):e9 (in eng).
 42. Rouwkema J, Rivron NC, & van Blitterswijk CA (2008) Vascularization in tissue engineering. (Translated from eng) *Trends Biotechnol* 26(8):434-441 (in eng).
 43. Tsigkou O, *et al.* (2010) Engineered vascularized bone grafts. (Translated from eng) *Proc Natl Acad Sci U S A* 107(8):3311-3316 (in eng).

Chapter 4

Micofabrication of self-remodeling tissues

N.C. Rivron¹, E.J. Vrij¹, J. Rouwkema², R. Truckenmüller^{1,3}, A. Barradas¹, S. , Le Gac³, J. de Boer¹, A. van den Berg³, C.A. van Blitterswijk¹

- 1- Department of Tissue Regeneration, MIRA -Institute for Biomedical Technology and Technical Medicine- University of Twente, Enschede , The Netherlands.
- 2- Department of Biomechanical Engineering, MIRA -Institute for Biomedical Technology and Technical Medicine- University of Twente, Enschede, The Netherlands.
- 3- BIOS - the Lab-on-a-Chip Group, MESA+ -Institute for Nanotechnology- University of Twente, Enschede, The Netherlands.

In vitro-generated tissues hold promises as models and as surgical implants. Here, we show the microfabrication of geometric, millimeter-scale tissues prone to self-modeling and self-organization. Tissues were built by sequential template-guided assembly of cells into microscale clusters and millimeter-scale tissues. The free-standing tissues compacted and deformed according to their initial outer and inner geometries. When formed by human mesenchymal stem cells and human umbilical vein endothelial cells, tissues remodeled either freely or in interaction with the template and reproducibly formed internal gradients of cellular compaction and tissue-scale vascular networks. Finally, these millimeter-scale tissue units can be combined and spontaneously fuse into centimeter-scale implants of clinical relevance. Self-organization is a simple and powerful engineering process to generate self-constructing tissues with wide applications in regenerative medicine.

Introduction

In vitro-generated tissues have an important potential as models for tissue development (1) and as implants for tissue replacement (2-4). The classical approach to fabricate tissues relies on a biomaterial scaffold mimicking the architecture/function of the natural tissue and a cell population providing a biological interface. This proved successful for orthopedic implants using solid scaffolds (3-4) or urologic implants using soft membranes (2). However this approach is mainly dictated by the properties of the scaffold and limits the spatial organization of cells into 3D tissue structures. As an alternative, scaffold-free implants as cell sheets (5) or microtissues (6) have an important potential of integration, survival and organization. Here, we developed microfabricated platforms to sequentially aggregate, assemble and culture arrays of 3D scaffold-free tissues.

A major challenge in tissue engineering lies in finding simple processes to form complex tissues. Typically, engineered tissues are achieved by assembling cells in precise geometries reminiscent of the original tissue structures (7) and organization is further promoted through external stimulation (8-9). Such approach requires complex and expensive machines. Here, we present a simple, accessible approach to form tissues through stochastic assembly and directed self-organization. Self-organization refers to a range of decentralized pattern-formation processes without external guidance or blueprint (10). We show strategies to direct the autonomous tissue deformation by modulating inner and outer geometries and we demonstrate their subsequent heterogeneous regionalization, organization and differentiation.

Upon assembly, tissues spontaneously fused into tissues of clinically relevant size (centimeter-scale). This approach is simple, versatile and can be used routinely at low cost. It allows for the parallel culture of hundreds of autonomously organizing tissues of high cellular density, in an array format. This represent a first step toward self-constructing tissues.

Results

Technical overall approach

We reasoned that scaffold-free, free-standing tissues would provide maximum degrees of freedom for remodeling and organization. We used a two-steps microfabrication approach to assemble cells into millimeter-scale tissues with different geometric shapes (bottom-up approach). First, we fabricated agarose templates termed MicroWell Arrays (MWAs). We used MWAs to assemble cells into microscale clusters that were then used as building blocks for tissues fabrication. In a second step, the same approach was used to assemble microscale cell clusters into millimeter-scale tissues in Shaped Well Arrays (SWAs). Cell clusters spontaneously fused into continuous, free-standing tissues adopting the geometry of the well. These millimeter-scale tissue units were further assembled and spontaneously fused into centimeter-scale, tissues of clinically relevant size.

Formation of microscale cell clusters

Agarose templates were built by replica molding from a silicone or SU-8 master via an intermediate Polydimethylsiloxane (PDMS) negative replica as a simple, efficient and conventional technique to replicate microscale structures (11). Here, PDMS templates were used to routinely cast inexpensive, non-adherent agarose well arrays for tissue culture (pink templates, figure 1a). Cells were passively seeded on the MWAs and spontaneously formed clusters (Figure 1b) within 12 hours. Using two different MWAs (well diameters of 200 and 400 μm , well depth of 200 μm) and seeding densities, a range of highly reproducible cell clusters (diameters from 70 to 300 micrometers, see figure 1b and d) of human Mesenchymal Stem Cells (hMSC, 48 hours) spontaneously assembled. The clusters' size evolved over-time at different rate depending on the culture medium (Figure 1e).

To assess for the potential of different cell types, we seeded 6 different cell types (hMSC, bovine Primary Chondrocytes (bPC), mouse premyoblast (C2C12), mouse Embryonic Stem Cells (mESC), human Umbilical Vein Endothelial Cells (huvEC) and mouse Embryonic Fibroblast (mEF)) (number of cells: 0.4 millions/MWA) on MWAs (200 μm well di-

ameter). The clusters evolved in circularity and size from 24 to 120 hours (Figure 1f). Based on their macroscale characteristics, we classified them into three families. The first family comprised hMSC, bPC and C2C12 and was characterized by clusters which compacted and improved circularity overtime. These three cell types achieved similar rates of compaction as determined by the change in projection area (PA) (rates of compaction of 1.8 ; 1.5 and 1.7 respectively) and similar high circularity as determined by circularity ($\text{Circularity} = 4\pi(\text{area}/\text{perimeter}^2) = 0.9$). The second family included chO and mESC and was characterized by a growth of the cell clusters. The rates of increasing PA were respectively 1.5 and 1.8 when circularity either increased or stabilized (0.9 and 0.7 respectively). The third family which included huVEC and mEF did not evolve overtime maintaining similar PA, low circularity and low coherence. These observations demonstrated different potential for different cell types for subsequent use as building blocks for tissue fabrication.

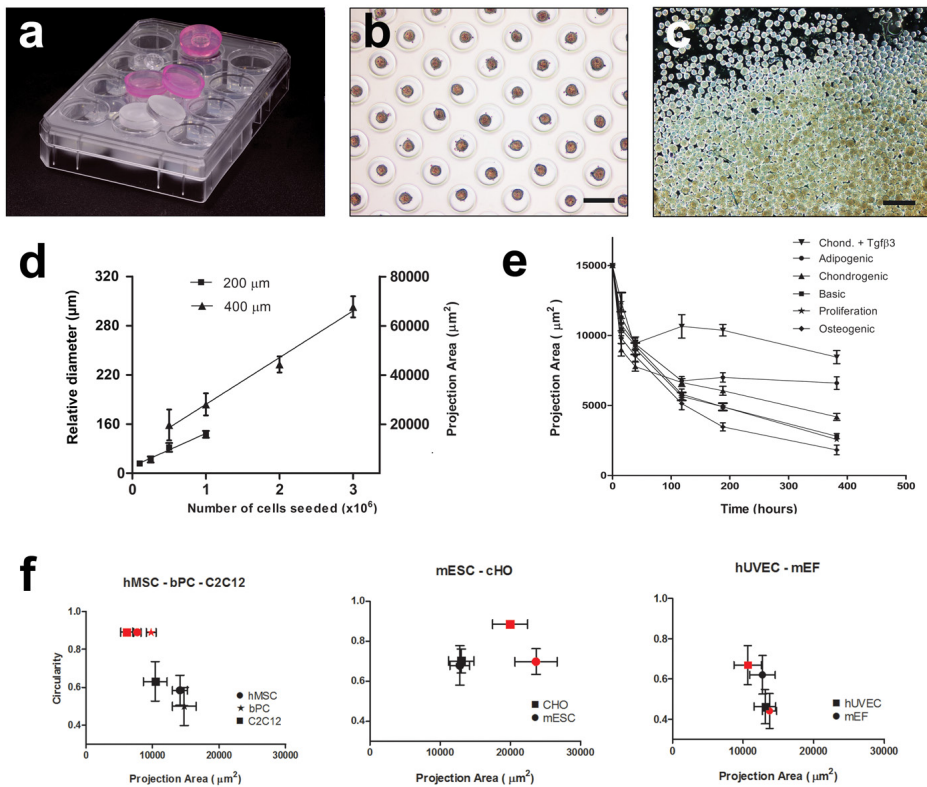


Figure 1: Microscale cell clusters spontaneously assembled on MicroWells Arrays.

MicroWells arrays (MWA) of agarose (pink templates, a) were routinely casted from PDMS templates (transparent templates, a) and placed in conventional well-plates. Upon stochastic seeding, cells felt in the microwells and rapidly (12h) and spontaneously formed cell clusters (b, scale bar is 200 μm) which could easily be flushed out (c, scale bar is 200 μm). Using 2 different MWA with wells of respectively 200 and 400 micrometers, cell clusters ranging from 70 to 300 micrometers' diameter were formed (d) which evolved differently in different medium (e). Based on their Projected area (PA) and Circularity, cell clusters of 6 different cell types were sorted in three different families with respectively a decreasing PA and increasing circularity (f, left), increasing PA (f, center) and stable PA and circularity (f, right). The black signs represent the clusters' characteristics after 20 hours and the red signs the characteristics after 120 hours.

Assembly of millimeter-scale tissues

In a second step, the same approach was used to assemble microscale cell clusters into millimeter-scale tissues in Shaped Well Arrays (SWAs, fig. 2a-f). Cell clusters were flushed out of the MWAs (Figure 1c) and passively seeded on the SWAs (1mm² PA/well, 500 µm depth, 15 to 25 wells/SWA, fig 2b-d). They fused within 24 hours and formed a continuous tissue adopting the shape of the well (fig 2e-f). To assess the necessity of a pre-condensation step (MWA), we compared the evolution of the tissues when formed either with a pool of single cells or a pool microtissues previously cultured on the MWAs (hMSC). Tissues assembled from a single cell suspension rapidly compacted, deformed and formed a sphere. On the contrary, tissues assembled from precondensed microtissues compacted to a lesser extent and maintained their original disc-shape (figure 2g). Resulting tissues are 3D, scaffold-free, free-standing with a PA of 1mm² and a height of approximately 300 micrometers. These results demonstrate that an intermediate step of precondensation into cell clusters is essential, at least for the cell types characterized by high compaction rates (first family, figure 1f), to form shaped millimeter-scale tissues.

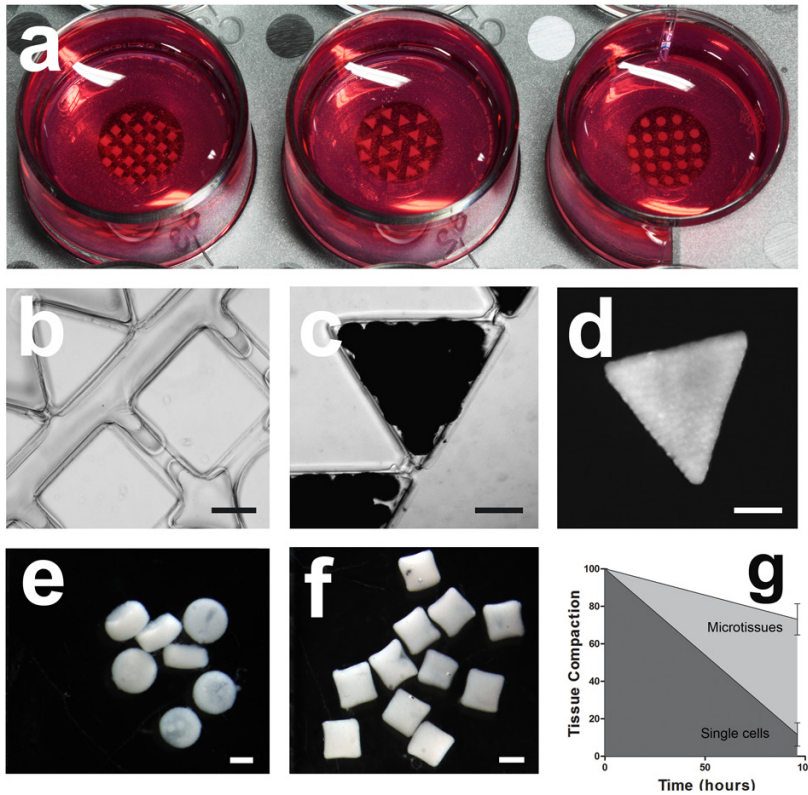


Figure 2: Assembly into millimeter-scale tissues

Microscale clusters were used as building blocks to form millimeter-scale tissues on agarose Shaped Wells Arrays (SWA, a). Microscale clusters were passively seeded on to SWA (b, c) and spontaneously fused to form continuous tissues adopting the shape of the wells (d). The tissues are scaffold-free, free-standing and can easily be flushed out of the SWA (d-f). The step of microscale clusters precompaction on MWAs is essential, at least for hMSC, to prevent the important deformation and compaction of the tissue as demonstrated by seeding both single cells and microscale clusters on the SWA (g). Scale bars are 500 μm .

Tissue remodeling and external geometries

Upon seeding of cell clusters on the SWAs, tissues compacted, deformed and finally stabilized their shape (150 hours). We tested the influence of the time of incubation of cell clusters on the MWA on the subsequent remodeling of tissues on the SWAs. Squared tissues formed of bPC (2 days on the MWA) underwent a minimal remodeling when cultured with Tgfb1 and maintained their initial geometry (shape factor=0.945, shape factor_{perfect square}=1, shape factor_{perfect circle}=0.91, 7 days, fig. 3d). Squared tissues formed of hMSC cultured for 3 days on the MWAs rapidly compacted and remodeled their shape to a circle (shape factor=0.91, 7 days, fig. 3d). This deformation was attenuated by either a longer incubation on the MWAs (5 days on the MWAs, shape factor=0.92,) or by the incorporation of 8% hUVECs in the clusters (5 days on the MWAs, shape factor=0.93,). On the other hand, clusters of hMSC cultured for more than 7 days and clusters of bPC cultured for more than 3 days failed to properly fuse and to form a continuous tissue (data not shown). Compaction and deformation reached a steady state after 6 days (Fig. 3d). This result demonstrated that the plasticity of cell clusters and the subsequent speed of tissue remodeling decreased upon culture and that an adequate time-window of culture on the MWA can be adjusted, for each cell type. These results also demonstrated an isotropic deformation of disc-like tissues and an anisotropic deformation of square-like tissues which underwent a more important deformation in corners compared to sides.

To overcome the anisotropic remodeling and subsequent loss of shape, we designed geometric tissues which compensated for these corner effects. Compensated geometries underwent high local deformation in the corners and a subsequent anisotropic remodeling toward predicted shapes (Figure 3c, SD1). Upon deformation, compensated geometries led to better shapes compared to the corresponding non-compensated geometries (shape factor_{Comp. Square}=0.97, shape factor_{Normal Square}=0.94, figure 3e).

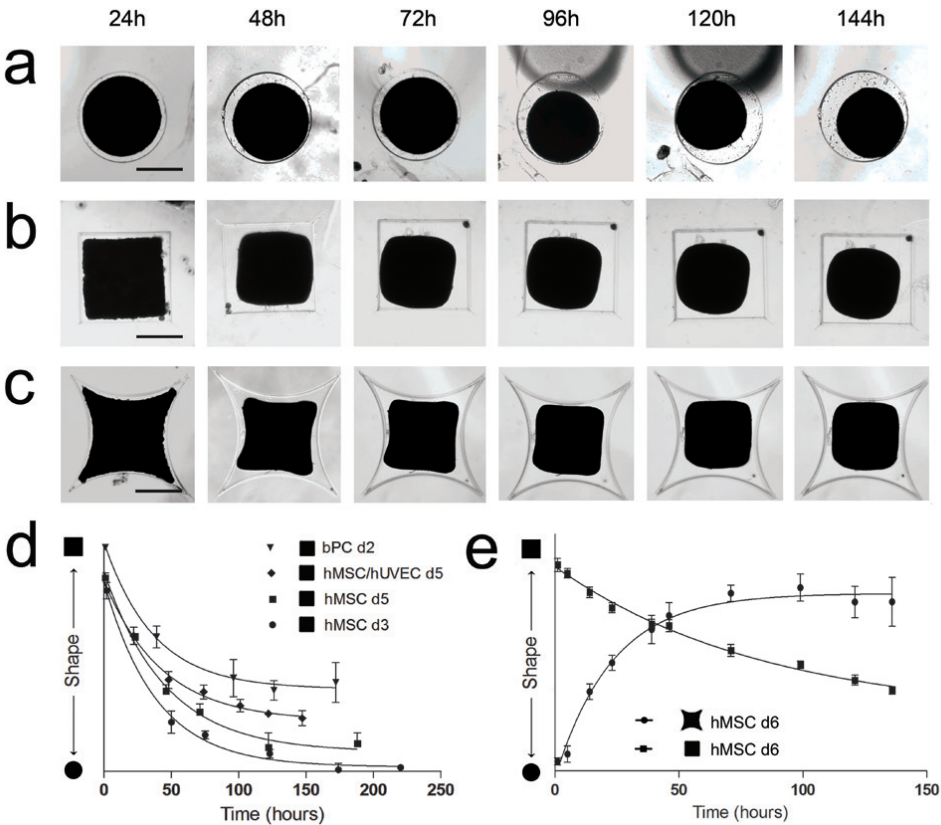


Figure 3: Tissue remodeling and external geometries

Upon culture on the SWA, tissues compacted and deformed according to their external geometries and stabilized their shapes after ~150 hours. Disc-shaped tissues remodeled isotropically (a) whereas squared-shaped tissues remodel anisotropically with tissue corners displacing more rapidly compared to their respective sides (b). To overcome this anisotropic remodeling and subsequent loss of shape, geometric tissues which compensated for these corner effects were designed (star-shaped wells) which progressively remodeled toward predicted shapes (squared-shaped and triangular-shaped tissues)(c and SD1). The time of incubation on the MWA influenced subsequent remodeling of the tissue. An appropriate time-window specific to each cell type(s) must be adjusted to form a continuous tissue with controllable remodeling properties (here, squared-shaped tissues of bPC, hMSC or hMSC and huvEC) (d). Compensated geometries (star-shaped wells) have, upon remodeling, a final better squared-shape than normal square geometries (e). Scale bars are 500 μm .

Tissue remodeling and internal geometries

Because the external tissue geometry directed an anisotropic deformation, we tested the influence of the internal geometries on subsequent tissue remodeling. We added pits or columns with different geometries inside the wells of SWAs. Upon seeding, ring-like tissues fused and compacted around these columns (Figure 4a-d). Upon compaction, a circular column inside a circular well induced an isotropic compaction into a ring (6 days on the MWAs and 5 days on the SWAs, circularity=0.82). In opposition, a star shaped column in the same well induced anisotropic deformation leading to a more squared tissue (circularity=0.69) (Figure 2d). Similarly, tissues starting from a square geometry compacted toward either a circle (circularity=0.80) or a polygon (circularity=0.63) depending on the orientation of the internal star-shaped pit (Figure 2d).

These observations demonstrated that the internal geometry of tissues can dictate its remodeling. It suggested that tissues are interspersed by streams of mechanical forces regulated by the geometry.

We then designed geometric tissues which, upon compaction, progressively interact physically with the template (Figure 2e-g). These complex complementary shapes can further be used as modules to form iterative tissue structures.

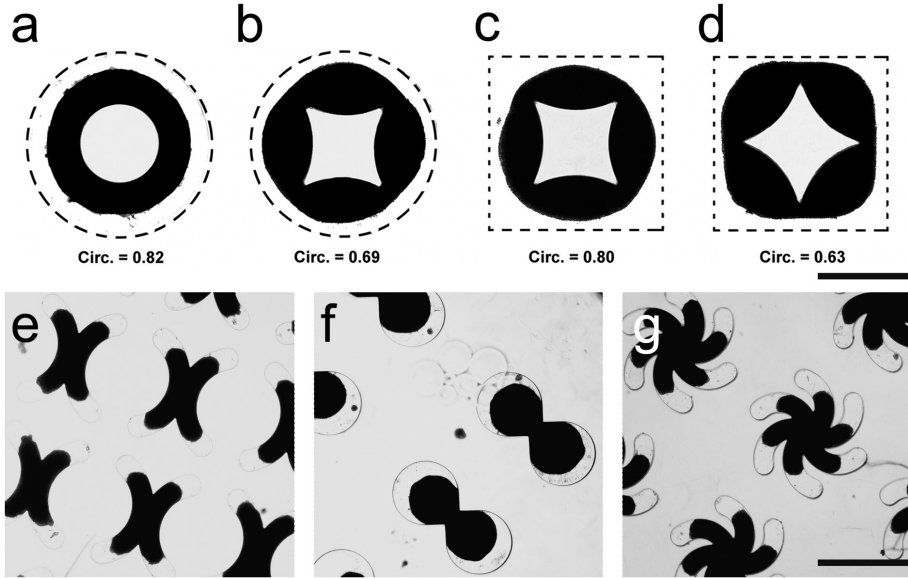


Figure 4: Tissue remodeling, internal geometries and interaction with the template

The internal geometry influenced the tissue deformation upon compaction (hMSC). When circular pits were inserted into the wells, ring-like tissues compacted isotropically (a). Contrarily, a star shaped pit in the same well induced an anisotropic deformation leading to a more polygonal (square) tissue (b). Tissues starting from a square geometry compacted toward either a circle (c) or a polygon (d) depending on the orientation of the internal star-shaped pit. Images are an average projection of 5 tissues. Complex complementary shapes can be form which progressively interact with the template and can subsequently be used as modules to assemble iterative tissue structures (e-g). Scale bars are 500 μm .

Tissue regionalization and differentiation

Large tissue constructs are prone to a lack of diffusion of oxygen. We previously demonstrated that this problem can be alleviated by the formation of a primitive vascular network that can anastomose with the host vasculature upon implantation (12). The co-culture of hMSC and hucEC support the formation of such a primitive vascular network (CD31+ cells) (13). Here we tested the possibility to use a co-cultured cell clusters as an initial microscale unit that would, upon assembly and fusion, form a network at a tissue-scale. We seeded both cell types on the same MWAs, cultured the clusters for 5

days and then transferred to SWAs. Upon fusion (24 hours), CD31+ cells were first found as round clusters distributed across the tissue (figure 5a, b). In a second step, the CD31+ cells elongated and formed a primitive vascular network (120 hours, figure 5c). This result demonstrate the possibility to form a primitive vascular network at the tissue-scale through random assembly and directed organization. Because geometric tissues deformed anisotropically (*corner-effect*), we observed the internal distribution of cells nuclei as an indicator of tissue compaction. Using a profile plot of normalized integrated intensities of Dapi around concentric circles, we demonstrated a significant increased tissue compaction from the tissue center to the periphery (Figure 5D, SD2). This result suggest that the important displacement of the tip induced local tissue compaction. Corner regions might be characterized by geometry-induced mechanical stress as already described using mathematical models (14-15).

In a third experiment, we tested the potential of bPC to differentiate *in vitro* into a cartilage-like tissue. We cultured bPC for 2 days on the MWA and transferred the clusters on the SWA. Clusters fused and were further cultured for 21 days with Tgfb β 3 (10 ng/ml). We assessed the formation of a proteglycans-rich extra-cellular matrix thus demonstrating the possibility to form large tissues producing their own scaffold (figure 5e).

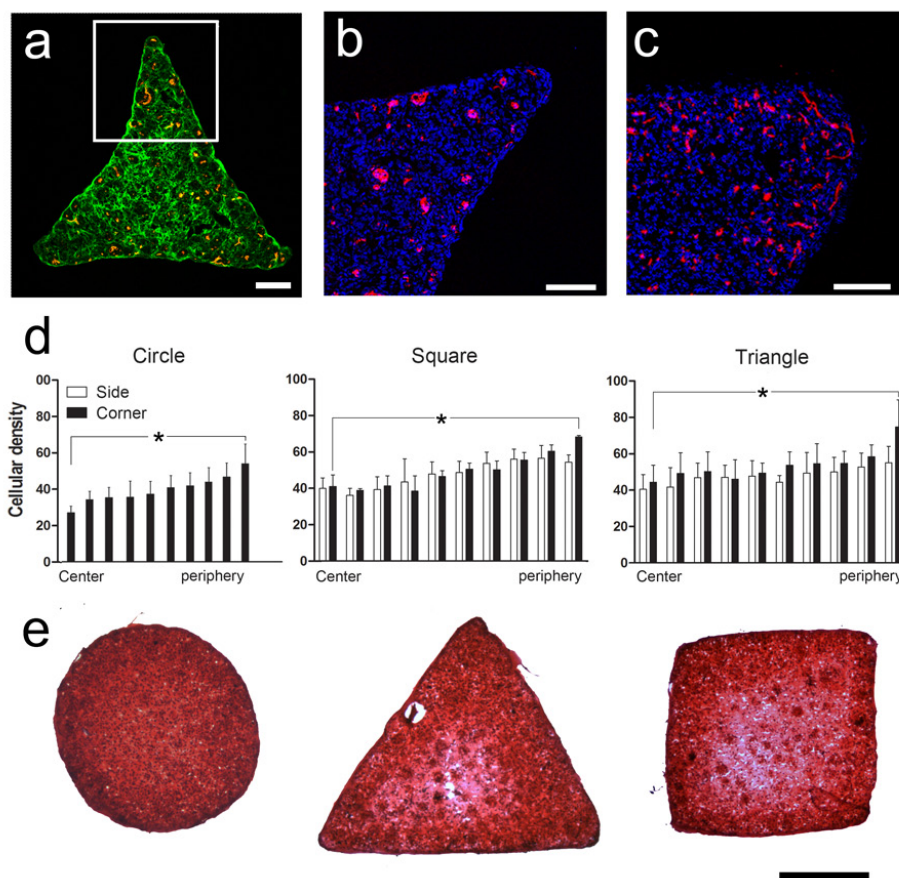


Figure 5: Tissue regionalization and differentiation.

Microscale clusters of hMSC and huVEC seeded on SWA fused into a continuous tissue (24 hours, F-actin in green and CD31 in red, a, scale bar is 200 micrometers) including rounded clusters of CD31+ cells (close up of the tissue tip, nuclei in blue and CD31 in red, b, scale bar is 200 micrometers). These clusters elongated overtime to form primitive vascular structures at the tissue scale (150 hours, c, scale bar is 200 micrometers). Upon tissue remodeling, a gradient of tissue compaction formed from the tissue center to the periphery as measured using a radial plot of nuclei density. Tissue compaction was found higher in the tissue corners compared to the periphery and the center, an observation which correlates with the macroscopic displacement of the tissue. Self-remodeling tissues form heterogeneous regions of tissue density upon compaction (d). bpC were cultured for differentiation and formed an extensive scaffold of extracellular matrix after 21 days as revealed using Safarin-O staining.

Puzzle-like assembly at a clinically relevant size

For therapeutic uses, a challenge lies in achieving grafts of centimeter-scale size. Extending the bottom-up approach, we used millimeter-scale tissue units to assemble clinically relevant tissues. Tissue units were deposited in agarose molds of adequate shapes and then assembled in cylinders (figure 6a) or sheets (figure 6c). Within 24 hours, tissues fused into centimeter-scale tissues (figure 6b, d). The shape of the tissue units and their arrangement dictated the shape of the final tissue which can be adjusted to the defect site. The tissue can be easily manipulated upon fusion of the units using surgical instruments and implanted to replace defective tissues (figure 6d).

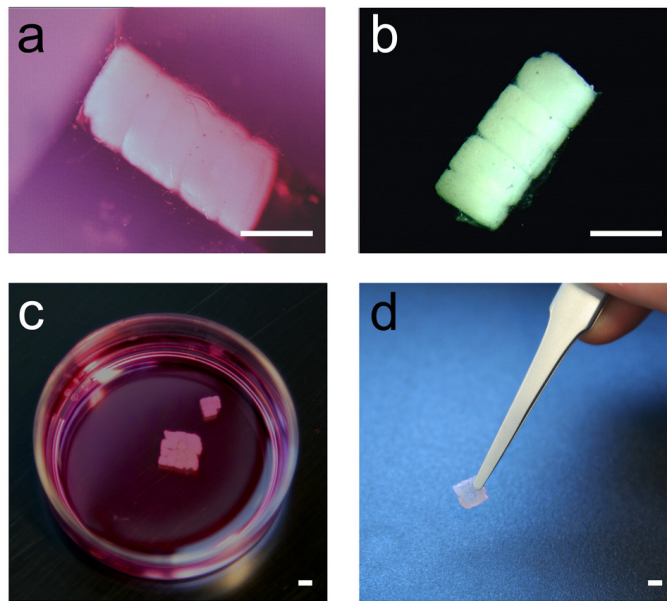


Figure 6: Puzzle-like assembly at a clinically relevant size.

Millimeter-scale tissues were further assembled into centimeter-scale tissues (a, c, scale bar is 1 mm). The shapes of the individual millimeter-scale tissues and their respective adjustment defines the final shape of the graft which can thus be adapted to the implantation site. The individual millimeter-scale tissues rapidly and spontaneously fused upon culture and can be easily handled for subsequent use (b, d, scale bar is 1 mm).

Discussion

We described an accessible and powerful process for the formation of scaffold-free tissues as tissue models and surgical implants. We specifically characterized the macroscale behavior of multicellular aggregates of different cell types as a prerequisite to fine-tune the conditions of tissue assembly. The range of behaviors observed demonstrate context-dependent boundary conditions (cell type, medium, timing). We demonstrated that a first step of precondensation into cell clusters is essential to limit subsequent tissue compaction and deformation rate. A time-window was specifically adjusted for hMSC and hMSC/huVEC to form a continuous tissue with controllable remodeling properties. These results demonstrate that the plasticity of clusters of hMSC decrease overtime, possibly due to a stabilization of cell-cell contacts and to the production of extra-cellular matrix. Within this time-window, the internal and external geometry of the tissue can be designed to promote an anisotropically remodeling toward predicted shapes. Interestingly, this anisotropic deformation correlated with the formation of internal heterogeneity and local tissue compaction (*corner/peripheral-effect*).

Developing tissues are dynamic systems which remodel and organize based on biological and physical heterogeneity. Such heterogeneity is a key mechanism which bridges the molecular scale to the tissue scale and allows for the emergence of forms and organization in tissues (16). The described heterogeneous deformation and compaction might be correlated, in further experiments, to an heterogeneous tissue organization/differentiation. Directed self-organization thus led to autonomous mechanisms of tissue regionalization upon contraction, compaction and deformation. Resulting heterogeneous tissue modules can be assembled into tissues of clinically relevant size.

Based on these results, we speculate that the combination of self-organizing tissue modules and modular tissue assembly might allow for the fabrication of tissues mimicking the iterative structures and function of organs at a clinically relevant size.

A major challenge in tissue engineering lies in finding simple processes to form complex tissues. Current approaches are often based on the assembly of artificial scaffolds and cells mimicking the final architecture of the desired tissue. Such an approach is mostly directed by the properties of the scaffold and requires complex and expensive machines. In clear opposition, here, we present a powerful and accessible approach to direct *in vitro* tissue

organization in a process reminiscent of natural development. In sum, we demonstrate that self-organization is a simple and powerful engineering process to generate complex tissues. This clearly opens new possibilities to form self-constructing tissues with wide impacts in tissue engineering and regenerative medicine.

Materials and Methods

Cell culture and reagents. Human bone marrow aspirates were obtained from donors after written informed consent, and human mesenchymal stem cells were isolated and expanded as already described (4). During experiments, human mesenchymal stem cells and bovine primary chondrocytes were cultured in Differentiation medium composed of Dulbecco's Modified Eagle's Medium supplemented with 10^{-7} M dexamethasone, 50 mg/ml ascorbate 2-phosphate, 40 mg/ml proline, 100 mg/ml pyruvate, and 50 mg/ml ITS1+ Premix (Becton–Dickinson, MA: 6.25 mg/ml insulin, 6.25 mg/ml transferrin, 6.25 ng/ml selenious acid, 1.25 mg/ml bovine serum albumin, 5.35 mg/ml linoleic acid), 100U/mL penicillin (Life Technologies), 100 mg/mL streptomycin (Life Technologies). Human umbilical vein endothelial cells were purchased from Lonza (Lonza, group Ltd. Switzerland) and cultured in endothelial growth medium-2 (Cambrex). C2C12, mouse embryonic fibroblast, Chinese hamster ovarian were cultured in Dulbecco's Modified Eagle's Medium supplemented with 10% fetal bovine serum ((FBS; Life Technologies), 100U/mL penicillin (Life Technologies), 100 mg/mL streptomycin (Life Technologies).

MicroWell Array and Shaped Well Array fabrication. Micropatterned agarose chips for non-adherent cell culture were formed by replica molding. Patterned elastomeric stamps of poly(dimethylsiloxane) (PDMS; Sylgard 184, Dow Corning) were replicated from either etched silicon wafers or SU-8/silicon wafers according to established protocols (11) and sterilized 10 minutes in 100% ethanol. A 4% agarose solution (Ultra pure agarose, Invitrogen) was casted on the PDMS stamp, demolded upon solidification and placed in a 12 well plate (S1). After wetting using corresponding Differentiation medium (500 microliters), a concentrated suspension of cells was seeded and allowed to settle for 15 minutes on the chip. Excess cells were rinsed away with culture medium and 1.5 milliliters of medium was added. Half of the medium was changed every day of culture. Upon culture on the MWAs, cell clusters were gently flushed out using culture medium, centrifuged (1300 rpm, 1 minute), resuspended in the culture medium and seeded on the SWAs. Cell clusters were allowed to settle in the wells for 1 minutes and excess cell clusters were washed away and seeded again for optimal seeding. The seeded chips were centrifuged (1300 rpm, 1 minute)

and 1.5 milliliter of culture medium was added. Half of the medium was changed every day of culture.

Immunohistochemical analysis. After harvesting, tissues were frozen in Cryomatrix at -60°C . Sections ($7\text{ }\mu\text{m}$) were cut using a cryotome. Sections were fixed in cold acetone for 5 min, air-dried, rehydrated for 10 min, after which they were incubated for 30 min with 10% FBS in PBS to block nonspecific background staining. Sections were incubated with monoclonal mouse anti-human CD31 antibody (Dako), a monoclonal mouse anti-human for 1 h. Sections were washed in PBS and subsequently incubated with the secondary antibody (Alexa Fluor 488 antibody, Invitrogen). Samples were counterstained with Dapi (Sigma). Pictures were taken using a confocal microscope (Leica LSM500). Cartilage formation was assessed by safari-O staining.

Measurements of tissues macroscopic behavior. *Projection area.* Pictures of the tissues are taken using a Nikon Eclipse TE300 microscope equipped with Nikon Digital Signt DS Fi1 digital camera and imaging system. Images are imported into Image J and a B&W mask picture is created using a threshold. The resulting picture is analysed using Image J to measure the area of each tissue.

Shape maintenance. Shape are graded by quantifying the overlapping area (OA) of the projected area of the tissue to a perfect shape of identical surface area. Shape factor = OA.

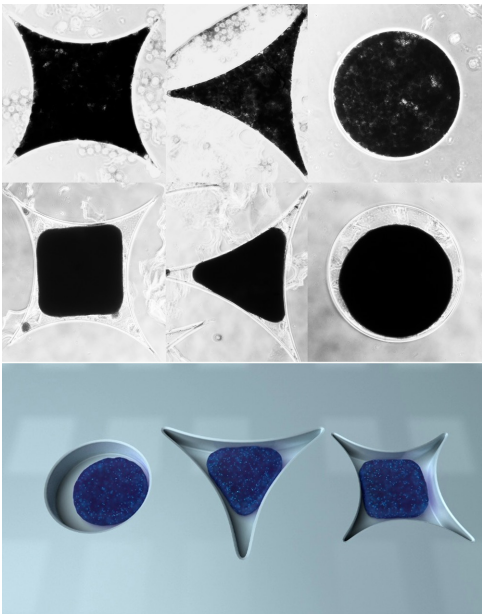
Circularity. Circularity was measured using an Image J plugin. A picture of taken and a mask of each tissue was made as described for the measurement of the projection area. The circularity of the mask was measured as followed. $\text{circularity} = 4\pi(\text{area}/\text{perimeter}^2)$

Cellular density. Cellular density was measured using a Radial Profile Plot. Image J plugin by Paul Baggethun. This plugin produces a profile plot of normalized integrated intensities around concentric circles as a function of distance from a point in the image. The intensity at any given distance from the point represents the sum of the pixel values around a circle. This circle has the point as its center and the distance from the point as radius. The integrated intensity is divided by the number of pixels in the circle that is also part of the image, yielding normalized comparable values. The profile x-axis can be plotted as pixel values or as values according to the spatial calibration of input image. <http://rsb.info.nih.gov/ij/>

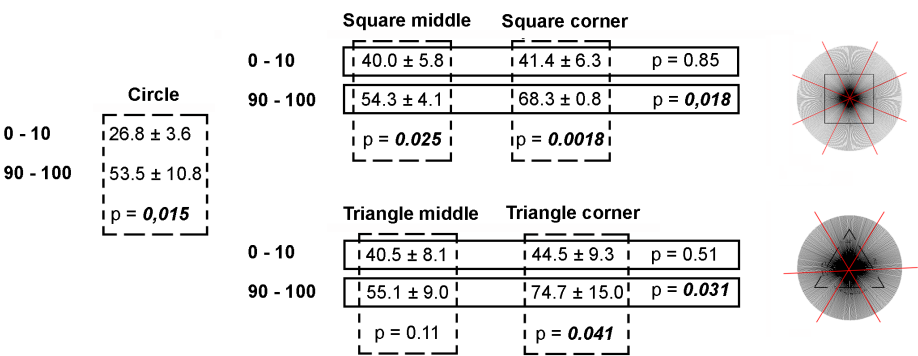
Chapter 4

plugins/radial-profile.html.

Supplementary informations



SD1: Compensated geometries. Geometries were designed which promote the progressive remodeling toward predicted shapes. Top row is after seeding, middle row is after 150 hours, bottom row is an artistic view.



SD2: Statistical analysis of the tissue density. The analysis is done using a radial plot as described in the methods and as schematically depicted in the above drawing. The statistical differences between different groups was determined using a student T-Test, $n=3$. 0-10 represents the first 10% of the distance from the center to the periphery (central part of the tissue) and 90-100 represents the last 10% of this same distance (periphery). The shapes' middles and corners are delimited by the red lines.

1. Nelson CM, Vanduijn MM, Inman JL, Fletcher DA, & Bissell MJ (2006) Tissue geometry determines sites of mammary branching morphogenesis in organotypic cultures. (Translated from eng) *Science* 314(5797):298-300 (in eng).
2. Atala A, Bauer SB, Soker S, Yoo JJ, & Retik AB (2006) Tissue-engineered autologous bladders for patients needing cystoplasty. (Translated from eng) *Lancet* 367(9518):1241-1246 (in eng).
3. Moroni L, *et al.* (2008) Regenerating articular tissue by converging technologies. (Translated from eng) *PLoS One* 3(8):e3032 (in eng).
4. Siddappa R, *et al.* (2008) cAMP/PKA pathway activation in human mesenchymal stem cells in vitro results in robust bone formation in vivo. (Translated from eng) *Proc Natl Acad Sci U S A* 105(20):7281-7286 (in eng).
5. Shimizu T, Yamato M, Kikuchi A, & Okano T (2001) Two-dimensional manipulation of cardiac myocyte sheets utilizing temperature-responsive culture dishes augments the pulsatile amplitude. (Translated from eng) *Tissue Eng* 7(2):141-151 (in eng).
6. Kelm JM, *et al.* (2004) Design of artificial myocardial microtissues. (Translated from eng) *Tissue Eng* 10(1-2):201-214 (in eng).
7. Liu Tsang V, *et al.* (2007) Fabrication of 3D hepatic tissues by additive photopatterning of cellular hydrogels. (Translated from eng) *FASEB J* 21(3):790-801 (in eng).
8. Luhmann T, Hanseler P, Grant B, & Hall H (2009) The induction of cell alignment by covalently immobilized gradients of the 6th Ig-like domain of cell adhesion molecule L1 in 3D-fibrin matrices. (Translated from Eng) *Biomaterials* (in Eng).
9. Matsumoto T, *et al.* (2007) Three-dimensional cell and tissue patterning in a strained fibrin gel system. (Translated from eng) *PLoS One* 2(11):e1211 (in eng).
10. Camazine S, *et al.* (2001) Self-organization in biological systems. *Princeton University Press*.
11. Xia Y, *et al.* (1996) Complex Optical Surfaces Formed by Replica Molding Against Elastic Masters. (Translated from eng) *Science* 273(5273):347-349 (in eng).
12. Levenberg S, *et al.* (2005) Engineering vascularized skeletal muscle tissue. (Translated from eng) *Nat Biotechnol* 23(7):879-884 (in eng).
13. Rouwkema J, de Boer J, & Van Blitterswijk CA (2006) Endothelial cells assemble into a 3-dimensional prevascular network in a bone tissue engineering construct. (Translated from eng) *Tissue Eng* 12(9):2685-2693 (in eng).
14. Ruiz SA & Chen CS (2008) Emergence of patterned stem cell differentiation within multicellular structures. (Translated from eng) *Stem Cells* 26(11):2921-2927 (in eng).
15. Nelson CM, *et al.* (2005) Emergent patterns of growth controlled by multicellular form and mechanics. (Translated from eng) *Proc Natl Acad Sci U S A* 102(33):11594-11599 (in eng).
16. Engler AJ, Humbert PO, Wehrle-Haller B, & Weaver VM (2009) Multiscale modeling of form and function. (Translated from eng) *Science* 324(5924):208-212 (in eng).

Chapter 5

Endogenous tissue contractility spatially regulates angiogenesis

N.C. Rivron¹, E.J. Vrij¹, R. Truckenmüller^{1,3}, J. Rouwkema², S. Le Gac³,
A. van den Berg³, C.A. van Blitterswijk¹

- 1- Department of Tissue Regeneration, MIRA -Institute for Biomedical Technology and Technical Medicine- University of Twente, Enschede , The Netherlands.
- 2- Department of Biomechanical Engineering, MIRA -Institute for Biomedical Technology and Technical Medicine- University of Twente, Enschede, The Netherlands.
- 3- BIOS - the Lab-on-a-Chip Group, MESA+ -Institute for Nanotechnology- University of Twente, Enschede, The Netherlands.

Stereotyped patterns of the vascular system are locally controlled by genetically hard-wired cell behaviors and shaped at the tissue-scale by gradients of angiogenic molecules induced, for example, by hypoxia. Using arrays of free-standing micro-fabricated tissues of human mesenchymal stem cells and human umbilical vein endothelial cells, we found that endogenous tissue contractility collectively generated by the cells induces local tissue deformations, compactions and the formation of stereotyped patterns of Capillary-Like Structures. This emergence correlated with the autonomous formation of a long-range gradient of Vascular Endothelial Growth Factor by graded production and with the local over-expression of the corresponding receptor VEGFR2. We propose that endogenous tissue contractility is a tissue-scale morphogenetic regulator of the angiogenic microenvironment and angiogenesis, a finding with wide implications in regenerative medicine and cancer biology.

Introduction

Tissues are self-deforming systems whose endogenous forces participate in the coordination of morphogenetic mechanisms by patterning gene expression (1) or cellular division (2). These endogenous forces can induce local compactions or mechanical deformations which are thought to act in unison with, for instance, gradients of morphogens to shape and maintain tissue forms and functions (3).

The vascular system is a mechanosensitive organ (4) forming organized and stereotyped networks of cords which further mature into veins, arteries or capillaries. The perturbation of this order is a hallmark of a wide range of malignant, inflammatory, ischemic, infectious and immune disorders including cancer, arthritis and blindness (5). Patterns in the vascular network are thought to be mainly shaped by tissue hypoxia which regulates cellular sprouting through a graded production of Vascular Endothelial Growth Factor (VEGF) (6) and to be then mainly remodeled by the haemodynamic flow which locally regulates, for instance, the expression of the VEGFR2 (7). Here we investigated the role of endogenous tissue contractility and deformation in regulating the angiogenic environment and the formation of patterns of Capillary-Like-Structures (CLS).

Results

We aimed at mimicking the early events of angiogenesis in engineered tissues using hMSC which can generate forces (8), produce VEGF (9) and hucEC which express the CD31 endothelial marker. This system supports the formation of a CD31+ primitive vascular network as a relevant model for early angiogenesis (10). We assembled geometric millimeter-scale tissues by using a two-step bottom-up approach of sequential aggregation of cells on microfabricated non-adherent agarose templates (Fig. 1a, S1) (11).

Within 5 days, geometric tissues reproducibly compacted, deformed and finally stabilized their shapes (Fig. 1b, S2). Disc-shaped tissues compacted isotropically whereas squared-shaped tissues compacted anisotropically with a preferential displacement of the corners compare to sides ($p=0.0015$, $n=10$, S3). To compensate for this tip-effect, geometries were designed which remodeled toward a square (Fig. 1b, second row). This anisotropic remodel-

eling and deformation suggests a geometry-induced heterogeneous distribution of internal forces as already observed and modeled in multicellular systems (12).

Microscale clusters first spontaneously organized into an inner core of CD31+ cells (Asterisk, fig. 1c) and an external layer of CD31- cells possibly according to differences in cellular affinity (strength of adhesion molecules) and in cortical tension that determines stable association and sorting (13-15). Clusters strongly and transiently expressed peripheral filamentous actin (F-actin) upon fusion with neighbors (Fig. 1c, 24 hours, S3). After 24 hours, CD31+ cells were F-actin intense, started to sprout into CLS (Asterisk, fig. 1d) and formed some lumens (Asterisk, fig. 3d).

Upon tissue compaction and deformation (day 5), CLS had preferentially formed in the peripheral regions of tissues and more densely in the corners of tissues (Fig. 1e and S4). Interestingly, this preferential growth of CLS correlated with the regions of higher displacements and shape deformation (S3).

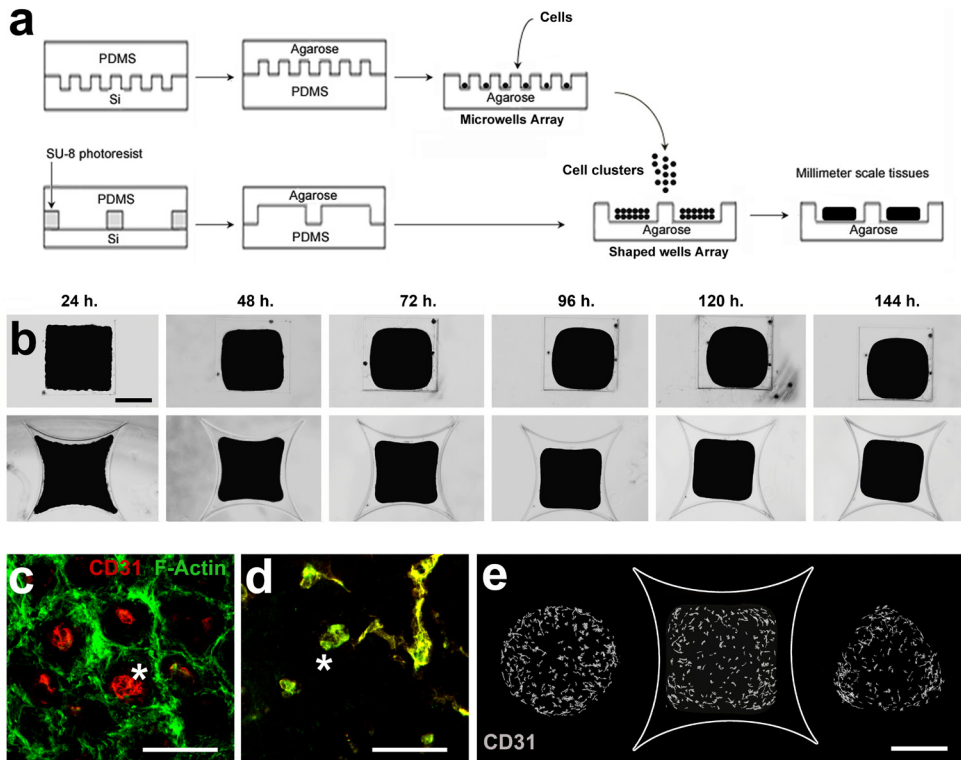


Fig.1. Microfabricated tissues autonomously remodeled and formed stereotyped patterns of CLS.

(a) 3D millimeter-scale tissues were sequentially assembled by cellular aggregation in non-adherent well arrays. (b) Free-standing tissues compacted, deformed and finally stabilized their shapes (scale bar 500 microns). Tissue geometries induced either an isotropic remodeling (disc-shaped tissues) or an anisotropic remodeling with a more important deformation of tissues corners (squared-shaped tissues)(see also fig. S2). (c) Cell clusters of hucEC and hMSC first spontaneously formed a CD31+ core and a CD31- external layer which generated an F-actin intense interface upon fusion with neighbors (24 hours). (d) After 24 hours, CD31+ cells were F-actin+ and sprouted from the original clusters (d, asterisk, scale bar 100 μ m). (e) Upon tissue remodeling, CLS were preferentially found in the peripheral region of circular tissues and in the peripheral and corner regions of squared and triangular tissues (scale bar 500 μ m).

We tested the possibility of impairing tissue remodeling by blocking specific forces-generating elements in cells. Non muscle Myosins II A, B and C (NMM II) and F-actin are likely to be main generators of forces in hMSC (16). We tested the effect of specific inhibitors of these elements (Blebistatin and Y27632) on tissue remodeling. Blebistatin blocks the activation of NMM II ATPase and impairs its interaction with F-actin. Y27632 suppresses p160ROCK (Rho associated coiled-coil containing protein kinase) and inhibits the phosphorylation of Myosin Light Chain and the formins-dependent formation of F-actin stress fibers (17). Tissues with Blebistatin or Y27632 alone compacted and deformed similarly to controls (normal compaction) but tissues exposed to Blebistatin and Y27632 relaxed within 4 hours (from 78% to 84% of their initial projected area, $p=0.0002$, $n=10$, Fig. 2a-b). Their compaction was further impaired compared to tissues exposed to one or no compound (70% of compaction against 58% after 144 hours, $p=6.10^{-7}$, $n=10$)(Fig. 2a-b). This tissue relaxation demonstrated the internal pre-stress, tensional state generated by the actin-myosin complex. The synergistic effect of Blebistatin and Y27632 suggested a combined role of actin bundle growth and myosin activity in the generation of internal tension and an intrinsic robustness of the mechanisms regulating the actin-myosin interaction. Tissue compaction was impaired but not stopped completely which implies a contribution of other cytoskeletal components or other mechanisms in tissue contractility.

Upon tissue compaction and deformation, cell nucleus staining revealed a gradient of increasing cellular density from the tissue center to the periphery which correlated with an

increase of NMM II and F-actin (Fig. 2b). These gradients disappeared when compaction was impaired (Fig. 2b and 3a). This internal heterogeneity in force-generating elements suggest an heterogeneous distribution of internal forces and correlates with local deformation and compaction (fig. S2). This might result directly from local cellular density or be generated by a dynamic positive feed-back loop of tension-mediated actomyosin regulation as already reported during *Drosophila* development (18).

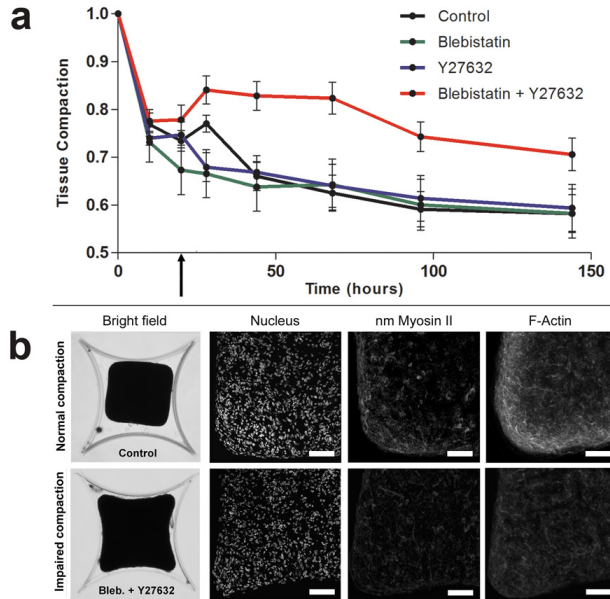


Fig. 2. Tissue compaction and deformation depends on an actomyosin tension collectively generated. (a) The combined inhibition of non muscle Myosin II (Blebistatin) and Rho associated protein kinase p160ROCK (Y27632) starting from 24 hours (see black arrow) relaxed the internal tissue tension (28 hours) and impaired the compaction (150 hours). (b) Tissue compaction resulted in a gradient of cellular density (density of nuclei) and a peripheral tissue layer with a concentration of force-generating elements (nm Myosin II and F-Actin, stack of 5 images)(scale bar 100 μ m) which was impaired when contraction was impaired. Standard deviations are shown for n=10.

We quantified the contribution of increased cellular density (number of nuclei/surface area unit) to the increase in the CLS. Tissue density was homogenous in the tissue center but a gradient was observed in the peripheral region (Fig. 3b, 2.2 fold increase in the last quartile compared to the first). This gradient was impaired when compaction was impaired (1.4 fold). Concomitantly, the den-

sity of CLS increased by 4.8 fold (2 fold when compaction was impaired) and the density of CLS/nucleus by 2.5 fold (1.4 fold upon compaction impairment, see color map, fig. 3a). The gradient of cellular density contributed to 48% of the increase in CLS (first quartile compared to last quartile, fig. 3c). This demonstrated that tissue contractility induced more than a strict compaction and suggested a more complex role for endogenous contractile forces. Indeed, the contribution of cellular density increased to 73% when compaction was impaired (Fig. 3c). Angiogenesis can be driven by tissue hypoxia due to the lack of oxygen diffusion which regulates the production of angiogenic factors (6). Tissues were designed with dimensions alleviating such a lack of oxygen diffusion and the formation of a hypoxic environment (tissue thickness ~ 300 micrometers). We tested this hypothesis by looking at the hypoxia inducible factor (HIF1a) which controls VEGF production (6). This factor was mostly cytoplasmic and homogeneously expressed across the tissue which suggests that preferential angiogenesis is not driven by localized hypoxia in this system (fig. S5). Indeed, when compaction was impaired, capillaries formed homogeneously throughout the whole tissue. The total CD31+ surface area increased from the center to the periphery of the tissues (fig. S4) which suggested a preferential elongation in the main plan of the tissue, a cellular migration of CD31+ cells toward the periphery or a local increase in proliferation as already proposed (19). We tested the hypothesis that preferential CLS formation was due to either a local proliferation or apoptosis using standard BrdU incorporation and TUNEL assays, respectively. Interestingly, proliferation was limited to the CD31+ cells (day 4), represented 0.3 to 1% of the total cell number (over 12 hours, day 1 to day 5) and was not restricted to the peripheral regions (Fig. S6). We could not detect significant apoptosis using a TUNEL assay (data not shown). These observations confirm that CLS are formed by sprouting and proliferation as already proposed (19) and suggest a deformation/compaction-induced local proliferation. The phenotypes of capillaries were different across the tissue sections: In regions of higher compaction and deformation, capillaries were thin, shaped and mostly elongated perpendicular to the preferential direction of tissue displacement (Fig. 3d, left, white arrows). This suggested a role for mechanical stress as endothelial cells have been reported to elongate perpendicular to externally applied mechanical stress (20-21). When internal tension was impaired, the basal level of angiogenesis was similar (fig. S7) but CLS grew more homogeneously throughout the tissue, were wider, tortuous and randomly oriented (Fig. 3a and d).

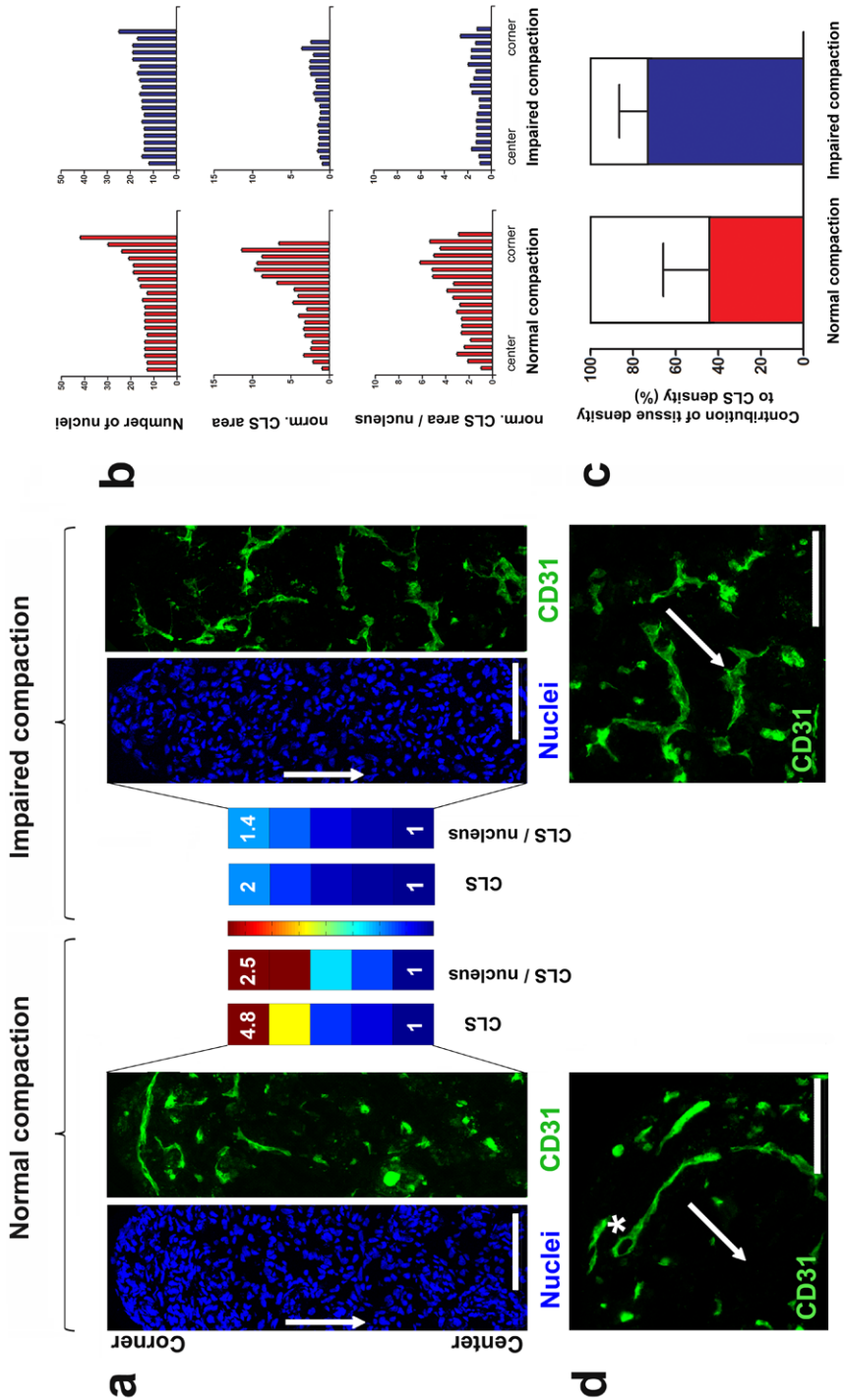


Fig. 3. Tissue contractility regulates local compaction and the preferential formation and directionality of CLS. (a) Tissue contractility induced the formation of local regions of compaction and deformation which correlated with the formation of CLS (from the center to periphery: 4.8 fold increase in CLS, 2.5 fold increase in CLS/nucleus, see color-maps). This preferential growth was impaired when contractility was impaired. (b, c) The increased cellular density (b) contributed to 48% of the increased CLS density during normal compaction and for 73% when compaction was impaired (c). (d) Tissue contractility induced the formation of thin CLS which formed some lumens (asterisk, d left) and elongated perpendicular to the tissue displacement (white arrows, a and d). This phenotype and directionality was impaired when compaction was impaired (d, right)(scale bars are 100 μ m). Standard deviations are shown for n=3 samples x 10 sections/sample.

Because the CLS within our microfabricated tissues exhibited patterned behavior in regions of higher tissue compaction and deformation and because hMSC are mechanosensitive cells (8, 16) which can modulate their VEGF expression in response to external mechanical stress (22), we tested the possibility that tissue contractility can regulate the production of VEGF in hMSC. Immunofluorescence using an antibody recognizing all different VEGF isoforms revealed the formation of a gradient of VEGF with an increasing intensity from the tissue center to the tissue periphery (Fig. 4a). VEGF was partly cytoplasmic (fig. S8) and cells in the peripheral region produced 50% more VEGF/nucleus compared to cells located in the center ($p=0.034$, $n=3 \times 10$)(Fig. 4b). When compaction was impaired, the total amount of VEGF produced in compacting tissues decreased by 2 fold compared to tissues with impaired compaction ($p=0.032$, $n=3 \times 10$)(Fig. 4c). Tissue contraction was subsequently responsible for the upregulation of VEGF expression and the formation of a gradient at least through direct compaction and the graded upregulation of VEGF production in regions of higher deformation and compaction. This does not exclude a possible contribution of an expansion of the gradient by diffusion.

Endothelial cells are mechanosensitive cells which can transcriptionally regulate the expression of the VEGFR2 receptor based on the mechanical properties of their microenvironment (4, 7). We tested the possibility that CD31+ cells responded to the tissue contraction by modulating their expression of the VEGFR2. VEGFR2 expression was restricted to CD31+ cells (fig. S9). Upon contraction, CD31+ cells in regions of higher compaction and deformation expressed higher level of VEGFR2 compared to cells in the central region (5

fold increase, $p=0.002$, $n=3 \times 8$, fig. 4d-e). The weakest VEGFR2 intensity was founded in the center of tissues with impaired compaction and the strongest intensity in the periphery of tissues with normal compaction (17 fold increase, see color map, fig. 4d-e). When contraction was impaired, the peripheral over-expression of VEGFR2 was abolished (Fig. 4d-e). Interestingly, the region of VEGFR2 intense expression was more localized, did not fully overlap with the region of maximum expression of VEGF and correlated with the region of higher tissue density and remodeling.

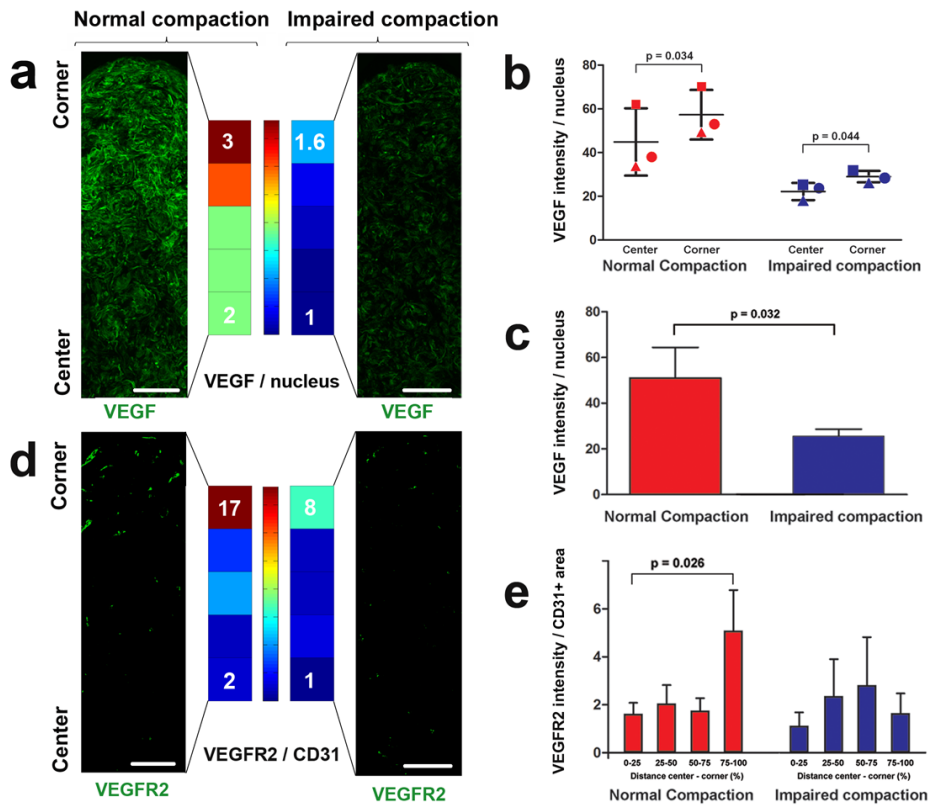


Fig. 4. Tissue contractility spatially regulates the angiogenic microenvironment through VEGF signaling. (a, b) Upon tissue compaction and deformation, a gradient of VEGF formed autonomously by graded production (a, left) which was impaired when tissue contractility was impaired (b, right). (c) The total expression of VEGF decreased by 2 folds when contractility was impaired (see also fig. S8). (d, e) Upon normal compaction, the VEGF receptor VEGFR2 was over-expressed in the peripheral region compared to the central region which was impaired when tissue contractility was impaired. Standard deviations are shown for $n=3$ samples \times 8 sections/sample.

Discussion

Taken together, these data show that endogenous tissue contractility can spatially regulate the angiogenic environment and angiogenesis. During branching morphogenesis of mouse lung epithelium, increased cell proliferation at distal sites of newly formed buds correlated with elevated cytoskeletal tension associated with the curvature (23). Similarly, endothelial cells can proliferate in response to mechanical stress (12, 24). These mechanisms might explain, in further investigations, how contractile forces generated within or in an adjacent tissue might have a long-range control over capillary formation with possible relevance in regenerative medicine (during tissue healing, angiogenesis is preceded by wound-contracting fibroblasts (25-26)) or in cancer biology (tumors are dependent on angiogenesis and stiffer than normal tissues due to an elevated endogenous tension (27)). Concomitantly with the classical model depicting a graded concentration of molecules diffusing from a source (28), here, contracting mesenchymal interstitial cells can form a gradient of molecules through compaction and graded production. This study demonstrates that complex behaviors can emerge from simple properties in engineered biological systems with an unexpected degree of self-organization. In addition to the realization of a critical step in tissue engineering, this system provides a platform for the direct and quantitative *in vitro* testing of a wide range of mechanisms during vascular development and homeostasis. This is, to the best of our knowledge, the first demonstration of a role for tissue contractility as a long-range mechanism coordinating morphogenesis through the formation of a gradient of a molecule and the local regulation of its corresponding receptor.

Materials and methods

Cell culture and reagents.

Human mesenchymal stem cells. Human Bone marrow aspirates were obtained from donors after written informed consent, and hMSCs were isolated and proliferated as follow. Aspirates were resuspended by using 20-gauge needles, plated at a density of 5×10^5 cells per square centimeter and cultured in hMSC proliferation medium containing α -MEM (Life Technologies), 10% FBS (Cambrex), 0.2 mM ascorbic acid (Asap; Life Technologies), 2 mM l-glutamine (Life Technologies), 100 units/ml penicillin (Life Technologies), 10 μ g/ml streptomycin (Life Technologies), and 1 ng/ml basic FGF (Instruchemie). Cells were grown at 37°C in a humid atmosphere with 5% CO₂. Medium was refreshed twice a week, and cells were used for further sub-culturing or cryopreservation. For experiments, the hMSC medium (termed Exp. Medium) was serum-free and composed of Dulbecco's Modified Eagle's Medium supplemented with 10⁻⁷ M dexamethasone, 50 mg/ml ascorbate 2-phosphate, 40 mg/ml proline, 100 mg/ml pyruvate, and 50 mg/ml ITS 1 Premix (Becton–Dickinson, MA: 6.25 mg/ml insulin, 6.25 mg/ml transferrin, 6.25 ng/ml selenious acid, 1.25 mg/ml bovine serum albumin, 5.35 mg/ml linoleic acid). Cells were trypsinised prior to seeding on agarose chips.

Human umbilical vein endothelial cells. Human umbilical vein endothelial cells (HUVECs) were purchased from Lonza (Lonza, group Ltd. Switzerland). Cells were grown at 37°C in a humid atmosphere with 5% carbon dioxide (CO₂) in endothelial growth medium-2 (Cambrex). Cells were routinely split at a 1:5 ratio and cultured in fewer than 5 passages. Only HUVECs from passage 3 or 4 were used to seed the coculture experiments.

Immunohistochemical analysis. After harvesting, tissues were frozen in Cryomatrix at -60°C. Sections (7 μ m) were cut with a cryotome. Sections were fixed in cold acetone for 5 min and air-dried. Sections were rehydrated for 10 min, after which they were incubated for 30 min with 10% FBS in PBS to block nonspecific background staining. Sections were incubated with monoclonal mouse anti-human CD31 antibody (Dako), a monoclonal rabbit anti-human VEGF Carboxyterminal end antibody (Abcam), a monoclonal rabbit anti-human VEGFR2 antibody (Cell Signaling), a rabbit anti-human HIF1 α antibody

(Abcam) or Phalloidin-Alexa fluor 488 conjugated antibody (Invitrogen) for 1 to 4 hours. Sections were washed in PBS and subsequently incubated with the secondary antibody (Alexa Fluor 488 or 594 antibody, Invitrogen). Samples were counterstained with Dapi (Sigma). Pictures were taken using a confocal microscope (Leica LSM500). Quantifications on fig. 3 and 4 were done on thresholded images. Quantification on fig. S5 was done without a threshold. A threshold was applied on images based on size and circularity (Image J) to select for the CD31+ structures which elongated in the main plane of the tissue in opposition to structures which did not elongate or elongated in another plane. Thresholded CD31+ structures were termed Capillary-Like Structures (CLS). For quantification of fig. 3 and 4, images were divided into 20 boxes from the center to the periphery. Each box was used for quantification of either the number of nuclei, the area of CLS, the intensity of VEGF fluorescence or the intensity of the VEGFR2 fluorescence. Results were used to create gradient color-maps or graphics.

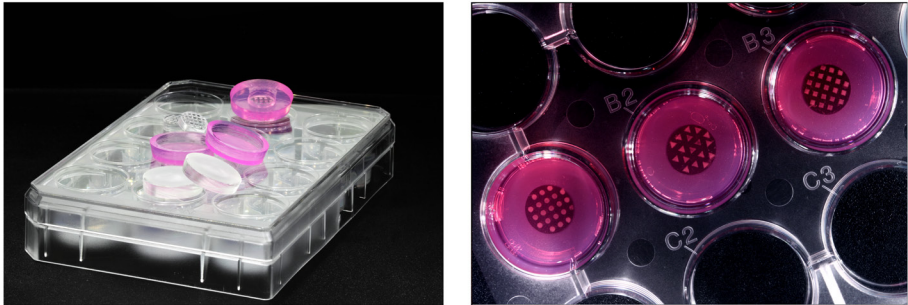
MicroWell Array (MWA) and Shaped Well Array (SWA) agarose chips. Micropatterned agarose chips for non-adherent cell culture were formed by replica molding. Patterned elastomeric stamps of poly(dimethylsiloxane) (PDMS; Sylgard 184, Dow Corning) were replicated from either etched silicone wafers or SU-8/silicone wafers and sterilized 10 minutes in 100% ethanol. A 4% agarose solution (Ultra pure agarose, Invitrogen) was casted on the PDMS stamp, demolded upon solidification and placed in a 12 well plate (S1). After wetting using corresponding Exp. medium (500 microliters), a concentrated suspension of cells (0.4 millions) was allowed to settle for 15 minutes on the chip. Excess cells were rinsed away with culture Exp. medium and 1.5 milliliters of Exp. medium was added. Cell clusters (~500 cells/cell cluster) spontaneously fused within 24 hours and could then be used as building blocks for tissue assembly. Half of the medium was changed every day of culture. After 150 hours of incubation on the MWAs, cell clusters were gently flushed out using Exp. medium, centrifuged (1300 rpm, 1 minute), resuspended in the Exp. medium and seeded on the SWAs. Cell clusters were allowed to settle in the wells for 1 minutes and excess cell clusters were washed away and seeded again for optimal seeding (~600.000 cells/tissue, thickness~250 μ m). The seeded chips were centrifuged (1300 rpm, 1 minute) and 1.5 milliliter of Exp. medium was added. Half of the medium was changed every day of culture.

Co-culture. A co-culture of 92% hMSC and 8% huVEC was used for all experiments. A total of 1.4 million cells was seeded on each MWAs containing 2800 wells. Cell clusters spontaneously formed within 24 hours and were further cultured for 160 hours. Cell clusters were then transferred to SWAs. Seven MWAs were used to seed a SWA of star shapes containing 15 tissues. Cell clusters were allowed to fuse for 24 hours. At this time point, Blebistatin (50 mM, Sigma-Aldrich) and Y-27632 (10 mM, Calbiochem) were added. Half the medium was replaced every day with constant total concentrations of 50 mM of Blebistatin and 10 mM of Y-27632 until day 5.

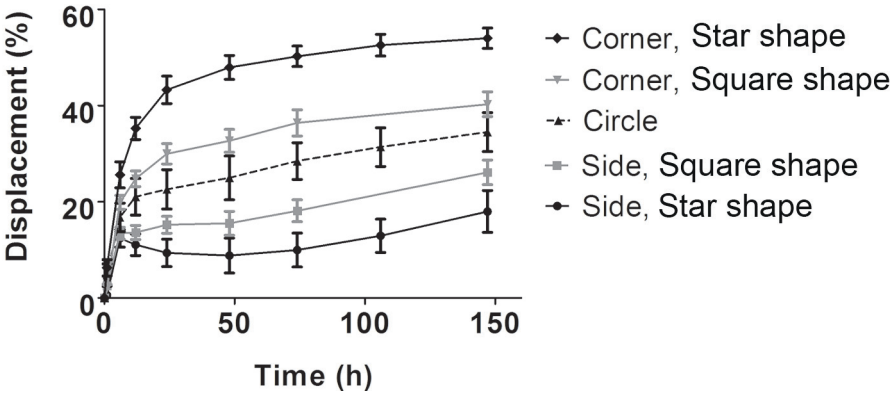
Quantification using color maps. Color maps (figures 3) show values, in 5 consecutive regions ranging from the tissue center to the tissue corners, of CLS density (scale from 1 to 4.8) and CLS/nucleus density (scale from 1 to 2.5) normalized to the central region. Values are an average of 24 images from 3 biological samples. The same scale is used for normal and impaired compaction. Contribution of tissue density to CLS density was measured as the expected CLS density due to a strict effect of compaction as compared to experimental CLS density. Color maps (figure 4) show values for VEGF density per nucleus (scale 1 to 3) and VEGFR2 intensity per CD31+ area (scale 1 to 17) in 5 consecutive regions ranging from the tissue center to the tissue corner and normalized to the region of weakest intensity of both normal and impaired compaction. Values are an average of 24 images from 3 biological samples.

Statistics. Differences between groups are determined using a Student's T-test as followed. Figure 2a, n=10, two-tailed distribution, unpaired samples. Figure 4b, n=3, two-tailed distribution, paired samples. Figure 4c, n=3, two-tailed distribution, unpaired samples. Figure 4e, n=3, two-tailed distribution, unpaired samples. Figure S5, n=3, two-tailed distribution, paired samples. Figure S6, n=3, two-tailed distribution, unpaired samples.

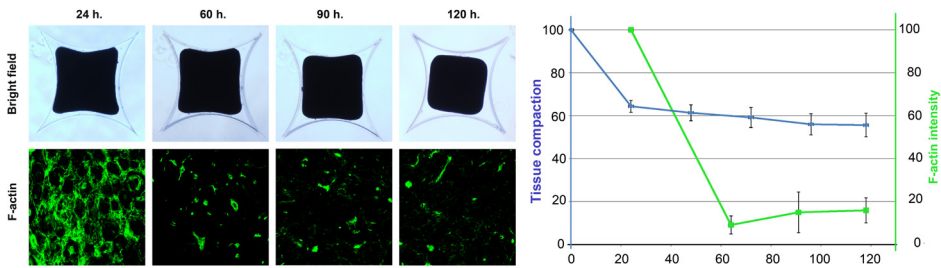
Supplementary informations



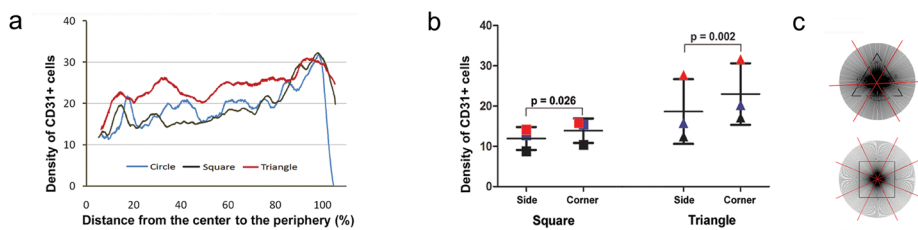
S1. Tissue arrays. Tissue arrays are routinely fabricated in agarose (pink templates, left picture) by replica molding from a silicone or SU-8 master via an intermediate Polydimethylsiloxane (PDMS) stamp with topographies (transparent template, left picture). Agarose templates are placed in conventional culture plates and used for non-adherent cell culture. Tissue arrays of disc-, triangle- and square-shaped tissues cultured on microfabricated agarose templates in a conventional 12-well plate.



S2. Tissue displacement. The displacement of tissue borders was measured as relative to the initial distance between the center and the border using bright field pictures (n=5). Displacement = 100 - % of the original distance. Standard deviations, n=10.

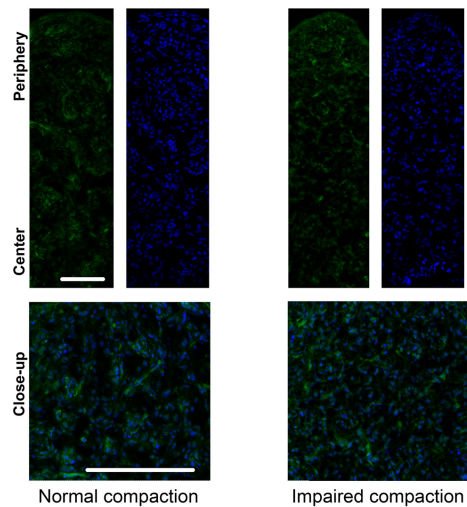


S3. The timeline of tissue compaction correlates with the F-actin intensity. Tissue compaction was assessed using bright field images and quantified by measuring the projected area of tissues (n=5). F-actin fluorescent intensity was assessed using a phalloidin staining and was quantified using an histogram plot (Image J)(Standard deviations, n=5).

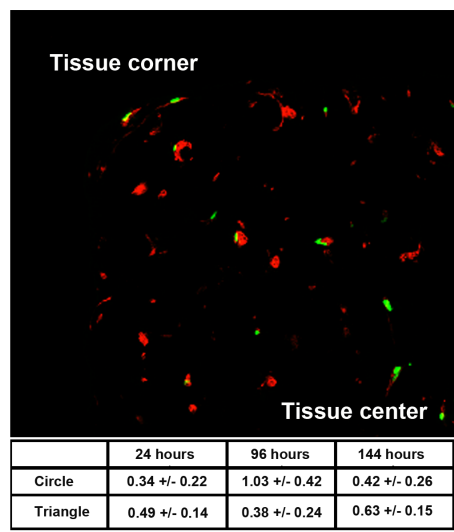


S4. Density of CD31+ cells. Radial Profile Plot were done using 5 images of the total cross-section of a tissue for 3 different biological samples. Image J (<http://rsbweb.nih.gov/ij/>) was used to produce a profile plot of normalized integrated intensities around concentric circles as a function of distance from a point in the image. The intensity at any given distance from the point represents the sum of the pixel values around a circle. This circle has the point as its center and the distance from the point as radius. The integrated intensity is divided by the number of pixels in the circle that is also part of the image, yielding normalized comparable values (see <http://rsb.info.nih.gov/ij/plugins/radial-profile.html>). For the density of CD31+ cells as a function of the distance from the center to the periphery (S5, a), values at similar distances on each spoke were averaged.

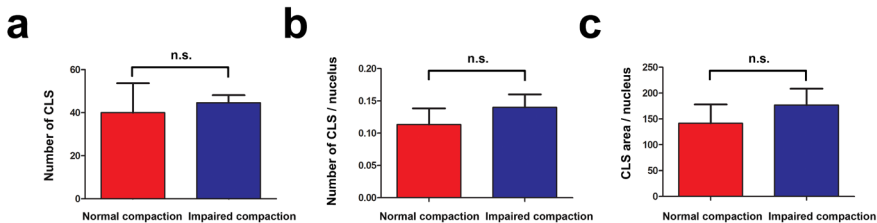
For the density of CD31+ cells in sides compared to corner (S5, b), shapes were divided into 6 or 8 equal areas, as depicted by the red spokes in c, values from each spoke and each area were averaged. The value is the average for one samples sides and its respective corners. The statistical significance is calculated using a T-Test (one tail distribution, paired, standard deviations, n=3).



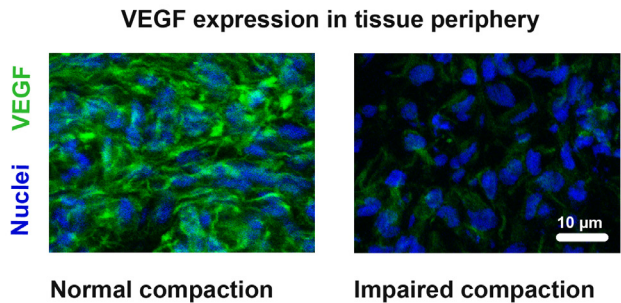
S5. Tissue hypoxia is homogeneous. Angiogenesis is mainly driven, during diseases and traumas, by local hypoxia which attract blood vessels through the activation of HIF1a which regulates VEGF production. HIF1a is constantly produced and degraded in the cytoplasm of cells and translocate to the nucleus upon hypoxia. Here, using antibody staining, we found that HIF1a is partly cytoplasmic and homogeneously expressed across the tissues. This suggest that the preferential formation of CLS and of VEGF production are not controlled by localized hypoxia. Scale bars are 100 micrometers.



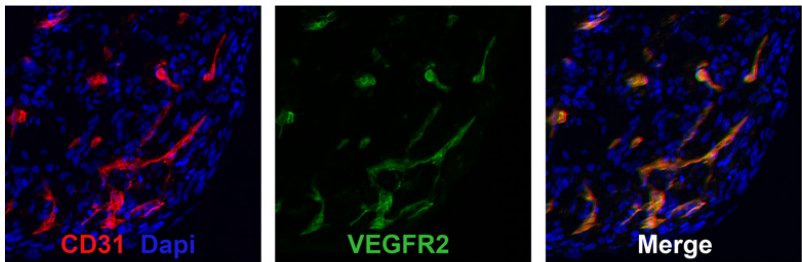
S6. Cellular proliferation. Cellular proliferation was assessed by BrdU incorporation over a period of 12 hours ending at 24, 96 and 144 hours of culture. Proliferating cells (green) are restricted to the CD31+ cells and are not limited to the tissue periphery (Standard deviations, n=3.).



S7. Average total number and area of CLS. The total average of number of CLS (a), number of CLS per nucleus (b) and CLS area per nucleus (c) were similar during normal compaction and impaired compaction. 24 images were quantified from 3 different samples. Statistical differences between normal compaction and impaired compaction was not significant (T-Test, one tail distribution, paired). Note that the wide phenotype of the CLS when compaction was impaired probably influenced the slight increase in the total CLS area. Standard deviations, $n=3$.



S8. VEGF is mainly cytoplasmic and overexpressed upon tissue contraction. VEGF production is visualized using a specific antibody for all isoforms. Left panel is a representative picture of VEGF intensity in the tissue periphery of compacting tissue. Right panel is a representative picture of VEGF intensity in the tissue periphery of tissues with impaired compaction.



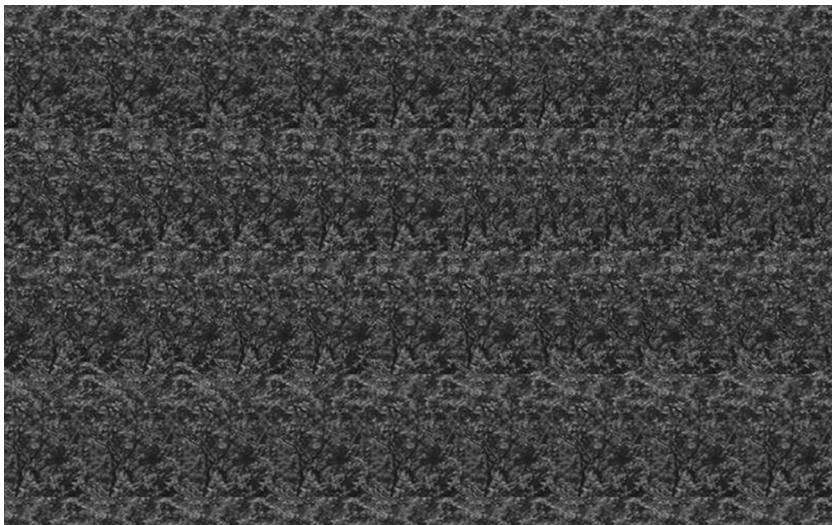
S9. VEGFR2+ cells strictly overlaps with CD31+ cells. CD31 and VEGFR2 in consecutive cuts.

1. N. Desprat, W. Supatto, P. A. Pouille, E. Beaupaire, E. Farge, *Dev Cell* **15**, 470 (Sep, 2008).
2. L. Hufnagel, A. A. Teleman, H. Rouault, S. M. Cohen, B. I. Shraiman, *Proc Natl Acad Sci U S A* **104**, 3835 (Mar 6, 2007).
3. M. A. Wozniak, C. S. Chen, *Nat Rev Mol Cell Biol* **10**, 34 (Jan, 2009).
4. A. Mammoto *et al.*, *Nature* **457**, 1103 (Feb 26, 2009).
5. P. Carmeliet, *Nat Med* **9**, 653 (Jun, 2003).
6. D. Shweiki, A. Itin, D. Soffer, E. Keshet, *Nature* **359**, 843 (Oct 29, 1992).
7. A. Shay-Salit *et al.*, *Proc Natl Acad Sci U S A* **99**, 9462 (Jul 9, 2002).
8. R. McBeath, D. M. Pirone, C. M. Nelson, K. Bhadriraju, C. S. Chen, *Dev Cell* **6**, 483 (Apr, 2004).
9. D. Zisa, A. Shabbir, G. Suzuki, T. Lee, *Biochem Biophys Res Commun* **390**, 834 (Dec 18, 2009).
10. J. Rouwkema, J. de Boer, C. A. Van Blitterswijk, *Tissue Eng* **12**, 2685 (Sep, 2006).
11. N. C. Rivron *et al.*, *Biomaterials* **30**, 4851 (Oct, 2009).
12. C. M. Nelson *et al.*, *Proc Natl Acad Sci U S A* **102**, 11594 (Aug 16, 2005).
13. T. Hayashi, R. W. Carthew, *Nature* **431**, 647 (Oct 7, 2004).
14. G. W. Brodland, *J Biomech Eng* **124**, 188 (Apr, 2002).
15. T. Lecuit, P. F. Lenne, *Nat Rev Mol Cell Biol* **8**, 633 (Aug, 2007).
16. A. J. Engler, S. Sen, H. L. Sweeney, D. E. Discher, *Cell* **126**, 677 (Aug 25, 2006).
17. M. Uehata *et al.*, *Nature* **389**, 990 (Oct 30, 1997).
18. P. A. Pouille, P. Ahmadi, A. C. Brunet, E. Farge, *Sci Signal* **2**, ra16 (2009).
19. S. Huang, D. E. Ingber, *Nat Cell Biol* **1**, E131 (Sep, 1999).
20. T. Matsumoto *et al.*, *PLoS One* **2**, e1211 (2007).
21. Y. C. Yung, J. Chae, M. J. Buehler, C. P. Hunter, D. J. Mooney, *Proc Natl Acad Sci U S A* **106**, 15279 (Sep 8, 2009).
22. V. Bassaneze *et al.*, *Stem Cells Dev*, (Sep 15, 2009).
23. H. Nogawa, K. Morita, W. V. Cardoso, *Dev Dyn* **213**, 228 (Oct, 1998).
24. C. S. Chen, M. Mrksich, S. Huang, G. M. Whitesides, D. E. Ingber, *Science* **276**, 1425 (May 30, 1997).
25. W. W. Kilarski, B. Samolov, L. Petersson, A. Kvanta, P. Gerwins, *Nat Med* **15**, 657 (Jun, 2009).
26. J. Rouwkema, N. C. Rivron, C. A. van Blitterswijk, *Trends Biotechnol* **26**, 434 (Aug, 2008).
27. J. Folkman, *N Engl J Med* **285**, 1182 (Nov 18, 1971).
28. L. Wolpert, *J Theor Biol* **25**, 1 (Oct, 1969).
29. We thank M. Berger, K. Ma and H. Unadkat for their technical suggestions and assistance; H. Tank and J. de Boer for comments on the manuscript. This work was supported by funds from the STW, The Netherlands, project TKG 6716.

Chapter 6

Tissue complexity

This chapter discusses the results of this thesis and gives an overview of currently known patterning mechanisms during vascular development. We then discuss current limits and restrictions in investigating and understanding the mechanisms of pattern formation in living organisms and the possible contribution of microfabricated multicellular systems.



Looking for the underlying pattern: Reality is hard to see.

Tissue complexity - or *how I learned to stop worrying and love biology*

1- What did we learn from these experiments?

Vascular development is a process central to tissue engineering and regenerative medicine and we speculate that *in vitro* engineered vasculatures will contribute to solve both therapeutic and fundamental problems in regenerative medicine.

First, due to its function in mass transport and its inductive role in organogenesis (i.e. liver [1], pancreatic [2] and others [3]) the vasculature is a critical therapeutic target to enhance tissue survival and to contribute to new tissue formation during regeneration processes. Second, the engineering of microfabricated *in vitro* models of vascular development will allow for the investigation of fundamental questions on vessel morphogenesis and pattern formation in a context more closely mimicking *in vivo* situations.

The first part of this thesis (**chapter 3**) is dedicated to the engineering of a vascularized graft as a template for endochondral bone regeneration. We showed the formation of a vasculature inside a graft, its *in vitro* maturation using the morphogen Sonic Hedgehog and its contribution to robustly improve the *in vivo* process of bone formation. These experiments demonstrate that only a mature vasculature can efficiently contribute to tissue formation. Indeed, the density of vascular lumens formed *in vitro* correlated with the density of lumens perfused *in vivo*. This raises questions on the stability of *in vitro* formed vascular structures and role of the flowing blood in selecting, maintaining and promoting further maturation of the engineered blood vessels. This approach aimed at mimicking the regenerative process of endochondral bone repair which is critically dependent on vascularization and occurs in large and mechanically challenged bone defects. We show for the first time the formation of clinically relevant amount of bone tissue from a vascularized graft, by a combination of intramembranous ossification and endochondral ossification. The remodeling of the graft observed *in vivo* is reminiscent of the formation of a bone callus during endochondral bone repair. Following the proof of concept experiment of pre-

vascularization [4] using cell lines (clinically non-applicable) for skeletal muscle tissue, we demonstrate the possibility to use pre-vascularization for endochondral bone formation using clinically relevant human primary cells and serum-free medium. These experiments open the possibility to form efficient grafts for the treatment of large and mechanically challenged bone defects.

The second part of this thesis (**chapter 4, 5**) is dedicated to the microfabrication of multicellular systems prone to autonomous remodeling and organization. Free-standing, geometric tissues were built using microfabricated templates, in a bottom-up approach, up to the centimeter-scale, . Using hMSC and huvEC, we demonstrate that these multicellular systems can autonomously and heterogeneously remodel their shape, spatially regulate the VEGF signaling by forming gradients of VEGF and VEGFR2 expression and form stereotyped patterns of vascular structures. This experiment demonstrate the possibility to form self-organizing artificial tissues which contract, deform and organize in ways reminiscent of naturally developing tissues. This is, to the best of our knowledge, the first experiment showing artificial tissues which stereotypically and autonomously remodel their shape and create stereotyped patterns. From the engineering point-of-view, this experiment shows the possibility to form, in parallel, high numbers of self-organizing tissues as building blocks to form grafts. From the scientific point-of-view, this experiment shows the possibility to investigate mechanisms of pattern formation in microfabricated tissues and suggest that the forms/boundaries of tissues and endogenous forces feed-back to control their remodeling and organization. During angiogenesis, the formation of VEGF gradients is thought to be mainly regulated by underlying gradients of hypoxia [5]. Concomitantly, here we propose that tissue forms/boundaries and endogenous forces can spatially regulate the VEGF signaling and angiogenesis thus integrate local signals at the global, tissue level.

2- Pattern formation during vascular development

In the following text, I will discuss the current knowledge regarding the morphogenesis and formation of organized patterns in the vascular tree which involves the formation of branches, their transformation into tubes, the control of their branching, size and direction.

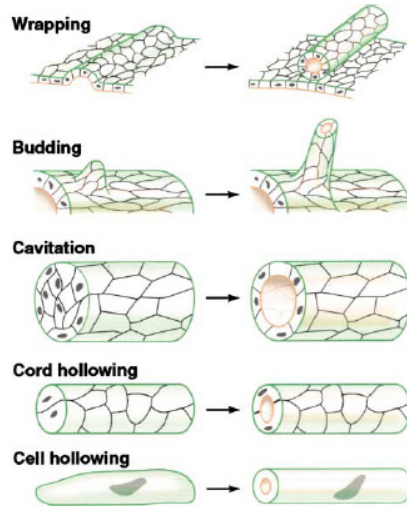
Vascular morphogenesis results from the combination of numerous overlapping processes: (i) processes not precisely controlled; for example, if vascular development occurs randomly to fill available space, (ii) precise iterative genetic processes at the microscale by repeated use of mechanisms, as in fractal models [6-7], (iii) self-organized processes meaning emergent processes resulting from numerous local fluctuating behaviors, (iv) template processes through guidance of environmental cues (i.e. the neuronal network, physical gradients of forces or gradients of soluble molecules, extracellular matrix or hypoxia). We will try to depict the respective contributions of each patterning process in forming and remodeling the vascular tree and describe the currently known underlying mechanisms.

Upon differentiation from mesodermal progenitor cells form round and unbranched blood islands which then elongates and sprout in cord-like structures. Upon interconnection, these structures form a non-hierarchical lattice (honeycomb-like structure), the plexus, which then lumenize. This process of plexus formation is probably guided by an underlying templates (i.e. hypoxia/VEGF gradients, neural guidance) [8] and is patterned by a Notch-Dll4 self-organization process [9].

Upon connection to the heart and the first heart-beat, this plexus progressively remodels into a fractal-like hierarchical network (i.e. tubes of different sizes) and specializes (i.e. acquisition of arterio-venous identity, tissue-specific identity). During remodeling, the control of vascular development is increasingly taken over by feedback signals derived from vascular function, including blood flow, pressure and tissue-specific cues including local metabolic state and tissue compliance [10-11]. The orderly structure of the vasculature emerges as each vascular segment reacts to the local conditions and stimuli that it experiences, according to a common set of genetically determined responses.

Classical descriptions of the morphogenetic movements resulting in tubular structures

suggest five different categories of wrapping, budding, cavitating, cord hollowing and cell hollowing (vesicle coalescence) [12]. Blood vessels have been observed to form by budding, cavitation, cord hollowing and cell hollowing.



Morphological processes of tube formation

Wrapping: a portion of an epithelial sheet invaginates and curls until the edges of the invaginating region meet and seal, forming a tube that runs parallel to the plane of the sheet..

Budding: a group of cells in an existing epithelial tube (or sheet) migrates out and form a new tube as the bud extends. The new tube is a direct extension of the original tube.

Cavitation: the central cells of a solid cylindrical mass of cells are eliminated to convert it into a tube.

Cord hollowing: a lumen is created de novo between cells in a thin cylindrical cord.

Cell hollowing: a lumen forms within the cytoplasm of a single cell, spanning the length of the cell.

(courtesy of B. Lubarsky)

Genetic control of vascular development. The initial specification of the endothelial progenitor cells and the early branching patterns are believed to be controlled by genetics (see table 1 in the appendix for references). This genetic control argues that specific clusters of genes are sequentially and reiteratively activated. Indeed, bFGF (basic Fibroblast Growth Factor) and VEGF are two molecules which are

critical for the differentiation of mesodermal progenitor cells into endothelial cells and bFGF is iteratively activated at branching sites during vascular development [13]. Molecular pathways are then modified at each stage of branching by genetic feedback controls to give distinct branching outcomes [14]. The expression of arterial and venous-specific molecules before the onset of the blood flow also argues for a genetic predetermination of the vasculature [15]. Sequential gene activation drives local molecular/cellular behaviors but explains with difficulties the spatial and temporal emergence of organization. Beyond genes, complementary organizing and regulatory principles are necessary [14, 16]. For instance, why is a specific mesodermal progenitor cell differentiating among a population and what controls the numbers and spatial distribution of mesodermal cells that will follow this differentiation path? What are the principles underlying the controlled organization of these endothelial cells into blood islands structures? Is this controlled by a genetically hardwired program including a genetic clock and pre-determined gene expression patterns or, for example, by random fluctuating, explorative behaviors and feedback controls? How are these genetic programs interacting with the physical environment?

Mechano-transductional control of vascular development. The seminal work of Donald E. Ingber argues for an important contribution of microscale cellular mechanical forces regulating the genetic expression patterns of endothelial cells [17]. This genetic interplay with physical forces permit to regulate the switch from proliferation to apoptotic and differentiation programs of endothelial cells [18]. Local mechanical deformations of the endothelial cells (external or endogenous forces) modulate cellular behavior through adherents cell junctions (i.e. cadherins), binding to the extra-cellular matrix (i.e. integrins) and the cytoskeleton (i.e. actin-myosin, Rho and Rac signaling)[19]. Similarly, at the multicellular level, internal patterns of stress can induce local proliferation [20] and the site of initiation of budding by local extracellular matrix remodeling [21]. These microscale mechanical forces might act as stabilizers channeling genetic expression and cellular behaviors during the differentiation and the assembly of vascular structures.

Local inhibition, competition and spacing control of vascular morphogenesis.

A question in vascular morphogenesis is how do some cells take on specific roles within a local group of cells? This problem was addressed through a process of local competition/inhibition [9]. Among fluctuating but relatively homogenous population of cells, a cell differentiate and simultaneously creates a local signal preventing neighboring cells to differentiate. The initial angiogenic sprouting and acquisition of the *tip* (leading) cell and *stalk* (following) cell phenotypes is based on gene expression (Notch/Dll4) but is dynamically organized through “social interactions” and lateral inhibition [9]. The *tip* phenotype is the default response to VEGF stimulation. VEGFR2 activation by VEGF-A results in the up-regulation of Dll4 ligands. Dll4 binds to Notch1 on neighboring cells, leading to the down-regulation of VEGFR2 [9]. Upon fluctuation and competition, a quantitative difference of Dll4 favors one cell follow the VEGF gradient and concomitantly prevents lateral cells from assuming the lead [9, 22-23]. Upon initial competition, cooperation might take place [23-24]. The iteration of the process allows the precise spacing between branching sites and the adequate ratio between *tip* and *stalk* cells required for correct sprouting and branching patterns. This self-organized process allows for the integration of molecular signals at the multicellular level and the coordination of a morphogenetic process. This conserved mechanism was described for tracheal [23] and vascular branching [9] but also for the regulation of the size of the developing wing of the *fruitfly* [25-26].

Channeling of the angiogenic sprout away from the mother vessel. Interesting mechanisms were discovered lately which are channeling and guiding the nascent angiogenic sprout away from the mother vessel. These mechanisms are based on the formation of short gradients of inhibitors along the mother vessel which prevent the sprouting vessel to form a closed loop back to the mother vessel. Nascent angiogenic sprouts are guided away by short gradients of inhibitors of the soluble molecule Flt-1 (VEGFR1) [27-28] or possibly by the sprouting inhibitor Tgf β [29] which are both produced by the mother vessel itself. Interestingly, the profile of the gradient is modulated by local remodeling events (i.e. remodeling of the extra-cellular matrix) and by the geometry of the of the blood vessel (the curvature of a blood vessel reduces the range of the gradient and thus favors sprouting). These mechanisms allow, in conjunction with exogenous

VEGF-A, for the local guidance of the sprout away from the mother vessel.

Flow control of vascular development. Haemodynamic flow continuously remodels the identity (i.e. arterial/venous identity) of blood vessels depending on local cues [30] and regulates the global patterning of arteries and veins in peripheral organs such as the yolk sac by selection/regression of vessels [11]. The flow selects capillaries of the initial plexus which then grow according to the forces they experience (positive feed-back loop). The enlargement is limited by the maximum pressure exerted by and the distance from the heart (negative feed-back loop). When the flow is stopped (heart removal), the vasculature spreads indefinitely by forming only small vessels [11]. Hemodynamic flow drives the fusion of small caliber vessels into large tubes, the selective disconnection and transfer of endothelial cells from the arterial system to the venous system and the guidance of lumenized vessel sprouts [30]. This adaptation relies on the local conditions and stimuli, according to a common set of genetically determined responses [31]. Numerous molecular elements are involved in the sensing and response to flow, from integrins and cadherins at the cell surface (see D.E. Ingber, above) to shear-stress-responsive-elements on gene promoters [30].

Hypoxia guidance of vascular development. As discussed in the introduction, hypoxia is a driving force of vascular development acting as an underlying template. Regions which become hypoxic upregulate HIF by stopping its degradation. Stable HIF1 α controls the expression of VEGF which attracts blood vessels through a graded production. The range of action is partly regulated by the diffusivity of the different isoforms of VEGF. Following vessel ingrowth in the target tissue, proper oxygenation results in a down regulation of HIF and a return to an homeostatic situation. This autonomous system provides a template for the directional growth of both tracheal [24] and vascular organs [32].

Nervous guidance of vascular development. The vascular system and the neuronal system develop alongside one another and uses common axon guidance molecules (see introduction). It is not known whether one comes first or not and possibly act as a guiding template for the other [33].

Tissue endogenous forces guidance of vascular development. Local mechanical properties of tissues (i.e. tissue compliance) and deformation fields has been often suggested to form a path which guides vascular development. Using mathematical modeling, it was shown that the endogenous forces exerted by the tissue is sufficient to remodel the vascular network and create straight vessels with regular branching angles [11]. In **chapter 5**, we show that the endogenous tissue contractility of the surrounding cellular environment can also provide patterning signals through a spatial regulation of the VEGF signaling and the formation of a gradient. This experiment suggest that the form/boundaries of tissues can feed-back to create an heterogeneous distribution of mechanical stress and VEGF signaling components leading to vascular pattern formation.

This synthesis of current state-of-the-art in patterning processes during vascular morphogenesis emphasizes the numerous overlapping patterning mechanisms and the difficulty to predict a vascular architecture *a priori*.

3- Investigating tissue morphogenesis using *in vitro* models

3-1 Morphogenesis as an emergent phenomena

Despite the complexity and intrinsic instability of biological systems (i.e. gene expression noise and fluctuation), tissues are incredibly robust to variations, stereotyped on large-scales and can self-repair. For example, many embryos ablated from part of their cells develop correctly, an adult liver partly ablated will re-grow to its initial size and newts can regenerate amputated limbs. From the engineering point-of-view, these properties are extremely inspiring.

Here we discuss evidences that tissue organization and morphogenesis results from system-level properties which emerge from large population of cells [34] according to sets of genetically pre-determined responses. Such organization is characterized by the emergence of structures at the global level of a system solely from numerous, iterative interactions among its lower level components [34] and regulated by positive and negative feed-back loops which are bridging *local* cell programs and *global* tissue behavior. Such emergent behavior and feedback control mechanisms produce complex and robust patterning behaviors in tissues [35]. The increasing importance of feed-back signals derived from vascular function (i.e. blood flow, tissue-specific metabolic state and compliance) and the local adaptation/organization of the vasculature according to local conditions and stimuli discussed previously are reflecting these large-scale self-organized mechanisms. In addition, the experiment in **chapter 5** and others [11, 18, 20, 29, 36-39] demonstrate that self-organization can lead to pattern formation in engineered multicellular system and opens opportunities to investigate these mechanisms *in vitro* and to apply them for tissue regeneration therapies.

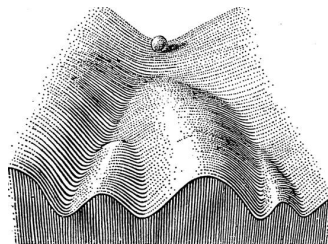
From this point of view, we will (i) discuss possible current restrictions in studying and understanding morphogenesis, (ii) an alternative experimental approach to the problem of pattern formation conducted in the field of self-organization, (iii) depict an example of emergent behavior during embryonic development and finally, (iv) discuss the possibility that microfabricated multicellular systems can provide integrated models to investigate the questions of emergence in morphogenesis.

3-2 Conceptual restrictions in understanding morphogenesis

Developing and regenerating tissues are complex systems. Despite the inventory of biological elements and their interconnections (human genome project, molecular biology), we still have a primitive understanding of the system-level dynamic leading to the organization of tissues, organs, organisms [40].

First, beyond their individual components (genes, proteins, RNA, microRNA, enzymes...), cells form signaling networks, protein complexes or protein interaction networks whose regulatory nature is not formally understood. Indeed, these regulatory networks use stochasticity (stochasticity during transcription [41-42]), noise (gene expression noise [43-45]) and fluctuation (transcriptome fluctuations [43]) to refine and extend their molecular and physical machinery. Molecular pathways form large networks using hypersensitivity (using microRNAs), by-pass and numerous feed-back loops to built tightly regulated and robust processes. These regulatory networks generate emergent behaviors which are probably as important as their individual components. For example, these emergent behaviors are currently thought to channel cell fate decision by creating attractor states leading for instance to cellular differentiation in discrete cell types [46] and the intrinsic heterogeneity of populations of cells [43, 47].

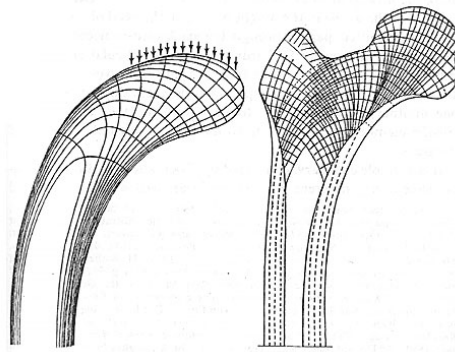
Over 50 years ago Waddington presented an epigenetic landscape as a metaphoric picture of development (see figure and appendix) [48]. This view was lately formalized by control theory and complex system theory and confirmed experimentally [43, 46, 49-51] which suggests that the control of cell fate by genes has both deterministic and stochastic elements. Complex regulatory networks define stable molecular states towards which individual cells are drawn over time, whereas stochastic fluctuations in gene and protein expression levels drive transitions between coexisting attractors, ensuring robustness at the population level.



Epigenetic landscape of Waddington. A metaphorical view of the modulation of development by genes, 1957 (see appendix).

These findings confirmed that (i) the regulatory patterns of biological networks are at least as important as the individual signaling components and (ii) that cell behaviors are channeled by these regulatory networks toward phenotypical states. There is thus a fundamental gap between understanding the components of the genetic and molecular pathways of cells and understanding cell behaviors, patterns of cell behaviors and multicellular organization. In this view, the classical approach of one gene *knock-out* is both powerful and limited. It proved useful for the few master-keys (i.e. VEGF [52-53]) which are critical nodes to the regulatory networks but do not permit to investigate less central genes (i.e. among many examples, PHD2 plays an important role during angiogenesis but knock-out mice for PHD2 have a normal phenotype [54]) whose disturbance can be *buffered* or compensated and do not give a phenotype.

Second, cells, tissues and organs are regulated by the physical environment. D'Arcy Thompson postulated in 1917, that the shape of organisms are directly imposed by the action of physical forces, by opposition to the internal (genetically-driven) forces [55]. For example, organisms of small size (and cells [38]) are shaped by surface tension whereas bigger animals are shaped by gravity. In his view, the shape of an object is a diagram of forces and physical constraints are orchestrating the organization of organisms.



Head of a crane (machine) and of a femur. From Culmann and Wolf, 1866. “The spatial arrangement of bone trabeculae are lines of physical constraint, the direction of the lines of tension and compression exerting on the structure under a physical load” (D’Arcy Thompson, On growth and forms).

Strikingly, while the organisms described by Thompson are objects whose life has been excluded, his intuition was lately proven experimentally. Macroscale mechanical forces (i.e. “Julius Wolf’s law” for bone remodeling), microscale tensional forces at the cell surface and inside the cell (tensegrity model of D.E. Ingber) [56], the osmotic swelling of cells [57-58], the surface tension-induced segregation of cells [37] or the shear of fluids [10, 59] are physical phenomena regulating genes/molecular signalling pathways, cellular phenotypes and tissue morphogenesis [40]. As depicted in **chapter 5**, beyond individual cells, tissues are shaped by emergent behaviors at the population level which arise from their interactions inside a physical frame (tissue form and contractility). Physical phenomena shape biological systems and can also be seen as attractors in the sense of Waddington: They channel the possibilities of biological forms.

Based on these observations, it is clear that the integration of genes and molecular networks in the study of multicellular organization will require to understand their emerging properties, the roles of stochasticity or the systemic control and regulatory mechanisms. This explains why, for example, a signal in a specific context will cause a cell to differentiate while elsewhere lead to mitosis and in a third context will induce cell death. In general, the outcome of the signaling event is not determined by the signal itself but by the physical and developmental state of the cell. While integrated on large-scales and regulated by feedback loops, these modulations give rise to patterned cellular behaviors and tissue architectures.

3-3 Pattern formation: learning from self-organization?

One important contribution to the study of systemic control and regulatory mechanisms in biology is the field of self-organization which is most successfully applied to the behavior of social animals [34]. Up to this point in this thesis, we used the term self-organization as a phenomenological, not as a mechanistic term, to depict the macroscale autonomous organization of the tissue. However, self-organization also refers to a range of pattern formation processes in the physical and biological world in which order and structures emerge at the global level of a system solely from numerous, iterative interactions among the lower level components of the system [34]. The rules specifying interactions among the system’s components are executed using only local information, using feed-forward and feed-back loops, without reference to the global pattern. Re-

markably, very complex structures result from the iteration of simple behaviors performed by individuals relying on only local information [34]. This is classically studied in colonies of social insects (i.e. ants or bees), sand grains assembling into rippled dunes but also in cells, tissues and organs: homeostasis (the self-maintaining nature of systems from the cell to the whole organism) or the chromatin and cytoskeletal assembly in cells (for precise example of self-organization in the cell, please see appendix) are two well studied examples of respectively large- and small scale self-organized phenomena. During tissue morphogenesis, the lamellar “plywood” structure of collagen fibers in bone lamellae (formed in **chapter 3**) result from a self-organization process: they are determined to a large extent by local stress-strain conditions and by the intrinsic chemical properties of the collagen molecules rather than being specifically cell-directed [60-63]. Interestingly, such organizational phenomena do not necessitate external guidance, blueprints, recipes or pre-existing templates (for counter-examples of self-organization, please see appendix).

This approach of organizational phenomena leading to pattern formation emphasize the importance of systemic regulatory networks. It uses relatively simple stimulus-response which are executed in a probabilistic manner and contrast with the complexity of the emergent collective phenomenon. Both chemically- and physically-induced feed-back loops initiate, control, regulate and stop the phenomena.

The interest of discussing the experimental approach in the field of self-organization in animal behaviors lies in its focus on the dynamic of control and regulatory mechanisms rather than on individual components. Beyond the simple analogy between morphogenesis and social animal behavior, the question lies in the possibility that self-organized processes also plays an important role during multicellular pattern formation.

In the first part of the thesis the CD31⁺ cells self-organize to form branched networks which are decently arranged, distributed, connected and stop growing at some point ; in the second part of this thesis, the tissues autonomously deform their shape up to a point of equilibrium (they do not round up) and spatially organized the VEGF signaling and the patterns of capillaries. The mechanisms involved allow for the emergence of patterns without external guidance or stimulation. It is though relevant to speculate that our vascular patterns are formed by self-organization or directed self-organization (because an initial shape is imposed using a template). In the first part of this thesis, a morphogen was used to

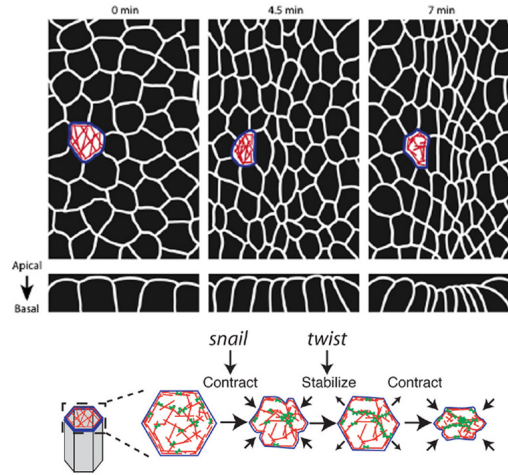
trigger several cellular processes (formation of vascular lumens, overexpression of collagen type X mRNA). Morphogens are, by definition signaling molecules which act directly on cells to produce specific cellular responses dependent on its concentration. As described in **chapter 3**, the distribution profile of the vascular lumens at a specific concentration of 10 nM was wider and normal as compared to other concentrations. This organization into a hierarchy and the normalization of the distribution profile of lumens is an emergent behavior of the vascular network. In the second part of the thesis, as described in **chapter 5**, the formation of the gradient of VEGF, the gradient of compaction and the vascular patterns can be seen as an emergent behavior of the multicellular construct and of the vascular network. The loss-of-function study (impaired compaction) show that the gradient of compaction, gradient of VEGF and vascular patterns arise from both the physical form of the tissue and the genetic regulatory network. Interestingly, the shape of the construct stabilize which suggest a negative feed-back of the remodeling probably due to a stabilization of the cell-cell interactions and to the production of extra-cellular-matrix. Further experiments are thus necessary to assess these regulatory loops.

3-4 Integrated models of pattern formation

3-4-1 Integrated *in vivo* models: *drosophila*

The study of epithelial invagination (wrapping) in *Drosophila* embryo is relevant of current restrictions in the study of morphogenesis [64-65]. Epithelial folding is observed in numerous developmental processes including mesoderm invagination. Apical cell contraction is thought to trigger the formation of a ventral furrow by changing the morphology of epithelial cells from cuboidal to bottle-shaped, which causes the tissue to bend and fold.

Global mechanism: This furrow was first thought to be formed by continuous, synchronous apical constriction of epithelial cells, driven by a purse-string-like contraction of a cortical actin-myosin ring underlying apical adherent junctions [66]. Live imaging ruled out this hypothesis and revealed a more complex process whereby asynchronous, discontinuous pulsatile contractions of cells are leading to a smooth global contractile movement at the tissue-scale. Each cell displays a pulsing behavior, alternating between phases of rapid contraction and pauses where the cell apical surface area remains stable [64].



“Ratchet” model of epithelial invagination of A.C. Martin & E.F. Wieschaus.

Genetic regulation: Cellular constriction occurs by iteration of two successive waves of contraction. The first wave is a stochastic process mediated by randomly positioned mesodermal cells (~40%) and is controlled by the transcription factor Snail. The second wave immediately follows and is controlled by the transcription factor Twist which maintains and stabilizes the constriction of the cells between two contractions (“ratchet” mechanism). The iterative process temporally involves Snail and Twist and drives productive apical constriction.

Mechanical positive feed-back: The invagination requires a spatial redistribution of the motor protein Myosin II to the apical side of the constricting cells. The mechanical tissue deformation creates a positive feed-back loop which enhances the process of Myosin II redistribution [65] since impaired redistribution of Myosin II and mesoderm invagination are rescued by local mechanical deformation of the mesoderm with a micromanipulated needle.

Emergent tissue behavior from local stochastic events: The global tissue contraction at a steady rate results from the integration of stochastic, asynchronous contractions of individual cells which are physically coupled through cell-cell interactions. As E. Paluch and CP Heisenberg wrote, “Chaos begets order” [67]. The emergence of a continuous behavior of the system at the tissue-level from asynchronous, discontinuous contractions in individual

cells has already been observed during convergent extension in *Xenopus* [68] and therefore may represent a conserved cellular mechanism that drives precise tissue level behavior.

This example, which is currently one of the most advanced in terms of integrating signals at different scales, depicts the current frontier in morphogenesis. Beyond the deterministic gene-centered view, morphogenesis also results from emergent behaviors resulting from the integration of local stochastic events. These studies are using a relatively simple organism as a powerful model (rapidity, throughput, genetic manipulation, imaging) and currently cannot be done in living mammals. However, they reveal conserved mechanisms and open a perspective for a coherent framework whereby local behaviors are integrated at the tissue-scale through self-organized, partly stochastic processes emerging from populations and which orchestrate the organization of tissues and organs.

3-4-2 Integrated *in vitro* models: microfabricated systems

How to transit from a gene/molecule centered approach to a system approach in studying morphogenesis? How can engineer contribute to an integrated approach to the problems of pattern formation?

A *next step* solution is to look at dynamic, quantitative processes in these systems, focusing on the sequence of cellular and molecular processes (actuation mechanisms, forward- and feed-back loop mechanisms) rather than on their nature (genes/molecules). Here we propose that microfabricated multicellular systems can give new insights into the emergence of tissue-scale mechanisms of pattern formation.

Microfabricated tissue models add the possibility to built *by design* experimental models of intermediate complexity, between current cell culture protocols and *in vivo* situations, which achieve the minimal level of structural complexity prone to induce organization.

What are the advantages and limitations of such artificial multicellular systems?

Technical advantages. As described above, the main advantage is to integrate the biological complexity in engineered controllable systems. Models of intermediate complexity can be assembled and designed at will. These systems theoretically allow for (i) precise variations on, for example, the forms and dimensions, (ii) the spatial patterning of different genetically modified cell populations, (iii) the parallel culture of numerous units for screening

purposes (only limited by the number of cells), (iv) an important control over the environment using for example microfluidics (local delivery of a soluble factor or siRNA), (v) an easy manipulation of the units (i.e. laser ablation to locally disrupt mechanical tension [69-70]) and (vi) the possibility for live imaging. They should prove useful to recapitulate slices of tissue development and regeneration. Interestingly, direct nuclear reprogramming techniques opened perspectives to provide patient-derived cell sources to build these models [71].

Scientific advantages. Microfabrication approaches allow for the study of systems intermediate complexity with defined characteristic. The parameters of morphogenetic processes can be decoupled and studied independently. To illustrate this in the context of vascular development, we depict two classical examples of (i) single cell and (ii) pairs of two cells behavior analysis on microfabricated templates.

This intermediate complexity was achieved at the single cell level in a seminal experiment by Christopher S. Chen. Endothelial cells attached on microfabricated islands of increasing sizes were physically stretched with a continuous variation of the cell shape from small and round to fully spread. This continuous variation resulted in discrete, abrupt changes from apoptosis to differentiation and proliferation [18, 39]. In an analogy to the abrupt phase transitions of inorganic materials which result from the emergent properties of the atomic network, the discrete cellular fates were thus described as emerging from the interactions of the molecular machinery and physical constraints [72].

Another example using groups of two endothelial cells patterned, in the shape of a Bowtie, on top of an array of mechanical sensors demonstrated that tugging force at cell-cell junction in itself modulates the size of the adherent junction through myosin and Rac1. The experimental set up allows for a precise decoupling of the intracellular cellular forces and the intercellular tugging force. This mechanism was shown to regulate the sensitivity of cells to physiological regulators of vascular permeability (thrombin, SP1) and coordinate the assembly and disassembly of cellular junctions, thus possibly providing a mean to dynamically remodel the permeability of blood vessels according to the mechanical signal they locally experience [73].

These two examples are involving either single cells or two cells coupled. Despite their apparent simplicity, these set up allowed to reproduce complex phenomena and the precise

measurements of the dynamic forces and molecular machinery involved. Current improvement in microfabrication techniques will allow for the patterning of larger populations of cells arranged in three-dimensional conformations and will help to investigate the dynamic of regulatory networks (i.e. feedback loops) and emergent behaviors leading to pattern formation and morphogenesis.

Limitation. These experiments are strongly hypothesis-driven or relies on grossly reproducing architectures mimicking the tissue of interest. The self-organization of the multicellular system depends on the adequate matching of the components (i.e. the cell source and cell state) with the design (multicellular pattern or dimensions matching the cell source and cell state). This necessitate important knowledge of the *in vivo* situations and thus should be conducted in parallel to *in vivo* observations recapitulating the complete program.

4- Is a formal approach to morphogenesis possible?

In parallel to the necessary reductionist approach making the inventory of the basic biological building blocks (genes, proteins, enzymes...) and their interactions, the systemic control and regulatory principles of morphogenesis can be investigated dynamically and quantitatively at the tissue-scale using integrated *in vitro* models.

Indeed, from the explosion of complexity revealed by genetic, biochemical and molecular biology aroused some unexpected perspectives: Despite inherent complexity, developing multicellular organisms use conserved mechanisms to orchestrate morphogenetic movements (i.e. tissue compaction, elongation, bending or tubulation). This opened a perspective for conceptual frameworks explaining the stereotyped organization of organisms which might be applicable from the fruitfly to the human, from embryos to adult tissues and from physiological to pathological tissues. It attenuate the idea that multicellular organization is too complex to be understood, recapitulated and thus manipulated for therapeutic applications. Instead, it suggested that multicellular organization is not necessarily refractory to generalization and conceptualization.

However, beyond genes and molecules, we are just starting to grasp the importance of systemic processes and feedback control mechanisms which are used to integrate signals at the tissue-scale. These processes are partly stochastic, emergent and self-organized and are strongly contributing to the precise, robust and versatile orchestration of morphogenesis. Interestingly, these processes bridge local cellular/molecular processes to the emergence of forms and patterns in tissues and thereby connect reductionism to complexity [74].

In parallel to the observation of complex living organisms, artificial multicellular system might contribute to investigating these phenomena *in vitro*, benefit to the study of morphogenesis and to the development of strategies to promote tissue regeneration during diseases or following traumas.

5- Appendix to the discussion

Self-organization in the cell. A large part of the organization of the cell depends on self-assembly processes that do not dissipate energy and are based on thermodynamic equilibrium (i.e. compartmentalization of the nucleus in domains). However detailed examples of intracellular self-organizing behaviors include the formation of the chromatin spindle during the cell cycle [75-77], microtubules [78-80] and the regulation of cell shape through actin-myosin complexes [81-82]. The relation of this last example to cellular function was done by looking at chemotaxis and cell polarization since polarization can occur in the absence of any cue through spontaneous symmetry breaking [83-86]. The study of the emergence of forms in biology partly lack the understanding of how dynamic interactions between agents can lead to the emergence of patterns. Here, based on experiments described in this thesis and on previously described work, we speculate that self-organization might plays a role in the morphogenesis process of branching organs.

Counterexamples of self-organization: These examples are taken from the book of Scott Camazine [34]. The concept of self-organization in biological systems can be conveyed through counterexamples. A marching band forming immense letters on a football field provides one such example. Here the band's members are guided in their behavior by a set of externally imposed instructions for the movements of each band member that specify in fine detail the final configuration of the whole band. A particular member of the band may know that the instructions are to march to the 50-yard line, turn left 90 degrees and march 10 paces. To the extent that the band member follows this recipe for contributing to the pattern and ignores local information, such as position relative to neighbors, this pattern formation would not be considered self-organized. Similarly, a team of carpenters building a house is a pattern-formation process that functions without self-organization. Here members of the construction crew are guided in their collective behavior by predetermined externally imposed instructions expressed as blueprints, that precisely specify the final structure of the house. Letter formation by a marching band and house construction by a construction crew both involve pattern building in space. Let us also consider two counterexamples to self-organization that involve pattern building over time. One such example is oarsmen in a rowing team pulling on their oars in perfect synchrony with one an-

other and with appropriate adjustments of their stroke frequency. This pattern arises when each oarsman responds to the coxswain's shouted instructions indicating when to begin each stroke. Clearly, this is an example of a group generating a pattern by following explicit orders from a leader based on the overall state of the group members. The rhythmic contractions of muscle fibers in the heart are also a counterexample to self-organization. Here the pattern arises as the component building blocks (the muscle fibers), follow instructions from special excitable cells that act as an external pacemaker and send a rhythmic electrical signal to the fibers.

Difference between self-organization and self-assembly: in physic and biology, two types of emergent behavior contribute to morphogenesis, self-organization and self-assembly. In both cases, the final structure arise from the integration of isolated components in a functional construct, however, two differences dissociate them. First, upon self-assembly, the elements and their properties are not affected by their integration whereas their insertion during a self-organized process modify their comportment, for example, their kinetic of reaction. Second, once formed, a self-organized structure remains dependant from an external source of energy or matter whereas a self-assembled structure is a stable entity, relatively autonomous.

Waddington's epigenetic landscape: Waddington's view was that development occurs similarly to a ball rolling down a sloping landscape containing multiple 'hills' and 'valleys': as development progresses, cells take different paths down this landscape and so adopt different fates. In this view, differentiation is not terminal, but instead different cell states are maintained by epigenetic barriers which are balanced states of the underlying regulatory system that can be overcome given sufficient perturbation. This intuition was lately confirmed by experiments which provided evidences of multiple attractor states and the possibility to switch from one to another at the single cell level owing to transcriptome-wide fluctuations in protein expression levels [43, 46]. This view is also suggested by the reprogramming experiments which demonstrated the possibility to go "back up the hill" to a pluripotent state [87] but also directly from one differentiated state to another [88] upon disturbance of the transcriptome.

1. Matsumoto, K., et al., *Liver organogenesis promoted by endothelial cells prior to vascular function*. Science, 2001. **294**(5542): p. 559-63.
2. Lammert, E., O. Cleaver, and D. Melton, *Induction of pancreatic differentiation by signals from blood vessels*. Science, 2001. **294**(5542): p. 564-7.
3. Red-Horse, K., et al., *Endothelium-microenvironment interactions in the developing embryo and in the adult*. Dev Cell, 2007. **12**(2): p. 181-94.
4. Levenberg, S., et al., *Engineering vascularized skeletal muscle tissue*. Nat Biotechnol, 2005. **23**(7): p. 879-84.
5. Shweiki, D., et al., *Vascular endothelial growth factor induced by hypoxia may mediate hypoxia-initiated angiogenesis*. Nature, 1992. **359**(6398): p. 843-5.
6. Mandelbrot, B.B., *Stochastic models for the Earth's relief, the shape and the fractal dimension of the coastlines, and the number-area rule for islands*. Proc Natl Acad Sci U S A, 1975. **72**(10): p. 3825-3828.
7. Nelson, T.R. and D.K. Manchester, *Modeling of lung morphogenesis using fractal geometries*. IEEE Trans Med Imaging, 1988. **7**(4): p. 321-7.
8. Drake, C.J., *Embryonic and adult vasculogenesis*. Birth Defects Res C Embryo Today, 2003. **69**(1): p. 73-82.
9. Hellstrom, M., et al., *Dll4 signalling through Notch1 regulates formation of tip cells during angiogenesis*. Nature, 2007. **445**(7129): p. 776-80.
10. le Noble, F., et al., *Flow regulates arterial-venous differentiation in the chick embryo yolk sac*. Development, 2004. **131**(2): p. 361-75.
11. Nguyen, T.H., et al., *Dynamics of vascular branching morphogenesis: the effect of blood and tissue flow*. Phys Rev E Stat Nonlin Soft Matter Phys, 2006. **73**(6 Pt 1): p. 061907.
12. Lubarsky, B. and M.A. Krasnow, *Tube morphogenesis: making and shaping biological tubes*. Cell, 2003. **112**(1): p. 19-28.
13. Carmeliet, P., *Fibroblast growth factor-1 stimulates branching and survival of myocardial arteries: a goal for therapeutic angiogenesis?* Circ Res, 2000. **87**(3): p. 176-8.
14. Metzger, R.J. and M.A. Krasnow, *Genetic control of branching morphogenesis*. Science, 1999. **284**(5420): p. 1635-9.
15. Herzog, Y., N. Guttman-Raviv, and G. Neufeld, *Segregation of arterial and venous markers in subpopulations of blood islands before vessel formation*. Dev Dyn, 2005. **232**(4): p. 1047-55.
16. Metzger, R.J., et al., *The branching programme of mouse lung development*. Nature, 2008. **453**(7196): p. 745-50.
17. Roth-Kleiner, M. and M. Post, *Genetic control of lung development*. Biol Neonate, 2003. **84**(1): p. 83-8.
18. Chen, C.S., et al., *Geometric control of cell life and death*. Science, 1997. **276**(5317): p. 1425-8.
19. Mammoto, A., T. Mammoto, and D.E. Ingber, *Rho signaling and mechanical control of vascular development*. Curr Opin Hematol, 2008. **15**(3): p. 228-34.
20. Nelson, C.M., et al., *Emergent patterns of growth controlled by multicellular form and mechanics*. Proc Natl Acad Sci U S A, 2005. **102**(33): p. 11594-9.
21. Moore, K.A., et al., *Control of basement membrane remodeling and epithelial branching morphogenesis in embryonic lung by Rho and cytoskeletal tension*. Dev Dyn, 2005. **232**(2): p. 268-81.
22. Phng, L.K. and H. Gerhardt, *Angiogenesis: a team effort coordinated by notch*. Dev Cell, 2009. **16**(2): p. 196-208.
23. Ghabrial, A.S. and M.A. Krasnow, *Social interactions among epithelial cells during tracheal branching morphogenesis*. Nature, 2006. **441**(7094): p. 746-9.
24. Ghabrial, A., et al., *Branching morphogenesis of the Drosophila tracheal system*. Annu Rev Cell Dev Biol, 2003. **19**: p. 623-47.
25. Day, S.J. and P.A. Lawrence, *Measuring dimensions: the regulation of size and shape*. Development, 2000. **127**(14): p. 2977-87.
26. Lawrence, P.A., *Morphogens: how big is the big picture?* Nat Cell Biol, 2001. **3**(7): p. E151-4.
27. Chappell, J.C., et al., *Local guidance of emerging vessel sprouts requires soluble Flt-1*. Dev Cell, 2009. **17**(3): p. 377-86.
28. Kappas, N.C., et al., *The VEGF receptor Flt-1 spatially modulates Flk-1 signaling and blood vessel*

- branching. *J Cell Biol*, 2008. **181**(5): p. 847-58.
29. Nelson, C.M., et al., *Tissue geometry determines sites of mammary branching morphogenesis in organotypic cultures*. *Science*, 2006. **314**(5797): p. 298-300.
30. le Noble, F., et al., *Neural guidance molecules, tip cells, and mechanical factors in vascular development*. *Cardiovasc Res*, 2008. **78**(2): p. 232-41.
31. Jones, E.A., F. le Noble, and A. Eichmann, *What determines blood vessel structure? Genetic pre-specification vs. hemodynamics*. *Physiology (Bethesda)*, 2006. **21**: p. 388-95.
32. Gerhardt, H., et al., *VEGF guides angiogenic sprouting utilizing endothelial tip cell filopodia*. *J Cell Biol*, 2003. **161**(6): p. 1163-77.
33. Carmeliet, P. and M. Tessier-Lavigne, *Common mechanisms of nerve and blood vessel wiring*. *Nature*, 2005. **436**(7048): p. 193-200.
34. Scott Camazine, J.-L.D., Nigel R. Franks, James Sneyd, Guy Theraulaz, & Eric Bonabeau, ed. *Self-Organization in Biological Systems*. Studies in complexity. 2003, Princeton University Press.
35. Freeman, M., *Feedback control of intercellular signalling in development*. *Nature*, 2000. **408**(6810): p. 313-9.
36. Farge, E., *Mechanical induction of Twist in the Drosophila foregut/stomodaeal primordium*. *Curr Biol*, 2003. **13**(16): p. 1365-77.
37. Foty, R.A., et al., *Liquid properties of embryonic tissues: Measurement of interfacial tensions*. *Phys Rev Lett*, 1994. **72**(14): p. 2298-2301.
38. Lecuit, T. and P.F. Lenne, *Cell surface mechanics and the control of cell shape, tissue patterns and morphogenesis*. *Nat Rev Mol Cell Biol*, 2007. **8**(8): p. 633-44.
39. McBeath, R., et al., *Cell shape, cytoskeletal tension, and RhoA regulate stem cell lineage commitment*. *Dev Cell*, 2004. **6**(4): p. 483-95.
40. Mammoto, T. and D.E. Ingber, *Mechanical control of tissue and organ development*. *Development*, 2010. **137**(9): p. 1407-20.
41. Kupiec, J.J., *A chance-selection model for cell differentiation*. *Cell Death Differ*, 1996. **3**(4): p. 385-90.
42. Degenhardt, T., et al., *Population-level transcription cycles derive from stochastic timing of single-cell transcription*. *Cell*, 2009. **138**(3): p. 489-501.
43. Chang, H.H., et al., *Transcriptome-wide noise controls lineage choice in mammalian progenitor cells*. *Nature*, 2008. **453**(7194): p. 544-7.
44. Raj, A. and A. van Oudenaarden, *Nature, nurture, or chance: stochastic gene expression and its consequences*. *Cell*, 2008. **135**(2): p. 216-26.
45. Kaern, M., et al., *Stochasticity in gene expression: from theories to phenotypes*. *Nat Rev Genet*, 2005. **6**(6): p. 451-64.
46. Huang, S., et al., *Cell fates as high-dimensional attractor states of a complex gene regulatory network*. *Phys Rev Lett*, 2005. **94**(12): p. 128701.
47. Huang, S. and D.E. Ingber, *A non-genetic basis for cancer progression and metastasis: self-organizing attractors in cell regulatory networks*. *Breast Dis*, 2006. **26**: p. 27-54.
48. Waddington, C., ed. *The strategy of the genes*. . ed. L. George Allen & Unwin. 1957.
49. Ma'ayan, A., et al., *Formation of regulatory patterns during signal propagation in a Mammalian cellular network*. *Science*, 2005. **309**(5737): p. 1078-83.
50. Basso, K., et al., *Reverse engineering of regulatory networks in human B cells*. *Nat Genet*, 2005. **37**(4): p. 382-90.
51. Tyson, J.J., K. Chen, and B. Novak, *Network dynamics and cell physiology*. *Nat Rev Mol Cell Biol*, 2001. **2**(12): p. 908-16.
52. Carmeliet, P., et al., *Abnormal blood vessel development and lethality in embryos lacking a single VEGF allele*. *Nature*, 1996. **380**(6573): p. 435-9.
53. Ferrara, N., et al., *Heterozygous embryonic lethality induced by targeted inactivation of the VEGF gene*. *Nature*, 1996. **380**(6573): p. 439-42.
54. Mazzone, M., et al., *Heterozygous deficiency of PHD2 restores tumor oxygenation and inhibits metastasis via endothelial normalization*. *Cell*, 2009. **136**(5): p. 839-51.
55. Thompson, D.A., ed. *On Growth and Form*. 1917 Cambridge University Press.

56. Ingber, D.E., *Cellular mechanotransduction: putting all the pieces together again*. FASEB J, 2006. **20**(7): p. 811-27.
57. Horner, V.L. and M.F. Wolfner, *Mechanical stimulation by osmotic and hydrostatic pressure activates Drosophila oocytes in vitro in a calcium-dependent manner*. Dev Biol, 2008. **316**(1): p. 100-9.
58. Adams, D.S., R. Keller, and M.A. Koehl, *The mechanics of notochord elongation, straightening and stiffening in the embryo of Xenopus laevis*. Development, 1990. **110**(1): p. 115-30.
59. Adamo, L., et al., *Biomechanical forces promote embryonic haematopoiesis*. Nature, 2009. **459**(7250): p. 1131-5.
60. Bouligand, Y., et al., *Twisted architectures in cell-free assembled collagen gels: study of collagen substrates used for cultures*. Biol Cell, 1985. **54**(2): p. 143-62.
61. Cisneros, D.A., et al., *Observing growth steps of collagen self-assembly by time-lapse high-resolution atomic force microscopy*. J Struct Biol, 2006. **154**(3): p. 232-45.
62. Kadler, K.E., et al., *Collagen fibril formation*. Biochem J, 1996. **316** (Pt 1): p. 1-11.
63. Shapiro, F., *Bone development and its relation to fracture repair. The role of mesenchymal osteoblasts and surface osteoblasts*. Eur Cell Mater, 2008. **15**: p. 53-76.
64. Martin, A.C., M. Kaschube, and E.F. Wieschaus, *Pulsed contractions of an actin-myosin network drive apical constriction*. Nature, 2009. **457**(7228): p. 495-9.
65. Pouille, P.A., et al., *Mechanical signals trigger Myosin II redistribution and mesoderm invagination in Drosophila embryos*. Sci Signal, 2009. **2**(66): p. ra16.
66. Ettensohn, C.A., *Mechanisms of epithelial invagination*. Q Rev Biol, 1985. **60**(3): p. 289-307.
67. Paluch, E. and C.P. Heisenberg, *Chaos begets order: asynchronous cell contractions drive epithelial morphogenesis*. Dev Cell, 2009. **16**(1): p. 4-6.
68. Keller, R., D. Shook, and P. Skoglund, *The forces that shape embryos: physical aspects of convergent extension by cell intercalation*. Phys Biol, 2008. **5**(1): p. 015007.
69. Rauzi, M., et al., *Nature and anisotropy of cortical forces orienting Drosophila tissue morphogenesis*. Nat Cell Biol, 2008. **10**(12): p. 1401-10.
70. Steinmeyer, J.D., et al., *Construction of a femtosecond laser microsurgery system*. Nat Protoc, 2010. **5**(3): p. 395-407.
71. Saha, K. and R. Jaenisch, *Technical challenges in using human induced pluripotent stem cells to model disease*. Cell Stem Cell, 2009. **5**(6): p. 584-95.
72. Ingber, D.E., *Mechanical control of tissue morphogenesis during embryological development*. Int J Dev Biol, 2006. **50**(2-3): p. 255-66.
73. Liu, Z., et al., *Mechanical tugging force regulates the size of cell-cell junctions*. Proc Natl Acad Sci U S A, 2010. **107**(22): p. 9944-9.
74. Whitesides, G.M. and B. Grzybowski, *Self-assembly at all scales*. Science, 2002. **295**(5564): p. 2418-21.
75. Hetzer, M., O.J. Gruss, and I.W. Mattaj, *The Ran GTPase as a marker of chromosome position in spindle formation and nuclear envelope assembly*. Nat Cell Biol, 2002. **4**(7): p. E177-84.
76. Karsenti, E. and I. Vernos, *The mitotic spindle: a self-made machine*. Science, 2001. **294**(5542): p. 543-7.
77. Misteli, T., *Beyond the sequence: cellular organization of genome function*. Cell, 2007. **128**(4): p. 787-800.
78. Carazo-Salas, R.E. and P. Nurse, *Self-organization of interphase microtubule arrays in fission yeast*. Nat Cell Biol, 2006. **8**(10): p. 1102-7.
79. Daga, R.R., et al., *Self-organization of microtubule bundles in anucleate fission yeast cells*. Nat Cell Biol, 2006. **8**(10): p. 1108-13.
80. Janson, M.E., et al., *Crosslinkers and motors organize dynamic microtubules to form stable bipolar arrays in fission yeast*. Cell, 2007. **128**(2): p. 357-68.
81. Backouche, F., et al., *Active gels: dynamics of patterning and self-organization*. Phys Biol, 2006. **3**(4): p. 264-73.
82. Piekny, A., M. Werner, and M. Glotzer, *Cytokinesis: welcome to the Rho zone*. Trends Cell Biol, 2005. **15**(12): p. 651-8.
83. Devreotes, P.N. and S.H. Zigmond, *Chemotaxis in eukaryotic cells: a focus on leukocytes and Dic-*

Chapter 6

tyostelium. Annu Rev Cell Biol, 1988. **4**: p. 649-86.

84. Xu, J., et al., *Divergent signals and cytoskeletal assemblies regulate self-organizing polarity in neutrophils*. Cell, 2003. **114**(2): p. 201-14.

85. Maly, I.V., H.S. Wiley, and D.A. Lauffenburger, *Self-organization of polarized cell signaling via autocrine circuits: computational model analysis*. Biophys J, 2004. **86**(1 Pt 1): p. 10-22.

86. Wedlich-Soldner, R. and R. Li, *Spontaneous cell polarization: undermining determinism*. Nat Cell Biol, 2003. **5**(4): p. 267-70.

87. Takahashi, K. and S. Yamanaka, *Induction of pluripotent stem cells from mouse embryonic and adult fibroblast cultures by defined factors*. Cell, 2006. **126**(4): p. 663-76.

88. Vierbuchen, T., et al., *Direct conversion of fibroblasts to functional neurons by defined factors*. Nature, 2010. **463**(7284): p. 1035-41.

Glossary

Angiogenesis: the formation of new blood vessels by sprouting and proliferation from an existing one.

Vasculogenesis: the formation of new blood vessels “de novo” from endothelial progenitor cells.

Chemotactic: movement by a cell or organism in reaction to a chemical stimulus

Complexity: complexity and complex systems generally refer to a system of interacting units that displays global properties not present at the lower level. These systems may show diverse responses that are often sensitively dependent on both the initial state of the system and nonlinear interactions among its components. Since these nonlinear interactions involve amplification or cooperativity, complex behaviors may emerge even though the system components may be similar and follow simple rules. Complexity in a system does not require complicated components or numerous complicated rules of interaction.

Conserved : A gene, molecule or mechanism that has remained essentially unchanged throughout evolution. Conservation of a gene, molecule or mechanism indicates that it is unique and essential and changes are likely to be lethal.

Emergence: defines the arising of patterns in complex systems, out of a collective multiplicity of relatively simple interactions. This term underlies the spontaneity of the transformation and the impossibility to predict the final structure from a single component (i.e. in contrary to crystal growth). An emergent property cannot be understood simply by examining in isolation the properties of the system's components, but requires a consideration of the interactions among the system's components.

Extra cellular matrix: An insoluble protein scaffold on which cells reside. The ECM provides the mechanical structure and attachment sites for soluble factors and signals through cell surface receptors. Epithelial cells, endothelial cells and adipocytes rest on a specialized ECM called the basement membrane.

Morphogenesis: from the Greek morphê shape and genesis creation. Formation of the ordered tissue structures during the development and regeneration of a multicellular organism. It occurs through the coordination of patterned cellular behaviors (differentiation, migration, growth and death) and tissue movements. The word Morphogenesis was introduced in 1789 by Goethe in The Metamorphosis of Plants.

Reductionism: empirical reductionism is methodological mode of analysis implying the dissection of a biological entity or system into its constituent parts in order to better understand it. Fundamentalist reductionism is a statement about the nature of the world: living systems can be completely understood in terms of the properties of their constituent parts. Fundamentalist reductionism does not require emergent behavior and explains the whole strictly with the sum of its parts (adapted from (1)).

Self-organization: a process in which pattern at the global level of a system emerges solely from numerous interactions among the lower level components of the system. Moreover, the rules specifying interactions among the system's components are executed using only local information, without reference to the global pattern. The word Self-organization was introduced by Kant (2)

1. C. R. Woese, Microbiol Mol Biol Rev 68, 173 (Jun, 2004).
2. E. Kant, Ed., Critique de la Faculté de Juger, (1790).

Summary

Tissue engineering and regenerative medicine aim at restoring a damaged tissue by respectively recreating the tissue *in vitro*, as an implant, or by directly promoting its regeneration *in vivo*. The vasculature is central to these therapies since (i) blood vessels allow for the irrigation the defective tissue with oxygen, nutrients or circulating regenerative cells and (ii) blood vessels play an important role in producing local signals inducing the development of the surrounding tissue (see chapter 1). This thesis describes the *in vitro* formation of biological vascular networks for tissue engineering and regenerative medicine applications.

In chapter 3 we show the formation of a vascularized tissue, using human mesenchymal stem cells (hMSC) and human umbilical vein endothelial cells (huvEC), which mimics *in vivo* some aspects of the natural regenerative process occurring in large bone defects (endochondral bone repair). *In vitro*, the two cell types aggregated and spontaneously formed a primitive vasculature. We used Sonic hedgehog (Shh), a powerful morphogen reactivated upon bone fracture, to promote further maturation of the vasculature (lumen formation, different lumen size, distribution). When implanted subcutaneously in mice, the vasculature connected with the vasculature of the mice, was perfused with blood and, concomitantly, bone and cartilage tissues formed. The *in vitro* maturation of the vasculature was essential to become functional *in vivo*: (i) *in vitro* maturation (Shh-treatment) enhanced the *in vivo* perfusion of the implant and (ii) only the mature vasculature (Shh-treatment) induced a robust and consistent increase in bone formation as compared to non-vascularized implants. The implants progressively remodeled in a process similar to endochondral bone repair, forming of a vascularized bone callus-like tissue: Direct bone formation occurred in the periphery of the implant while a cartilage tissue formed in the internal part which underwent hypertrophy, osteoclasts digestion and progressive replacement by bone. This resulted in the formation of a full bone organ with a trabecular-like bone structure, blood vessels and apparent bone-marrow cavities. These vascularized implants mimicked ectopically several aspects of the regenerative process of endochondral bone repair via the formation of a vascularized callus-like tissue. This opens opportunities

for the treatment of large, mechanically challenged bone defects.

In Chapter 4, we developed a microfabrication technique to form scaffold-free, three-dimensional, geometric tissues by sequential assembly of cells into microscale clusters and millimeter-scale tissues. We demonstrate the versatility and applicability of this method for differentiated cells, adult stem cells and embryonic stem cells. When formed by hMSC, the endogenous forces generated by the cells induced an heterogeneous and stereotypical deformation of the tissues according to their external and internal geometries. This method allows for the parallel formation of high numbers of self-remodeling tissues as building blocks to form tissues or organs.

Using this method, we investigated in Chapter 5 a novel mechanism of vascular pattern formation regulated by endogenous contractility and tissue geometry. Self-remodeling tissues formed with hMSC and hucEC deformed heterogeneously and stereotypically. Tissue corners and periphery induced more important deformations which led to the formation of internal gradients of cellular compaction, gradients of VEGF molecules and a local over-expression of the corresponding receptor VEGFR2. This resulted in a preferential growth and directionality (patterns) of the vascular structures in tissue peripheries and corners. Loss-of-function studies using pharmacological inhibitors of cellular force generating elements impaired the formation of vascular patterns. This experiment shows the microfabrication of tissues which autonomously self-remodeled and organize vascular patterns in vitro in a process mimicking the naturally deforming, developing tissues. We thus propose that endogenous tissue contractility and geometry might act as a long-range patterning mechanisms during vascular morphogenesis.

In conclusion, these experiments show the applicability of the concept of pre-vascularization for endochondral bone tissue engineering. We demonstrate the possibility to form vascularized tissues in vitro which recapitulate in vivo a process similar to the natural regeneration of large and mechanically challenged bone defects. We then show the in vitro microfabrication of self-remodeling and self-organizing tissues which prove useful to investigate a long-range process of vascular pattern formation driven by

Summary

tissue geometry and endogenous forces. Based on this work and others (see chapter 2), we speculate that microfabricated tissue models are powerful tools which will contribute to the investigation and understanding of emergent self-organizing processes integrating of genetic and molecular signals at the tissue scale and driving the organization of tissue patterns and morphogenesis.

Samenvatting

De vakgebieden weefseltechnologie en regeneratieve geneeskunde richten zich op het herstellen van beschadigd weefsel door het opnieuw maken van het weefsel in vitro, als implantaat, of het op directe manier bevorderen van het herstel in vivo. Het bloedvatenstelsel speelt een centrale rol bij deze therapieën, omdat (1) de bloedvaten zorg dragen voor toevoer van zuurstof, voedingsstoffen en in het bloed circulerende regeneratieve cellen naar het beschadigde weefsel, en (2) de bloedvaten een belangrijke rol spelen bij de totstandkoming van locale prikkels welke het omliggende weefsel stimuleren tot verdere ontwikkeling (zie hoofdstuk 1). Dit proefschrift beschrijft de vorming van bloedvatenstelsels in vitro voor toepassingen in weefseltechnologie en de regeneratieve geneeskunde.

In hoofdstuk 3 tonen we de in vitro vorming van een gevasculariseerd stukje weefsel aan met behulp van menselijke mesenchymale stamcellen (hMSC) en menselijke endotheelcellen van de navelstrengader (huvEC). Dit bootst enkele aspecten van de natuurlijke in vivo regeneratieve processen van grote botdefecten na (endochondraal botherstel). In vitro aggregeren de twee celtypen en vormen spontaan een primitief vasculair netwerk. Een krachtig ‘morphogen’ genaamd Sonic hedgehog (Shh) werd gebruikt om de verdere rijping van het vasculair netwerk te bevorderen (vorming van lumen, verscheidene lumen groottes). Bij het onderhuids implanteren van deze gekweekte weefsels in een muis verbond het vasculair netwerk met het bloedvatenstelsel van de muis en werd doorbloed. Als gevolg werd er bot- en kraakbeenweefsel gevormd. De in vitro rijping van het vasculair netwerk was essentieel om in vivo de juiste functie te vervullen: (1) in vitro rijping (behandeling met Shh) bevorderde de in vivo perfusie van het implantaat en (2) alleen na de rijping van het vasculair netwerk induceerde deze een robuuste en consistente toename van botvorming vergeleken met niet-gevasculariseerde implantaten. De implantaten ontwikkelden zich op een progressieve manier, vergelijkbaar met endochondrale botvorming. Hierbij werd een gevasculariseerd stukje callus-achtig botweefsel gevormd. Directe botvorming vond plaats in de periferie van het implantaat, terwijl kraakbeen weefsel zich vormde in de inwendige delen, waar er sprake was van hypertrofie, digestie van osteoclasten en pro-

gressieve substitutie door botweefsel. Dit resulteerde in de vorming van een volledig 'botorgaan' inclusief een trabeculair-achtige botstructuur, bloedvaten en 'beenmergholtes'. De ectopische implantatie van deze gevasculariseerde weefsels vertoont overeenkomsten met verscheidene facetten van het natuurlijke regeneratieve proces van endochondraal botherstel via de vorming van gevasculariseerd callus-achtig weefsel. Dit biedt mogelijkheden voor het behandelen van grote en mechanisch complexe bot defecten.

In hoofdstuk 4 beschrijven we de ontwikkeling van een microfabricage techniek voor het vormen van driedimensionale geometrische stukjes weefsel, zonder gebruik te maken van 'scaffolds'. In plaats daarvan worden cellen op microschaal samengevoegd tot clusters, waarna deze vervolgens worden samengevoegd tot millimeterschaal weefsels. We tonen de veelzijdigheid en toepasbaarheid van deze methode aan voor gedifferentieerde cellen, stamcellen en embryonale stamcellen. Wanneer deze stukjes weefsel gevormd worden door hMSCs, induceren de door cellen gegenereerde endogene krachten een heterogene en specifieke vervorming van het stukje weefsel, afhankelijk van de externe en interne geometrie. Deze methode staat ons toe om eenvoudig grote aantallen zelfvormende stukjes weefsel te vervaardigen die kunnen dienen als bouwstenen voor weefsels en organen.

In hoofdstuk 5 beschrijven we het gebruik van bovenstaande methode als een nieuwe manier voor het vormen van vasculaire patronen, gereguleerd door endogene samen-trekking van het weefsel in combinatie met de geometrie van het weefsel. Zelfvormende stukjes weefsel, gevormd uit hMSCs en huvECs, vervormden op een heterogene en stereotypische manier. De hoeken en de periferie van de stukjes weefsel induceerden de grootste vervormingen welke leidden tot de vorming van inwendige gradiënten van cellulaire dichtheid, VEGF moleculen en een locale over-expressie van de overeenkomstige VEGFR2 receptoren. Dit resulteerde in een voorkeursrichting en -groei (patronen) van vasculaire structuren in de periferie en hoeken van de stukjes weefsel. Een functieverlies studie, waarbij farmacologische remmers toegediend werden om de door cellen gegenereerde krachten in te perken, resulteerde in het ontbreken van de vorming van vasculaire patronen. Dit experiment toont de microfabricage van stukjes weefsel welke zich in vitro

autonoom vervormen en organiseren in vasculaire patronen in een proces welke de natuurlijke vervorming en ontwikkeling van weefsels nabootst. We stellen dus dat de endogene samentrekking en geometrie van weefsels als lange-afstand mechanisme zouden kunnen dienen voor de patroonvorming tijdens vasculaire morfogenese.

Concluderend tonen deze experimenten de toepasbaarheid aan voor het concept van pre-vascularisatie voor endochondrale botvorming in weefseltechnologie. De mogelijkheid wordt gedemonstreerd om gevasculariseerde stukjes weefsel te vormen in vitro welke in vivo een proces imiteren gelijkend op de natuurlijke regeneratie van grote, mechanisch complexe botdefecten. We laten daarna zien dat de in vitro microfabricage van zelfvervormende en zelforganiserende stukjes weefsel nuttig blijkt voor het onderzoeken van een lange-afstand proces van vasculaire patroonvorming gedreven door de geometrie van het weefsel en endogene krachten. We suggereren, gebaseerd op dit werk en dat van anderen (zie hoofdstuk 2), dat de microfabricage van weefselmodellen een krachtig hulpmiddel is om bij te dragen aan het onderzoek en begrip van zelforganiserende processen omtrent de integratie van genetische en moleculaire prikkels in weefsels en het sturen van de organisatie van weefselpatronen en morfogenese.

Nicolas C. Rivron received an engineering and a master degree in biology from Universite de Technologie de Compiègne (Compiègne, France). He then worked in the R&D department of Medtronic at the *Material and Bioscience Center* (Minneapolis, USA) and in the *Heart Valve Research Division* (Santa Ana, USA) before starting a PhD in the *Department of Tissue Regeneration* at University of Twente (Enschede, The Netherlands). The research was performed on engineering vascular development, under the supervision of Prof. Clemens A. van Blitterswijk, the results of which are described in this thesis. He will start a post-doctoral position at the Hubrecht Institute (Utrecht, The Netherlands) in the *Pluripotent stem cells in development and disease group* of Prof. Niels Geijsen and supervise PhD research projects in the *Department of Tissue Regeneration*. On a personal level, he loves traveling around the world especially in mountainous areas, musics with soul, taking pictures with vintage cameras, cooking and eating, and friends.

Acknowledgements

Four years in the Netherlands, so little change, so many changes. I would first like to thank Clemens van Blitterswijk for giving me a chance with this PhD, you opened a door for me and showed me a whole new world. I thank you for the freedom and trust you gave me, which definitely exceeded my own confidence. It has been, scientifically, a very exciting time. I sincerely thank you for this. I would like to especially thank two people who helped me, taught me, and without whom my projects would not have been the same: thank you so much to you, Jeroen Rouwkema, for all these discussions we had, for the supervision in the early days, for listening to me and helping me clarify my thoughts, thank you also for your friendship that will continue over the years. And thank you so much to you, Roman Truckenmüller, for helping me so much with the experiments, for stepping up my projects, for sharing sooooo many ideas and for being my very good friend. You are one creative person living your life deeply and with an integrity that I admire. Thank you to Veda, Nils, Anne, Chris and Erik for working with me and helping me to achieve this work during those years. I (mostly) liked working together with you and it wouldn't have been the same without you. Erik, I am very happy to make up and realize these projects with you. I am sure we will have some good exciting times together in the coming years. Thank you to you, Hemant, for being such an amazing, irritating, inspired, lunatic, inspirational, annoying, attaching, hopeless, cheerful, unreasonable and passionate person and for all the excellent cooking you did for me during these 4 years. We'll have to be friends for the best and the worst. Some encounter cannot happen only by chance. Thanks to you, my friend Gustavo, with whom I spent so much time. We are so alike and so different we could have been brothers. Thanks God for our putative mother, that did not happen. Thank you, Anand, for being, simply, my very good friend, a rock of tranquility, for sharing so many thoughts, laughter (and movies). You know where to put your priorities: Chess and Renuka (and vice versa) are definitely worth it. Let's go and play cards in Utrecht. Thank you so much to you, Lorenzo, for your mentorship and for inspiring us to make our own way, machete in hand, through the beautiful and dangerous jungle of academia. I admire very much your commitment, your amazing capacity of work but, most of all, Yourself as an amazing human being with a smile on your face. Hugo, a good education lasts for a lifetime! We share quite a few excellent, idiosyncratic memories together and there will be

more! Thank you for those good friendship times we had. I can't wait to see you at the bar of the conference, or at the city hall of Braga when you'll run it. Thank you Jun for your kindness, your help and all the good moments we shared. I wish you the best to you and to Nan and will surely see you again, somewhere. Thank you to you, Bin for all the good moments we spent together, for the diner sessions, the long discussions, for being an amazing outlier and my friend. Thank you Anouk for being such a nice person, a caring colleague and a mother to all of us: being so kind and understanding is unbelievable! Thank you Jacqueline for making the lab a good place to be. I don't blame you for keeping the Histolab so messy (aih... don't punch me!) and apologize for being such a useless supervisor and for spending all the money. Thank you to Pamela for discussing mostly non work-related things, it really makes a difference. Thank you Jan for your advices throughout those years and for the good times we had and will have outside the Lab. Thank you very much Joyce for making our life a little bit Orange and for all the good times we had playing foot-ball together. Thank you Alice for being an amazing person with a great heart and a great personality, now that I am done, we'll go dancing again. Thank you Ling for sharing about China, football and green tea. Thank you Anandita for being so fully yourself and making me laugh so much when we work together. One day, we'll make bone! Thank you to Ana for being a friend I always feel comfortable with: Life so simple, life so sweet. Une grosse accolade a mon ami Juan pour toutes les soirées infernales, les moments de folies douce et ses monologues interminables qui ont jalonné ces années. On en a pas fini, on peut aussi vivre en dehors. Thanks to you Hugo (Andre) for being my friend, you are a clever person and no one will stop you. I'll see you soon. Thank you to Nathalie, Jeroen, Lilianna, Bjorn, Charlene, Elie, Janneke, Karolina, Nicole for making the TR atmosphere so good. Thanks to my friends in BPE, Mariana, Vishnu, Remko and last but not least, Tom for the good times and the help with the Chameleon and Confocal. Thanks to my music teacher and friend Benny. I never spent so much time in a course dancing and chatting and so less time playing the instrument, you truly know what is important. I thank you for the good times in Bolwerk and in De Tor. Thank you very much to you, Martin for helping and teaching me the joy of photography, for your friendship and for the very good, cheerful times we had together. Thank you to you, Bojan for being my very good friend, I hope you the best, back in Serbia, we'll meet again. Un grand merci a Papa, mon père géniteur et scientifique, grand maitre en ingénierie, qui y est pour beaucoup dans mes choix de vie, a Maman qui m'a tant aidé moralement durant

Acknowledgement

ces années et dont je suis si proche. Merci à l'ainé (Charles), à ma sœur puînée (Juliette), au petit (Simon), à la benjamine (Fanny), au tout petit « celui qui n'est pas né » et à son père, Sébastien pour me supporter et me supporter. Merci à Gero, mon fils, ma bataille, le fruit de mes entrailles. Merci à toi, Anne-Laure, pour être une personne si incroyable et pour avoir partager avec moi tout ces moments. Tu es inoubliable.

Appendix

Table 1: Lessons from knockout mice (Courtesy of RK Jain, Nature Medicine 9, 685 - 693 (2003))

Ligand/receptors/pathways

Gene	Survival	Phenotype				Ref.
		Vasculogenesis	Angiogenesis	Vessel maturation	Other	
<i>Vegf-A</i>	E10.5	Abnormal differentiation of blood island	Impaired angiogenesis	Impaired lumen formation Impaired special vessel organization		.2
<i>Vegf-B</i>	Alive				Atrial conduction abnormality	.4
<i>Vegf120/188</i> <i>Vegf120/164</i>	Alive Alive			Impaired arterial development		
<i>Vegf164/188</i>	Death postnatally		Impaired myocardial angiogenesis	Ischemic cardiomyopathy		
<i>Pgf</i>	Alive		Impaired pathological angiogenesis			
<i>VegfR-1</i>	E8.5	Disorganized EC				
<i>VegfR-2</i>	E8.5-9.5	Absent yolk sac blood island Reduced hematopoietic precursors				
<i>VegfR-3</i>	E9.5			Enlarged vessel lumens Cardiovascular failure		0
<i>Nrp1</i>	Alive	Impaired neural vascularization Disorder yolk sac vascular network		Agensis and transposition of the great vessels Persistent <i>truncus arteriosus</i>		1,12

Gene	Survival	Phenotype				Ref.
		Vasculogenesis	Angiogenesis	Vessel maturation	Other	
		Impaired vascular sprouting at the central nervous system and pericardium				
<i>Nrp1/2</i>	E8.5	Avascular yolk sac				3
<i>Nrp2</i>	Alive			Reduction of small lymphatic vessels and capillaries		4
<i>Jagged1</i>	E10			defects in remodeling of the embryonic and yolk sac vasculature		5
<i>Notch1/4</i>				Defect of angiogenic vascular remodeling		6
<i>EphB2 / 3</i>	E11.5	Defects in the remodeling of embryonic vascular network		Defects in the remodeling of embryonic vascular network		7
<i>Ephrin-B2</i>	E9.5		Defects in angiogenesis by both arteries and veins in the capillary network of the head and yolk sac	Defect of myocardial trabeculation		7-19
<i>Pdgf-A</i>	E10 or postnatal death				Loss of alveolar myofibroblasts Reduced number of oligodendrocytes Dysmyelination	0,21

Appendix

Gene	Survival	Phenotype				Ref.
		Vasculogenesis	Angiogenesis	Vessel maturation	Other	
					ion	
<i>Pdgf-B</i>	E17.5-18.5			Lack of pericyte Microvascular aneurysms		2,23
<i>Pdgf-Rα</i>	Death at birth				Abnormal neural crest development Abnormal somite pattern	4
<i>Pdgf-Rβ</i>	Death at birth				Hemorrhage, thrombocytopenia, anemia	5
<i>Edg-1</i>	E12.5-14.5			Deficiency of vascular smooth muscle cells/pericyte		6
<i>Edg-3</i>	Alive					7
<i>Galpa13</i>	Intra-uterin death		Impaired ability of endothelial cell to develop into organized vascular system	Impaired fibroblast movement		8
<i>Ang1</i>	E10.5			Dilated vessel Impaired vessel branching		9
<i>Ang2</i>	Alive	Incomplete development of the superficial vascular bed of the retina	Absence of the intermediate and deep vascular bed of the retina		Lymphatic defect	0,31

<i>Tie-1</i>	E13.5-14.5 Death immediately after birth			Leaky vessels, Edema Leaky vessels, Small heart	unexpanded alveoli	2,33
<i>Tie-2</i>	E10.5			Dilated vessels Impaired vessel branching		3
<i>Tgf-β1</i>	Alive or E10.5	Deficient extraembryonic hematopoiesis		Poor EC differentiation and hematopoiesis		4
<i>Tgf-βRII</i>	E10.5	Defects in yolk sac hematopoiesis and vasculogenesis				5
<i>Alk1</i>	E11.5			Severe arteriovenous malformation		6,37
<i>Alk5</i>	E10.5-11.5			Severe defects in vascular development	Absence of circulating red blood cell	8
<i>Endoglin (Tgf-βRIII)</i>	E11.5			Poor vascular SMC development Arrested EC remodeling		9
<i>Smad2</i>	Perigastrulation lethality				Defective in extraembryonic and mesoderm induction/formation Abnormalities in anterior-posterior axis formation	0-42
<i>Smad3</i>	1-10 months after birth				Accelerate wound healing	3-45
<i>Smad5</i>	E9-11.5		Defect of angiogenesis	Mesenchymal apoptosis	gut heart and craniofacial defect	6,47
<i>Fgf-2</i>	Alive			Delayed skin wound healing	Abnormal cortical neurogenesis	8,49
<i>Syk/Slp-76 pathway</i>	Alive				Failure to separate emerging lymphatic vessels from blood vessels	0

Appendix

Molecules of cell-cell interaction

Gene	Survival	Phenotype				ef.
		Vasculogenesis	Angiogenesis	Vessel maturation	Other	
<i>Ve-cadherin</i>	E9.5			Impaired vascular remodeling and maturation		1,52
<i>Cx37/40</i>	Perinatal death			Vessel dilatation and congestion especially in skin, testis, gastrointestinal tissue and lung		3
<i>Cx40</i>	Alive				Lower atrial and ventricular conduction velocity	4
<i>Cx43</i>	Death at birth			Right ventricular outflow tract obstruction		5
<i>Cd31</i>	Alive					6
Gene	Survival	Phenotype				ef.
		Vasculogenesis	Angiogenesis	Vessel maturation	Other	
<i>Cd148</i>	E11.5			Enlarged primitive vessels defective in vascular remodeling and branching with impaired pericyte investment adjacent to endothelial structure		7

Molecules of cell-matrix interactions

Gene	Survival	Phenotype				ef.
		Vasculogenesis	Angiogenesis	Vessel maturation	Other	
$\alpha_v\beta_3$	Alive				Defects in platelet aggregation and clot retraction, prolonged bleeding times, and cutaneous and gastrointestinal bleeding	8
$\alpha_v\beta_5$	Alive					9
β_8 <i>integrins</i>	midgestation			Distended and leaky capillary vessels and aberrant brain capillary pattern		0
<i>Mmp-2</i>	Alive					1
<i>Mmp-3</i>	Alive					2
<i>Pai-1</i>	Alive					3,64
<i>Tsp-1</i>	Alive				Impaired pulmonary homeostasis	5
Gene	Survival	Phenotype				ef.
		Vasculogenesis	Angiogenesis	Vessel maturation	Other	
<i>Tsp-2</i>	Alive			Increased vascular density	Abnormal bleeding time	6
<i>uPa</i>	Alive					7
<i>Collagen XVIII</i>	Alive				Eye abnormality	8

Appendix

Transcription factors

Gene	Survival	Phenotype				ef.
		Vasculogenesis	Angiogenesis	Vessel maturation	Other	
<i>Hey2</i> (<i>glidlock</i>)	Immediately after birth			Cardiac hypertrophy		9
<i>Bmx</i>	Alive					0
<i>Hif1α</i>	E11	Complete lack of cephalic vascularization		Cardiovascular malformation	Neural tube defect Reduction in the number of somites and abnormal neural fold formation	1,72
<i>Id1/3</i>	E10.5			Vascular malformation in the forebrain Absence of branching and sprouting of vessels into the neuroectoderm		3
<i>c-Myc</i>	E10.5	Profound defect of vasculogenesis			Defect of primitive erythrocytogenesis	4
<i>Prox1</i>	Alive				Budding and sprouting arrest and lymphatics defect	5

1. Carmeliet, P. et al. Abnormal blood vessel development and lethality in embryos lacking a single VEGF allele. *Nature* 380, 435-9 (1996).
2. Ferrara, N. et al. Heterozygous embryonic lethality induced by targeted inactivation of the VEGF gene. *Nature* 380, 439-42 (1996).
3. Aase, K. et al. Vascular endothelial growth factor-B-deficient mice display an atrial conduction defect. *Circulation* 104, 358-64 (2001).
4. Bellomo, D. et al. Mice lacking the vascular endothelial growth factor-B gene (*Vegfb*) have smaller hearts, dysfunctional coronary vasculature, and impaired recovery from cardiac ischemia. *Circ Res* 86, E29-35 (2000).
5. Stalmans, I. et al. Arteriolar and venular patterning in retinas of mice selectively expressing VEGF isoforms. *J Clin Invest* 109, 327-36 (2002).
6. Carmeliet, P. et al. Impaired myocardial angiogenesis and ischemic cardiomyopathy in mice lacking the vascular endothelial growth factor isoforms VEGF164 and VEGF188. *Nat Med* 5, 495-502 (1999).
7. Luttun, A. et al. Loss of placental growth factor protects mice against vascular permeability in pathological conditions. *Biochem Biophys Res Commun* 295, 428-34 (2002).
8. Fong, G.H., Rossant, J., Gertsenstein, M. & Breitman, M.L. Role of the Flt-1 receptor tyrosine kinase in regulating the assembly of vascular endothelium. *Nature* 376, 66-70 (1995).
9. Shalaby, F. et al. Failure of blood-island formation and vasculogenesis in Flk-1-deficient mice. *Nature* 376, 62-6 (1995).
10. Dumont, D.J. et al. Cardiovascular failure in mouse embryos deficient in VEGF receptor-3. *Science* 282, 946-9 (1998).
11. Kawasaki, T. et al. A requirement for neuropilin-1 in embryonic vessel formation. *Development* 126, 4895-902 (1999).
12. Yamada, Y. et al. Neuropilin-1 on hematopoietic cells as a source of vascular development. *Blood* 101, 1801-9 (2003).
13. Takashima, S. et al. Targeting of both mouse neuropilin-1 and neuropilin-2 genes severely impairs developmental yolk sac and embryonic angiogenesis. *Proc Natl Acad Sci U S A* 99, 3657-62 (2002).
14. Yuan, L. et al. Abnormal lymphatic vessel development in neuropilin 2 mutant mice. *Development* 129, 4797-806 (2002).
15. Xue, Y. et al. Embryonic lethality and vascular defects in mice lacking the Notch ligand *Jagged1*. *Hum Mol Genet* 8, 723-30 (1999).
16. Krebs, L.T. et al. Notch signaling is essential for vascular morphogenesis in mice. *Genes Dev* 14, 1343-52 (2000).
17. Adams, R.H. et al. Roles of ephrinB ligands and EphB receptors in cardiovascular development: demarcation of arterial/venous domains, vascular morphogenesis, and sprouting angiogenesis. *Genes Dev* 13, 295-306 (1999).
18. Wang, H.U., Chen, Z.F. & Anderson, D.J. Molecular distinction and angiogenic interaction between embryonic arteries and veins revealed by ephrin-B2 and its receptor Eph-B4. *Cell* 93, 741-53 (1998).
19. Gerety, S.S. & Anderson, D.J. Cardiovascular ephrinB2 function is essential for embryonic angiogenesis. *Development* 129, 1397-410 (2002).
20. Bostrom, H. et al. PDGF-A signaling is a critical event in lung alveolar myofibroblast development and alveogenesis. *Cell* 85, 863-73 (1996).
21. Fruttiger, M. et al. Defective oligodendrocyte development and severe hypomyelination in PDGFA knockout mice. *Development* 126, 457-67 (1999).
22. Leveen, P. et al. Mice deficient for PDGF B show renal, cardiovascular, and hematological abnormalities. *Genes Dev* 8, 1875-87 (1994).
23. Lindahl, P., Johansson, B.R., Leveen, P. & Betsholtz, C. Pericyte loss and microaneurysm formation in PDGF-B-deficient mice. *Science* 277, 242-5 (1997).
24. Soriano, P. The PDGF alpha receptor is required for neural crest cell development and for normal patterning of the somites. *Development* 124, 2691-700 (1997).

25. Soriano, P. Abnormal kidney development and hematological disorders in PDGF beta-receptor mutant mice. *Genes Dev* 8, 1888-96 (1994).
26. Liu, Y. et al. Edg-1, the G protein-coupled receptor for sphingosine-1-phosphate, is essential for vascular maturation. *J Clin Invest* 106, 951-61 (2000).
27. Ishii, I. et al. Selective loss of sphingosine 1-phosphate signaling with no obvious phenotypic abnormality in mice lacking its G protein-coupled receptor, LP(B3)/EDG-3. *J Biol Chem* 276, 33697-704 (2001).
28. Offermanns, S., Mancino, V., Revel, J.P. & Simon, M.I. Vascular system defects and impaired cell chemokinesis as a result of G α 13 deficiency. *Science* 275, 533-6 (1997).
29. Suri, C. et al. Requisite role of angiopoietin-1, a ligand for the TIE2 receptor, during embryonic angiogenesis. *Cell* 87, 1171-80 (1996).
30. Hackett, S.F., Wiegand, S., Yancopoulos, G. & Campochiaro, P.A. Angiopoietin-2 plays an important role in retinal angiogenesis. *J Cell Physiol* 192, 182-7 (2002).
31. Gale, N.W. et al. Angiopoietin-2 is required for postnatal angiogenesis and lymphatic patterning, and only the latter role is rescued by Angiopoietin-1. *Dev Cell* 3, 411-23. (2002).
32. Puri, M.C., Rossant, J., Alitalo, K., Bernstein, A. & Partanen, J. The receptor tyrosine kinase TIE is required for integrity and survival of vascular endothelial cells. *Embo J* 14, 5884-91 (1995).
33. Sato, T.N. et al. Distinct roles of the receptor tyrosine kinases Tie-1 and Tie-2 in blood vessel formation. *Nature* 376, 70-4 (1995).
34. Dickson, M.C. et al. Defective haematopoiesis and vasculogenesis in transforming growth factor-beta 1 knock out mice. *Development* 121, 1845-54 (1995).
35. Oshima, M., Oshima, H. & Taketo, M.M. TGF-beta receptor type II deficiency results in defects of yolk sac hematopoiesis and vasculogenesis. *Dev Biol* 179, 297-302 (1996).
36. Urness, L.D., Sorensen, L.K. & Li, D.Y. Arteriovenous malformations in mice lacking activin receptor-like kinase-1. *Nat Genet* 26, 328-31 (2000).
37. Oh, S.P. et al. Activin receptor-like kinase 1 modulates transforming growth factor-beta 1 signaling in the regulation of angiogenesis. *Proc Natl Acad Sci U S A* 97, 2626-31 (2000).
38. Larsson, J. et al. Abnormal angiogenesis but intact hematopoietic potential in TGF-beta type I receptor-deficient mice. *Embo J* 20, 1663-73 (2001).
39. Li, D.Y. et al. Defective angiogenesis in mice lacking endoglin. *Science* 284, 1534-7 (1999).
40. Weinstein, M. et al. Failure of egg cylinder elongation and mesoderm induction in mouse embryos lacking the tumor suppressor smad2. *Proc Natl Acad Sci U S A* 95, 9378-83 (1998).
41. Nomura, M. & Li, E. Smad2 role in mesoderm formation, left-right patterning and craniofacial development. *Nature* 393, 786-90 (1998).
42. Waldrip, W.R., Bikoff, E.K., Hoodless, P.A., Wrana, J.L. & Robertson, E.J. Smad2 signaling in extraembryonic tissues determines anterior-posterior polarity of the early mouse embryo. *Cell* 92, 797-808 (1998).
43. Datto, M.B. et al. Targeted disruption of Smad3 reveals an essential role in transforming growth factor beta-mediated signal transduction. *Mol Cell Biol* 19, 2495-504 (1999).
44. Yang, X. et al. Targeted disruption of SMAD3 results in impaired mucosal immunity and diminished T cell responsiveness to TGF-beta. *Embo J* 18, 1280-91 (1999).
45. Ashcroft, G.S. et al. Mice lacking Smad3 show accelerated wound healing and an impaired local inflammatory response. *Nat Cell Biol* 1, 260-6 (1999).
46. Chang, H. et al. Smad5 knockout mice die at mid-gestation due to multiple embryonic and extraembryonic defects. *Development* 126, 1631-42 (1999).
47. Yang, X. et al. Angiogenesis defects and mesenchymal apoptosis in mice lacking SMAD5. *Development* 126, 1571-80 (1999).
48. Ozaki, H. et al. Basic fibroblast growth factor is neither necessary nor sufficient for the development of retinal neovascularization. *Am J Pathol* 153, 757-65 (1998).
49. Ortega, S., Ittmann, M., Tsang, S.H., Ehrlich, M. & Basilico, C. Neuronal defects and delayed wound healing in mice lacking fibroblast growth factor 2. *Proc Natl Acad Sci U S A* 95, 5672-7 (1998).
50. Abtahian, F. et al. Regulation of blood and lymphatic vascular separation by signaling proteins

- SLP-76 and Syk. *Science* 299, 247-51 (2003).
51. Carmeliet, P. et al. Targeted deficiency or cytosolic truncation of the VE-cadherin gene in mice impairs VEGF-mediated endothelial survival and angiogenesis. *Cell* 98, 147-57 (1999).
 52. Gory-Faure, S. et al. Role of vascular endothelial-cadherin in vascular morphogenesis. *Development* 126, 2093-102 (1999).
 53. Simon, A.M. & McWhorter, A.R. Vascular abnormalities in mice lacking the endothelial gap junction proteins connexin37 and connexin40. *Dev Biol* 251, 206-20 (2002).
 54. Kirchhoff, S. et al. Reduced cardiac conduction velocity and predisposition to arrhythmias in connexin40-deficient mice. *Curr Biol* 8, 299-302 (1998).
 55. Reaume, A.G. et al. Cardiac malformation in neonatal mice lacking connexin43. *Science* 267, 1831-4 (1995).
 56. Duncan, G.S. et al. Genetic evidence for functional redundancy of Platelet/Endothelial cell adhesion molecule-1 (PECAM-1): CD31-deficient mice reveal PECAM-1-dependent and PECAM-1-independent functions. *J Immunol* 162, 3022-30 (1999).
 57. Takahashi, T. et al. A mutant receptor tyrosine phosphatase, CD148, causes defects in vascular development. *Mol Cell Biol* 23, 1817-31. (2003).
 58. Hodivala-Dilke, K.M. et al. Beta3-integrin-deficient mice are a model for Glanzmann thrombasthenia showing placental defects and reduced survival. *J Clin Invest* 103, 229-38 (1999).
 59. Huang, X., Griffiths, M., Wu, J., Farese, R.V., Jr. & Sheppard, D. Normal development, wound healing, and adenovirus susceptibility in beta5-deficient mice. *Mol Cell Biol* 20, 755-9 (2000).
 60. Zhu, J. et al. β 8 integrins are required for vascular morphogenesis in mouse embryos. *Development* 129, 2891-2903 (2002).
 61. Itoh, T. et al. Unaltered secretion of beta-amyloid precursor protein in gelatinase A (matrix metalloproteinase 2)-deficient mice. *J Biol Chem* 272, 22389-92 (1997).
 62. Rudolph-Owen, L.A., Hulboy, D.L., Wilson, C.L., Mudgett, J. & Matrisian, L.M. Coordinate expression of matrix metalloproteinase family members in the uterus of normal, matrilysin-deficient, and stromelysin-1-deficient mice. *Endocrinology* 138, 4902-11 (1997).
 63. Carmeliet, P. et al. Plasminogen activator inhibitor-1 gene-deficient mice. I. Generation by homologous recombination and characterization. *J Clin Invest* 92, 2746-55 (1993).
 64. Carmeliet, P. et al. Plasminogen activator inhibitor-1 gene-deficient mice. II. Effects on hemostasis, thrombosis, and thrombolysis. *J Clin Invest* 92, 2756-60 (1993).
 65. Lawler, J. et al. Thrombospondin-1 is required for normal murine pulmonary homeostasis and its absence causes pneumonia. *J Clin Invest* 101, 982-92 (1998).
 66. Kyriakides, T.R. et al. Mice that lack thrombospondin 2 display connective tissue abnormalities that are associated with disordered collagen fibrillogenesis, an increased vascular density, and a bleeding diathesis. *J Cell Biol* 140, 419-30 (1998).
 67. Carmeliet, P. et al. Biological effects of disruption of the tissue-type plasminogen activator, urokinase-type plasminogen activator, and plasminogen activator inhibitor-1 genes in mice. *Ann N Y Acad Sci* 748, 367-81; discussion 381-2 (1995).
 68. Fukai, N. et al. Lack of collagen XVIII/endostatin results in eye abnormalities. *Embo J* 21, 153544 (2002).
 69. Gessler, M. et al. Mouse gridlock: no aortic coarctation or deficiency, but fatal cardiac defects in Hey2 $-/-$ mice. *Curr Biol* 12, 1601-4 (2002).
 70. Rajantie, I. et al. Bmx tyrosine kinase has a redundant function downstream of angiopoietin and vascular endothelial growth factor receptors in arterial endothelium. *Mol Cell Biol* 21, 4647-55 (2001).
 71. Iyer, N.V. et al. Cellular and developmental control of O₂ homeostasis by hypoxia-inducible factor-1 α . *Genes Dev* 12, 149-162 (1998).
 72. Ryan, H.E., Lo, J. & Johnson, R.S. HIF-1 α is required for solid tumor formation and embryonic vascularization. *EMBO J* 17, 3005-3015 (1998).
 73. Lyden, D. et al. Id1 and Id3 are required for neurogenesis, angiogenesis and vascularization of tumour xenografts. *Nature* 401, 670-7 (1999).
 74. Baudino, T.A. et al. c-Myc is essential for vasculogenesis and angiogenesis during development

Appendix

and tumor progression. *Genes Dev* 16, 2530-43 (2002).

75. Wigle, J.T. & Oliver, G. Prox1 function is required for the development of the murine lymphatic system. *Cell* 98, 769-78 (1999).

Table 2: Angiogenesis in diseases (courtesy of P. Carmeliet, Nature. 2005 Dec 15;438(7070):932-6.).

Diseases characterized or caused by abnormal or excessive (lymph)-angiogenesis

ORGAN	DISEASE IN MICE OR HUMANS
Numerous organs	Cancer (activation of oncogenes; loss of tumor suppressors) and metastasis; infectious diseases (pathogens express (lymph)-angiogenic genes ¹ , induce (lymph)-angiogenic programs ² or transform ECs ^{3,4} ; antimicrobial peptides or bacterial infections increase HIF-1 levels ⁵⁻⁷ ; HIV-Tat is angiogenic ⁸); vasculitis and angiogenesis in auto-immune disorders such as systemic sclerosis, multiple sclerosis, Sjögren's disease ⁹⁻¹¹ (in part by activation of mast cells and other leukocytes).
Blood and lymph vessels	Vascular malformations (Tie-2 mutation ¹²); DiGeorge syndrome (low VEGF/Nrp-1 expression ¹³); hereditary hemorrhagic telangiectasia (mutation of endoglin or ALK ^{14,15}); cavernous hemangioma (loss of Cx37/40 ¹⁶); cutaneous hemangioma (VG5Q mutation ^{17,18}); lymphatic malformations ¹⁹ ; transplant arteriopathy and atherosclerosis (plaques contain blood and lymph vessels ²⁰⁻²²)
Adipose tissue	Obesity (angiogenesis induced by fat diet; weight loss by angiogenesis inhibitors ²³ , anti-VEGFR2 inhibits preadipocyte differentiation via effects on ECs ²⁴ ; adipocytokines stimulate angiogenesis ²⁵ ; lymph induces preadipocyte differentiation ^{26,27} ;
Skin	Psoriasis (high VEGF and Tie2 ²⁸⁻³⁰), warts ² , allergic dermatitis (high VEGF and PIGF ^{31,32}), scar keloids ^{33,34} , pyogenic granulomas, blistering disease ³⁵ , Kaposi's sarcoma in AIDS patients ³ , systemic sclerosis ³⁶ .
Eye	Persistent hyperplastic vitreous syndrome (loss of Ang-2 ^{37,38} or VEGF164 ³⁹); diabetic retinopathy; retinopathy of prematurity ⁴⁰ ; choroidal neovascularization ⁴⁰ (TIMP-3 mutation ⁴¹)
Lung	Primary pulmonary hypertension (BMPR2 mutation; somatic EC mutations ⁴²⁻⁴⁴); asthma ⁴⁵ , nasal polyps ⁴⁶ , rhinitis ⁴⁷ ; chronic airway inflammation ⁴⁸ , cystic fibrosis ⁴⁹
Gastro-intestinal tract	Inflammatory bowel disease (ulcerative colitis ⁵⁰) and periodontal disease ⁵¹ , ascites, peritoneal adhesions ⁵² ; liver cirrhosis ⁵³⁻⁵⁵
Reproductive system	Endometriosis ^{56,57} , uterine bleeding, ovarian cysts ⁵⁸ , ovarian hyperstimulation ⁵⁹
Bone, joints	Arthritis and synovitis ⁶⁰⁻⁶³ , osteomyelitis ⁶⁴ , osteophyte formation ⁶⁵ ; HIV-induced bone marrow angiogenesis ⁶⁶
Kidney	Diabetic nephropathy (early stage: enlarged glomerular vascular tufts) ^{67,68}

Diseases characterized or caused by insufficient (lymph)-angiogenesis or vessel regression

ORGAN	DISEASE IN MICE OR HUMANS	ANGIOGENIC MECHANISM
Nervous system	Alzheimer's disease Amyotrophic lateral sclerosis; diabetic neuropathy Stroke	Vasoconstriction, microvascular degeneration and cerebral angiopathy due to EC toxicity by amyloid- β ^{69, 70} . Impaired perfusion and neuroprotection, causing motoneuron or axon degeneration due to insufficient VEGF production ⁷¹⁻⁷⁵ Correlation of survival with angiogenesis in brain ⁷⁶ ; stroke due to arteriopathy (Notch-3 mutations ⁷⁷)
Blood and Lymph vessels	Diabetes Hypertension Atherosclerosis Restenosis Lymphedema	Characterized by impaired collateral growth ⁷⁸ , and angiogenesis in ischemic limbs ⁷⁹ , but enhanced retinal neovascularization secondary to pericyte drop out ⁸⁰ . Microvessel rarefaction due to impaired vasodilation or angiogenesis ⁸¹⁻⁸³ . Characterized by impaired collateral vessel development ⁸⁴ Impaired reendothelialization after arterial injury ⁸⁵ Iatrogenic (post-surgery of breast cancer; elephantiasis caused by parasites); hereditary (VEGFR3 mutations) ⁸⁶ .
Gastro-intestinal tract	Gastric or oral ulcerations Crohn's disease	Delayed healing due to production of angiogenesis inhibitors by pathogens ^{87, 88} . Characterized by mucosal ischemia ^{50, 89}
Skin	Hair loss Skin purpura, telangiectasia, and venous lake formation Systemic sclerosis, Lupus	Retarded hair growth by angiogenesis inhibitors ⁹⁰ Age-dependent reduction of vessel number and maturation (SMC drop out) due to EC telomere shortening ⁹¹ . Insufficient compensatory angiogenic response ⁹²
Reproductive system	Preeclampsia Menorrhagia (uterine bleeding)	EC dysfunction, resulting in organ failure, thrombosis and hypertension due to deprivation of VEGF by soluble Flt1 ^{93, 94} . Fragility of SMC-poor vessels due to low Ang-1 production ⁹⁵
Lung	Neonatal respiratory distress syndrome (RDS) Pulmonary fibrosis, emphysema	Insufficient lung maturation and surfactant production in premature mice with low HIF-2/VEGF ⁹⁶ ; low VEGF levels in human neonates also correlate with RDS ⁹⁷ . Alveolar EC apoptosis upon VEGF inhibition ⁹⁸⁻¹⁰⁰ .
Kidney	Nephropathy (ageing; metabolic syndrome); glomerulosclerosis; tubulointerstitial fibrosis	Characterized by vessel dropout, microvasculopathy and EC dysfunction (low VEGF; high TSP1) ¹⁰¹⁻¹⁰³ ; recovery of glomerular/peritubular ECs in glomerulonephritis, thrombotic microangiopathy and nephrotoxicity is VEGF-dependent ¹⁰⁴ .
Bone	Osteoporosis, impaired bone fracture healing	Impaired bone formation due to age-dependent decline of VEGF-driven angiogenesis ¹⁰⁵ ; angiogenesis inhibitors prevent fracture healing ¹⁰⁶ ; osteoporosis due to low VEGF ¹⁰⁷ ; healing of fracture non-union is impaired by insufficient angiogenesis ⁶⁴
Heart	Ischemic heart disease, cardiac failure	Imbalance in capillary-to-cardiomyocyte fiber ratio due to reduced VEGF levels ^{108, 109}

Acquired resistance to anti-angiogenesis treatment

KNOWN MECHANISMS	HYPOTHETICAL MECHANISMS
<p>EC instability: In some human lymphomas, ECs have cytogenetic abnormalities ^{110, 111}.</p> <p>Multidrug resistance: ECs are chemoprotected by high levels of VEGF and other EC survival factors in tumors, which upregulate anti-apoptotic signals (survivin) and multidrug resistance-associated protein (MRP, BCRP) ¹¹²⁻¹¹⁵.</p> <p>EC radioresistance: Hypoxic activation of HIF-1 renders ECs resistant to irradiation ¹¹⁶.</p> <p>Vascular mimicry: A fraction of tumor vessels is lined by malignant cells ^{117, 118} and thus unresponsive to anti-angiogenic agents.</p> <p>Angiogenic switch: Tumor cell clones, expressing more of the same or other angiogenic factors, may become selected at advanced stages or in response to anti-angiogenic treatment (i.e. upregulation of PlGF and FGF-2 after VEGF inhibition ^{119, 120}, of VEGF after VEGFR or EGFR inhibition ¹²¹⁻¹²³, of IL-8 after HIF-1 inhibition ¹²⁴; etc). Anti-VEGF does not prevent activation of VEGFR2 by VEGF-C.</p> <p>Vascular independence: Mutant tumor cell clones (such as those lacking p53 or HIF-1) or inflammatory cells are able to survive in hypoxic tumors; their reduced vascular dependence impairs the anti-angiogenic response ^{125, 126}.</p> <p>Stromal cells: VEGF^{-/-} tumors recruit pro-angiogenic stromal fibroblasts via upregulation of PDGF-AA ¹²⁷.</p> <p>Lymphatics: Tumor cells metastasize via lymph vessels; their growth is not (necessarily) blocked by anti-angiogenic therapy ⁸⁶.</p> <p>Mature vessels: Pre-existing supply vessels are covered by SMCs and not easily pruned by EC-targeted treatment ^{128, 129}.</p> <p>Bone marrow-derived cells: Tumors or ischemic tissues recruit pro-angiogenic EPC, HSC and inflammatory cells independently of VEGF ¹³⁰⁻¹³³.</p> <p>Micro-environment: HIF-1^{-/-} glioma growth, metastasis and malignancy are dependent on the site, suggesting tissue-specific influences ¹³⁴.</p> <p>RTKIs: may not synergize with chemotherapy, possibly because they don't block Neuropilin-1.</p>	<p>Gene mutations: RTKI monotherapy often results in resistance due to the acquisition of novel mutations, gene amplification, reduced RTKI uptake or activation of downstream signaling pathways ^{123, 135, 136}. do VEGF-RTKIs induce similar phenomena? Do mutations of PDGFRs ¹³⁷ and Tie2 ¹² arise in tumor vessels?</p> <p>Cancer stem cells: Do cancer stem cells thrive better in hypoxic tumors after anti-angiogenic treatment?</p> <p>Endothelial cancer stem cells: Do somatic mutations in single EPCs contribute to tumor angiogenesis, as they do in clonal hemangiomas ¹³⁸?</p> <p>Vessel morphology: Is improvement of drug delivery by vessel normalization (too) transient ¹³⁹? Or is drug delivery inefficient due to excessive vessel pruning by prolonged anti-angiogenic treatment ¹³⁹? Become tumor vessels after anti-angiogenic treatment stabilized by an excess coverage with mural cells and therefore resistant to pruning ¹⁴⁰?</p> <p>Vessel cooption: Tumors coopt existing vessels ¹⁴¹, which may be less sensitive to anti-angiogenic treatment and require anti-vascular agents.</p> <p>Signaling redundancy: Does (epi)-genetic activation of signals downstream of VEGFRs bypass VEGF(R) inhibition, similar as increased PI3K activity in PTEN^{-/-} tumor cells impairs EGFR inhibition ^{123, 135, 136}?</p> <p>Receptor activation <i>in trans</i>: Blocking a ligand will not entirely eliminate RTK activation <i>in trans</i> by other receptors (VEGFR-2 by VEGFR1 ¹⁴², EGFR by IGF1 ^{123, 135, 136}). Heterodimerization with other receptors may also alter angiogenic signaling ¹⁴³.</p> <p>Tissue-specific angiogenesis: Do different signals regulate angiogenesis in the primary versus metastatic tumors?</p> <p>DNA repair: Hypoxic activation of HIF-1 (resulting from vessel pruning by anti-angiogenesis) inhibits DNA repair ¹⁴⁴; is this relevant for tumor ECs?</p> <p>Cell adhesion-mediated drug resistance: Are tumor ECs, most strongly adherent to ECM, resistant to chemo- and anti-angiogenic therapy ¹⁴⁵?</p> <p>Pharmaco-economics: The costs of combination anti-angiogenesis therapy are formidable.</p>

For more information, the reader is referred to the following reviews ¹⁴⁶⁻¹⁵⁰.

Adverse effects of VEGF inhibition

ADVERSE EFFECTS IN HUMANS	PHENOTYPES IN (ADULT) ANIMAL MODELS
<p>Thrombosis^{1,2}: Inhibition of VEGF increases the thrombo-embolic risk 2-fold in the general population¹⁵¹, but >8-fold in cancer patients, older than 65 years of age with a previous history of arterial thrombotic events (www.asco.org/ac/1,1003,12-002511-00_18-0034-00_19-003346,00.asp). The thrombotic risk may be related to the reduced release of fibrinolytic components¹⁵² and the increased release of fibrinolytic inhibitors (unpublished) and pro-coagulants¹⁵³, to the reduced release of NO (inhibitor of platelet aggregation and vasospasms)¹⁵⁴, and to EC dysfunction resulting from deprivation of VEGF vessel maintenance signals^{155, 156}.</p> <p>Hypertension^{1,2,4}: likely attributable to reduced vasodilation by NO, and possibly to pruning of normal vessels and effects on renal salt homeostasis^{83, 154, 157, 158}.</p> <p>Proteinuria and glomerulonephritis¹: related to the maintenance role of VEGF in podocyte functioning¹⁵⁹.</p> <p>Bleeding¹: in centrally located cavitory necrotic lung tumors, likely due to vessel disintegration.</p> <p>Gastro-intestinal perforation¹: presumably related to impaired wound healing.</p> <p>Preeclampsia: thrombosis, hypertension, renal dysfunction, edema due to EC dysfunction due to trapping of VEGF by elevated levels of endogenous soluble VEGFR1 (sFlt1)^{93, 94, 160}.</p> <p>Others: diarrhea¹⁻⁴, leukopenia^{1,2}, nausea^{2,3}, thrombophlebitis, neuropathy^{1,2}, vomiting², venous thrombosis², dizziness, hand and foot syndrome³, fatigue^{3,4}, rash³.</p>	<p>Pruning of quiescent vessels (up to 68%) in healthy organs, especially in endocrine organs with fenestrated ECs, but also in muscle and other organs^{157, 158}.</p> <p>CNS: low VEGF levels in mice cause ALS-like motoneuron degeneration⁷¹, while VEGF-lowering gene variants increase the risk of ALS and Alzheimer disease in humans^{72, 161}; VEGF inhibitors aggravate motoneuron degeneration in the SOD1^{G93A} mouse model of ALS (unpublished). Microvascular disruption may underly diabetic neuropathy, Alzheimer disease and other neurological disorders^{70, 75, 162, 163}. Inhibition of VEGF in the CNS impairs learning by decreasing neurogenesis¹⁶⁴.</p> <p>Kidney: heterozygous loss of VEGF in podocytes results in disappearance of EC fenestrations, loss of podocyte foot processes, proteinuria and hypertension¹⁵⁹.</p> <p>Lung: Inhibition or conditional loss of VEGF in the lung cause emphysema due to apoptosis of alveolar septal cell and bronchial epithelial cells^{99, 100}.</p> <p>Preeclampsia: delivery of sFlt1 causes hypertension, proteinuria and renal endotheliosis^{93, 94, 160}.</p> <p>Bone: VEGF inhibitors impair fracture healing¹⁶⁵.</p> <p>Reproduction: inhibition of VEGF prevents ovulation and embryonic development¹⁶⁶.</p> <p>Bone marrow: Inhibition of VEGF or VEGFR1 impairs hematopoietic recovery after myeloablation and inflammatory disease¹⁶⁷⁻¹⁶⁹.</p> <p>Heart & Limb: VEGF inhibition causes cardiac dysfunction and dilatation after pressure overload; prunes 64% of the capillaries in normoxic muscle with increased muscle fiber apoptosis and decreased myoblast fusion; and impairs functional recovery of ischemic hindlimbs^{109, 158, 170, 171}.</p> <p>Pancreas: VEGF inhibition impairs pancreas regeneration with progenitors (unpublished observations).</p>

¹ toxicity observed in patients receiving anti-VEGF antibody (Avastin) and chemotherapy (phase III trials); ²⁻⁴ toxicity in patients receiving RTKIs (Vatalinib²; Sorafenib³; Sutent⁴) and chemotherapy (phase III trials). For more detailed information, see ¹⁷².

1. Meyer, M. et al. A novel vascular endothelial growth factor encoded by Orf virus, VEGF-E, mediates angiogenesis via signalling through VEGFR-2 (KDR) but not VEGFR-1 (Flt-1) receptor tyrosine kinases. *Embo J* 18, 363-74 (1999).
2. Harada, K., Lu, S., Chisholm, D. M., Syrjanen, S. & Schor, A. M. Angiogenesis and vasodilation in skin warts. Association with HPV infection. *Anticancer Res* 20, 4519-23 (2000).
3. Barillari, G. & Ensoli, B. Angiogenic effects of extracellular human immunodeficiency virus type 1 Tat protein and its role in the pathogenesis of AIDS-associated Kaposi's sarcoma. *Clin Microbiol Rev* 15, 310-26 (2002).
4. Wang, H. W. et al. Kaposi sarcoma herpesvirus-induced cellular reprogramming contributes to the lymphatic endothelial gene expression in Kaposi sarcoma. *Nat Genet* 36, 687-93 (2004).
5. Frantz, S., Vincent, K. A., Feron, O. & Kelly, R. A. Innate immunity and angiogenesis. *Circ Res* 96, 15-26 (2005).
6. Li, J. et al. PR39, a peptide regulator of angiogenesis. *Nat Med* 6, 49-55 (2000).
7. Kempf, V. A. et al. Activation of hypoxia-inducible factor-1 in bacillary angiomatosis: evidence for a role of hypoxia-inducible factor-1 in bacterial infections. *Circulation* 111, 1054-62 (2005).
8. Urbinati, C. et al. Integrin $\alpha V\beta 3$ as a Target for Blocking HIV-1 Tat-Induced Endothelial Cell Activation In Vitro and Angiogenesis In Vivo. *Arterioscler Thromb Vasc Biol* (2005).
9. Kirk, S. L. & Karlik, S. J. VEGF and vascular changes in chronic neuroinflammation. *J Autoimmun* 21, 353-63 (2003).
10. Storkebaum, E., Lambrechts, D. & Carmeliet, P. VEGF: once regarded as a specific angiogenic factor, now implicated in neuroprotection. *Bioessays* 26, 943-54 (2004).
11. Ohno, A. et al. Dermatomyositis associated with Sjogren's syndrome: VEGF involvement in vasculitis. *Clin Neuropathol* 23, 178-82 (2004).
12. Vikkula, M. et al. Vascular dysmorphogenesis caused by an activating mutation in the receptor tyrosine kinase TIE2. *Cell* 87, 1181-90 (1996).
13. Stalmans, I. et al. VEGF: A modifier of the del22q11 (DiGeorge) syndrome? *Nat Med* 9, 173-82 (2003).
14. van den Driesche, S., Mummery, C. L. & Westermann, C. J. Hereditary hemorrhagic telangiectasia: an update on transforming growth factor beta signaling in vasculogenesis and angiogenesis. *Cardiovasc Res* 58, 20-31 (2003).
15. Lebrin, F., Deckers, M., Bertolino, P. & Ten Dijke, P. TGF-beta receptor function in the endothelium. *Cardiovasc Res* 65, 599-608 (2005).
16. Simon, A. M. & McWhorter, A. R. Vascular abnormalities in mice lacking the endothelial gap junction proteins connexin37 and connexin40. *Dev Biol* 251, 206-20 (2002).
17. Tian, X. L. et al. Identification of an angiogenic factor that when mutated causes susceptibility to Klippel-Trenaunay syndrome. *Nature* 427, 640-5 (2004).
18. Lambrechts, D. & Carmeliet, P. Medicine: genetic spotlight on a blood defect. *Nature* 427, 592-4 (2004).
19. Tille, J. C. & Pepper, M. S. Hereditary vascular anomalies: new insights into their pathogenesis. *Arterioscler Thromb Vasc Biol* 24, 1578-90 (2004).
20. Nakano, T. et al. Angiogenesis and lymphangiogenesis and expression of lymphangiogenic factors in the atherosclerotic intima of human coronary arteries. *Hum Pathol* 36, 330-40 (2005).
21. Kahlon, R., Shaper, J. & Gotlieb, A. I. Angiogenesis in atherosclerosis. *Can J Cardiol* 8, 60-4 (1992).
22. Khurana, R. et al. Placental Growth Factor Promotes Atherosclerotic Intimal Thickening and Macrophage Accumulation. *Circulation* (2005).
23. Rupnick, M. A. et al. Adipose tissue mass can be regulated through the vasculature. *Proc Natl Acad Sci U S A* 99, 10730-5 (2002).
24. Fukumura, D. et al. Paracrine regulation of angiogenesis and adipocyte differentiation during in vivo adipogenesis. *Circ Res* 93, e88-97 (2003).
25. Shibata, R. et al. Adiponectin stimulates angiogenesis in response to tissue ischemia through stimulation of amp-activated protein kinase signaling. *J Biol Chem* 279, 28670-4 (2004).
26. Harvey, N. L. et al. Lymphatic vascular defects promoted by Prox1 haploinsufficiency cause adult-

- onset obesity. *Nat Genet* 37, 1072-81 (2005).
27. Schneider, M., Conway, E. M. & Carmeliet, P. Lymph makes you fat. *Nat Genet* 37, 1023-1024 (2005).
28. Voskas, D. et al. A cyclosporine-sensitive psoriasis-like disease produced in Tie2 transgenic mice. *Am J Pathol* 166, 843-55 (2005).
29. Leong, T. T., Fearon, U. & Veale, D. J. Angiogenesis in psoriasis and psoriatic arthritis: clues to disease pathogenesis. *Curr Rheumatol Rep* 7, 325-9 (2005).
30. Xia, Y. P. et al. Transgenic delivery of VEGF to mouse skin leads to an inflammatory condition resembling human psoriasis. *Blood* 102, 161-8 (2003).
31. Oura, H. et al. A critical role of placental growth factor in the induction of inflammation and edema formation. *Blood* 101, 560-7 (2003).
32. Agha-Majzoub, R., Becker, R. P., Schraufnagel, D. E. & Chan, L. S. Angiogenesis: the major abnormality of the keratin-14 IL-4 transgenic mouse model of atopic dermatitis. *Microcirculation* 12, 455-76 (2005).
33. Yang, G. P., Lim, I. J., Phan, T. T., Lorenz, H. P. & Longaker, M. T. From scarless fetal wounds to keloids: molecular studies in wound healing. *Wound Repair Regen* 11, 411-8 (2003).
34. Gira, A. K., Brown, L. F., Washington, C. V., Cohen, C. & Arbiser, J. L. Keloids demonstrate high-level epidermal expression of vascular endothelial growth factor. *J Am Acad Dermatol* 50, 850-3 (2004).
35. Brown, L. F. et al. Increased expression of vascular permeability factor (vascular endothelial growth factor) in bullous pemphigoid, dermatitis herpetiformis, and erythema multiforme. *J Invest Dermatol* 104, 744-9 (1995).
36. Distler, O. et al. Uncontrolled expression of vascular endothelial growth factor and its receptors leads to insufficient skin angiogenesis in patients with systemic sclerosis. *Circ Res* 95, 109-16 (2004).
37. Gale, N. W. et al. Angiopoietin-2 is required for postnatal angiogenesis and lymphatic patterning, and only the latter role is rescued by Angiopoietin-1. *Dev Cell* 3, 411-23 (2002).
38. Hackett, S. F. et al. Angiopoietin 2 expression in the retina: upregulation during physiologic and pathologic neovascularization. *J Cell Physiol* 184, 275-84 (2000).
39. Stalmans, I. et al. Arteriolar and venular patterning in retinas of mice selectively expressing VEGF isoforms. *J Clin Invest* 109, 327-36 (2002).
40. Campochiaro, P. A. Ocular neovascularisation and excessive vascular permeability. *Expert Opin Biol Ther* 4, 1395-402 (2004).
41. Qi, J. H. et al. A novel function for tissue inhibitor of metalloproteinases-3 (TIMP3): inhibition of angiogenesis by blockage of VEGF binding to VEGF receptor-2. *Nat Med* 9, 407-15 (2003).
42. Voelkel, N. F. et al. Janus face of vascular endothelial growth factor: the obligatory survival factor for lung vascular endothelium controls precapillary artery remodeling in severe pulmonary hypertension. *Crit Care Med* 30, S251-6 (2002).
43. Yeager, M. E., Halley, G. R., Golpon, H. A., Voelkel, N. F. & Tuder, R. M. Microsatellite instability of endothelial cell growth and apoptosis genes within plexiform lesions in primary pulmonary hypertension. *Circ Res* 88, E2-E11 (2001).
44. Humbert, M. & Trembath, R. C. Genetics of pulmonary hypertension: from bench to bedside. *Eur Respir J* 20, 741-9 (2002).
45. Bai, T. R. & Knight, D. A. Structural changes in the airways in asthma: observations and consequences. *Clin Sci (Lond)* 108, 463-77 (2005).
46. Gosepath, J., Brieger, J., Lehr, H. A. & Mann, W. J. Expression, localization, and significance of vascular permeability/vascular endothelial growth factor in nasal polyps. *Am J Rhinol* 19, 7-13 (2005).
47. Kirmaz, C. et al. Increased expression of angiogenic markers in patients with seasonal allergic rhinitis. *Eur Cytokine Netw* 15, 317-22 (2004).
48. Baluk, P. et al. Pathogenesis of persistent lymphatic vessel hyperplasia in chronic airway inflammation. *J Clin Invest* 115, 247-57 (2005).
49. Shute, J., Marshall, L., Bodey, K. & Bush, A. Growth factors in cystic fibrosis - when more is not enough. *Paediatr Respir Rev* 4, 120-7 (2003).

50. Konno, S. et al. Altered expression of angiogenic factors in the VEGF-Ets-1 cascades in inflammatory bowel disease. *J Gastroenterol* 39, 931-9 (2004).
51. Suthin, K. et al. Enhanced expression of vascular endothelial growth factor by periodontal pathogens in gingival fibroblasts. *J Periodontal Res* 38, 90-6 (2003).
52. Molinas, C. R., Binda, M. M., Carmeliet, P. & Koninckx, P. R. Role of vascular endothelial growth factor receptor 1 in basal adhesion formation and in carbon dioxide pneumoperitoneum-enhanced adhesion formation after laparoscopic surgery in mice. *Fertil Steril* 82 Suppl 3, 1149-53 (2004).
53. Medina, J. et al. Evidence of angiogenesis in primary biliary cirrhosis: an immunohistochemical descriptive study. *J Hepatol* 42, 124-31 (2005).
54. Ward, N. L. et al. Angiopoietin-1 causes reversible degradation of the portal microcirculation in mice: implications for treatment of liver disease. *Am J Pathol* 165, 889-99 (2004).
55. Fernandez, M. et al. Inhibition of VEGF receptor-2 decreases the development of hyperdynamic splanchnic circulation and portal-systemic collateral vessels in portal hypertensive rats. *J Hepatol* (2005).
56. Groothuis, P. G., Nap, A. W., Winterhager, E. & Grummer, R. Vascular development in endometriosis. *Angiogenesis*, 1-10 (2005).
57. Hull, M. L. et al. Antiangiogenic agents are effective inhibitors of endometriosis. *J Clin Endocrinol Metab* 88, 2889-99 (2003).
58. Abd El Aal, D. E., Mohamed, S. A., Amine, A. F. & Meki, A. R. Vascular endothelial growth factor and insulin-like growth factor-1 in polycystic ovary syndrome and their relation to ovarian blood flow. *Eur J Obstet Gynecol Reprod Biol* 118, 219-24 (2005).
59. LeCouter, J. et al. Identification of an angiogenic mitogen selective for endocrine gland endothelium. *Nature* 412, 877-84 (2001).
60. Taylor, P. C. & Sivakumar, B. Hypoxia and angiogenesis in rheumatoid arthritis. *Curr Opin Rheumatol* 17, 293-8 (2005).
61. Szekanecz, Z., Gaspar, L. & Koch, A. E. Angiogenesis in rheumatoid arthritis. *Front Biosci* 10, 1739-53 (2005).
62. Lainer, D. T. & Brahn, E. New antiangiogenic strategies for the treatment of proliferative synovitis. *Expert Opin Investig Drugs* 14, 1-17 (2005).
63. Arima, K. et al. RS3PE syndrome presenting as vascular endothelial growth factor associated disorder. *Ann Rheum Dis* 64, 1653-5 (2005).
64. Hausman, M. R. & Rinker, B. D. Intractable wounds and infections: the role of impaired vascularity and advanced surgical methods for treatment. *Am J Surg* 187, 44S-55S (2004).
65. Luttun, A. et al. Revascularization of ischemic tissues by PlGF treatment, and inhibition of tumor angiogenesis, arthritis and atherosclerosis by anti-Flt1. *Nat Med* 8, 831-40. (2002).
66. Patsouris, E. et al. Increased microvascular network in bone marrow of HIV-positive haemophilic patients. *HIV Med* 5, 18-25 (2004).
67. Yamamoto, Y. et al. Tumstatin peptide, an inhibitor of angiogenesis, prevents glomerular hypertrophy in the early stage of diabetic nephropathy. *Diabetes* 53, 1831-40 (2004).
68. Schrijvers, B. F., Flyvbjerg, A., Tilton, R. G., Lameire, N. H. & Vriese, A. S. A neutralizing VEGF antibody prevents glomerular hypertrophy in a model of obese type 2 diabetes, the Zucker diabetic fatty rat. *Nephrol Dial Transplant* (2005).
69. de la Torre, J. C. Alzheimer's disease is a vasocognopathy: a new term to describe its nature. *Neurol Res* 26, 517-24 (2004).
70. Zlokovic, B. V. Neurovascular mechanisms of Alzheimer's neurodegeneration. *Trends Neurosci* 28, 202-8 (2005).
71. Oosthuysen, B. et al. Deletion of the hypoxia-response element in the vascular endothelial growth factor promoter causes motor neuron degeneration. *Nat Genet* 28, 131-8. (2001).
72. Lambrechts, D. et al. VEGF is a modifier of amyotrophic lateral sclerosis in mice and humans and protects motoneurons against ischemic death. *Nat Genet* 34, 383-94 (2003).
73. Störkebaum, E. et al. Treatment of motoneuron degeneration by intracerebroventricular delivery of VEGF in a rat model of ALS. *Nat Neurosci* 8, 85-92 (2005).
74. Azzouz, M. et al. VEGF delivery with retrogradely transported lentivector prolongs survival in a

- mouse ALS model. *Nature* 429, 413-7 (2004).
75. Storkebaum, E. & Carmeliet, P. VEGF: a critical player in neurodegeneration. *J Clin Invest* 113, 14-8 (2004).
76. Krupinski, J., Kaluza, J., Kumar, P., Kumar, S. & Wang, J. M. Role of angiogenesis in patients with cerebral ischemic stroke. *Stroke* 25, 1794-8 (1994).
77. Kalimo, H., Ruchoux, M. M., Viitanen, M. & Kalaria, R. N. CADASIL: a common form of hereditary arteriopathy causing brain infarcts and dementia. *Brain Pathol* 12, 371-84 (2002).
78. Waltenberger, J. Impaired collateral vessel development in diabetes: potential cellular mechanisms and therapeutic implications. *Cardiovasc Res* 49, 554-60 (2001).
79. Rivard, A. et al. Rescue of diabetes-related impairment of angiogenesis by intramuscular gene therapy with adeno-VEGF. *Am J Pathol* 154, 355-63 (1999).
80. Caldwell, R. B. et al. Vascular endothelial growth factor and diabetic retinopathy: role of oxidative stress. *Curr Drug Targets* 6, 511-24 (2005).
81. Boudier, H. A. Arteriolar and capillary remodelling in hypertension. *Drugs* 58 Spec No 1, 37-40 (1999).
82. Kubis, N., Richer, C., Domergue, V., Giudicelli, J. F. & Levy, B. I. Role of microvascular rarefaction in the increased arterial pressure in mice lacking for the endothelial nitric oxide synthase gene (eNOS3pt-/-). *J Hypertens* 20, 1581-7 (2002).
83. Sane, D. C., Anton, L. & Brosnihan, K. B. Angiogenic growth factors and hypertension. *Angiogenesis* 7, 193-201 (2004).
84. Van Belle, E. et al. Hypercholesterolemia attenuates angiogenesis but does not preclude augmentation by angiogenic cytokines. *Circulation* 96, 2667-74 (1997).
85. Gennaro, G., Menard, C., Michaud, S. E. & Rivard, A. Age-dependent impairment of reendothelialization after arterial injury: role of vascular endothelial growth factor. *Circulation* 107, 230-3 (2003).
86. Alitalo, K., Tammela, T. & T., P. Lymphangiogenesis in development and human disease. *Nature* (this volume) (2005).
87. Jenkinson, L., Bardhan, K. D., Atherton, J. & Kalia, N. *Helicobacter pylori* prevents proliferative stage of angiogenesis in vitro: role of cytokines. *Dig Dis Sci* 47, 1857-62 (2002).
88. Kim, J. S., Kim, J. M., Jung, H. C. & Song, I. S. *Helicobacter pylori* down-regulates the receptors of vascular endothelial growth factor and angiopoietin in vascular endothelial cells: implications in the impairment of gastric ulcer healing. *Dig Dis Sci* 49, 778-86 (2004).
89. Hatoum, O. A., Binion, D. G. & Gutterman, D. D. Paradox of simultaneous intestinal ischaemia and hyperaemia in inflammatory bowel disease. *Eur J Clin Invest* 35, 599-609 (2005).
90. Yano, K., Brown, L. F. & Detmar, M. Control of hair growth and follicle size by VEGF-mediated angiogenesis. *J Clin Invest* 107, 409-17 (2001).
91. Chang, E., Yang, J., Nagavarapu, U. & Herron, G. S. Aging and survival of cutaneous microvasculature. *J Invest Dermatol* 118, 752-8 (2002).
92. Mackiewicz, Z. et al. Increased but imbalanced expression of VEGF and its receptors has no positive effect on angiogenesis in systemic sclerosis skin. *Clin Exp Rheumatol* 20, 641-6 (2002).
93. Maynard, S. E. et al. Excess placental soluble fms-like tyrosine kinase 1 (sFlt1) may contribute to endothelial dysfunction, hypertension, and proteinuria in preeclampsia. *J Clin Invest* 111, 649-58 (2003).
94. Levine, R. J. et al. Circulating angiogenic factors and the risk of preeclampsia. *N Engl J Med* 350, 672-83 (2004).
95. Hewett, P. et al. Down-regulation of angiopoietin-1 expression in menorrhagia. *Am J Pathol* 160, 773-80 (2002).
96. Compnolle, V. et al. Loss of HIF-2alpha and inhibition of VEGF impair fetal lung maturation, whereas treatment with VEGF prevents fatal respiratory distress in premature mice. *Nat Med* 8, 702-10 (2002).
97. Tsao, P. N. et al. Vascular endothelial growth factor in preterm infants with respiratory distress syndrome. *Pediatr Pulmonol* 39, 461-5 (2005).
98. Kasahara, Y. et al. Inhibition of VEGF receptors causes lung cell apoptosis and emphysema. *J Clin*

- Invest 106, 1311-9 (2000).
99. Tang, K., Rossiter, H. B., Wagner, P. D. & Breen, E. C. Lung-targeted VEGF inactivation leads to an emphysema phenotype in mice. *J Appl Physiol* 97, 1559-66; discussion 1549 (2004).
 100. McGrath-Morrow, S. A., Cho, C., Zhen, L., Hicklin, D. J. & Tuder, R. M. Vascular endothelial growth factor receptor 2 blockade disrupts postnatal lung development. *Am J Respir Cell Mol Biol* 32, 420-7 (2005).
 101. Kang, D. H. et al. Impaired angiogenesis in the aging kidney: vascular endothelial growth factor and thrombospondin-1 in renal disease. *Am J Kidney Dis* 37, 601-11 (2001).
 102. Long, D. A., Mu, W., Price, K. L. & Johnson, R. J. Blood vessels and the aging kidney. *Nephron Exp Nephrol* 101, e95-9 (2005).
 103. Gealekman, O. et al. Endothelial dysfunction as a modifier of angiogenic response in Zucker diabetic fat rat: amelioration with Ebselen. *Kidney Int* 66, 2337-47 (2004).
 104. Schrijvers, B. F., Flyvbjerg, A. & De Vriese, A. S. The role of vascular endothelial growth factor (VEGF) in renal pathophysiology. *Kidney Int* 65, 2003-17 (2004).
 105. Martinez, P., Esbrit, P., Rodrigo, A., Alvarez-Arroyo, M. V. & Martinez, M. E. Age-related changes in parathyroid hormone-related protein and vascular endothelial growth factor in human osteoblastic cells. *Osteoporos Int* 13, 874-81 (2002).
 106. Yin, G. et al. Endostatin gene transfer inhibits joint angiogenesis and pannus formation in inflammatory arthritis. *Mol Ther* 5, 547-54 (2002).
 107. Pufe, T. et al. The role of vascular endothelial growth factor in glucocorticoid-induced bone loss: evaluation in a minipig model. *Bone* 33, 869-76 (2003).
 108. Jesmin, S. et al. Age-related changes in cardiac expression of VEGF and its angiogenic receptor KDR in stroke-prone spontaneously hypertensive rats. *Mol Cell Biochem* 272, 63-73 (2005).
 109. Shiojima, I. et al. Disruption of coordinated cardiac hypertrophy and angiogenesis contributes to the transition to heart failure. *J Clin Invest* 115, 2108-18 (2005).
 110. Hida, K. et al. Tumor-associated endothelial cells with cytogenetic abnormalities. *Cancer Res* 64, 8249-55 (2004).
 111. Streubel, B. et al. Lymphoma-specific genetic aberrations in microvascular endothelial cells in B-cell lymphomas. *N Engl J Med* 351, 250-9 (2004).
 112. Sawada, T., Kato, Y., Sakayori, N., Takekawa, Y. & Kobayashi, M. Expression of the multidrug-resistance P-glycoprotein (Pgp, MDR-1) by endothelial cells of the neovasculature in central nervous system tumors. *Brain Tumor Pathol* 16, 23-7 (1999).
 113. Diestra, J. E. et al. Frequent expression of the multi-drug resistance-associated protein BCRP/MXR/ABCP/ABCG2 in human tumours detected by the BXP-21 monoclonal antibody in paraffin-embedded material. *J Pathol* 198, 213-9 (2002).
 114. Mao, Q. & Unadkat, J. D. Role of the breast cancer resistance protein (ABCG2) in drug transport. *Aaps J* 7, E118-33 (2005).
 115. Tran, J. et al. A role for survivin in chemoresistance of endothelial cells mediated by VEGF. *Proc Natl Acad Sci U S A* 99, 4349-54 (2002).
 116. Moeller, B. J. et al. Pleiotropic effects of HIF-1 blockade on tumor radiosensitivity. *Cancer Cell* 8, 99-110 (2005).
 117. di Tomaso, E. et al. Mosaic tumor vessels: cellular basis and ultrastructure of focal regions lacking endothelial cell markers. *Cancer Res* 65, 5740-9 (2005).
 118. Maniotis, A. J. et al. Vascular channel formation by human melanoma cells in vivo and in vitro: vasculogenic mimicry. *Am J Pathol* 155, 739-52 (1999).
 119. Casanovas, O., Hicklin, D. J., Bergers, G. & Hanahan, D. Drug resistance by evasion of antiangiogenic targeting of VEGF signaling in late-stage pancreatic islet tumors. *Cancer Cell* 8, 299-309 (2005).
 120. Willet, C. G. & al, e. Surrogate markers for antiangiogenic therapy and dose-limiting toxicities for bevacizumab with radio-chemotherapy: continued experience of a Phase I trial in rectal cancer patients. *J Clin Oncol* (in press) (2005).
 121. Bocci, G. et al. Increased plasma vascular endothelial growth factor (VEGF) as a surrogate marker for optimal therapeutic dosing of VEGF receptor-2 monoclonal antibodies. *Cancer Res* 64, 6616-25 (2004).

122. Bianco, R., Troiani, T., Tortora, G. & Ciardiello, F. Intrinsic and acquired resistance to EGFR inhibitors in human cancer therapy. *Endocr Relat Cancer* 12, S159-S171 (2005).
123. Vilorio-Petit, A. M. & Kerbel, R. S. Acquired resistance to EGFR inhibitors: mechanisms and prevention strategies. *Int J Radiat Oncol Biol Phys* 58, 914-26 (2004).
124. Mizukami, Y. et al. Induction of interleukin-8 preserves the angiogenic response in HIF-1 α -deficient colon cancer cells. *Nat Med* 11, 992-7 (2005).
125. Yu, J. L., Rak, J. W., Coomber, B. L., Hicklin, D. J. & Kerbel, R. S. Effect of p53 status on tumor response to antiangiogenic therapy. *Science* 295, 1526-8 (2002).
126. Yu, J. L. et al. Heterogeneous vascular dependence of tumor cell populations. *Am J Pathol* 158, 1325-34 (2001).
127. Dong, J. et al. VEGF-null cells require PDGFR α signaling-mediated stromal fibroblast recruitment for tumorigenesis. *Embo J* 23, 2800-10 (2004).
128. Bergers, G., Song, S., Meyer-Morse, N., Bergsland, E. & Hanahan, D. Benefits of targeting both pericytes and endothelial cells in the tumor vasculature with kinase inhibitors. *J Clin Invest* 111, 1287-95 (2003).
129. Benjamin, L. E., Golijanin, D., Itin, A., Pode, D. & Keshet, E. Selective ablation of immature blood vessels in established human tumors follows vascular endothelial growth factor withdrawal. *J Clin Invest* 103, 159-65 (1999).
130. Butler, J. M. et al. SDF-1 is both necessary and sufficient to promote proliferative retinopathy. *J Clin Invest* 115, 86-93 (2005).
131. Guleng, B. et al. Blockade of the stromal cell-derived factor-1/CXCR4 axis attenuates in vivo tumor growth by inhibiting angiogenesis in a vascular endothelial growth factor-independent manner. *Cancer Res* 65, 5864-71 (2005).
132. Ceradini, D. J. et al. Progenitor cell trafficking is regulated by hypoxic gradients through HIF-1 induction of SDF-1. *Nat Med* 10, 858-64 (2004).
133. Okamoto, R. et al. Hematopoietic cells regulate the angiogenic switch during tumorigenesis. *Blood* 105, 2757-63 (2005).
134. Blouw, B. et al. The hypoxic response of tumors is dependent on their microenvironment. *Cancer Cell* 4, 133-46 (2003).
135. Cools, J., Maertens, C. & Marynen, P. Resistance to tyrosine kinase inhibitors: Calling on extra forces. *Drug Resist Updat* 8, 119-29 (2005).
136. Morgillo, F. & Lee, H. Y. Resistance to epidermal growth factor receptor-targeted therapy. *Drug Resist Updat* (2005).
137. Jones, A. V. & Cross, N. C. Oncogenic derivatives of platelet-derived growth factor receptors. *Cell Mol Life Sci* 61, 2912-23 (2004).
138. Bischoff, J. Monoclonal expansion of endothelial cells in hemangioma: an intrinsic defect with extrinsic consequences? *Trends Cardiovasc Med* 12, 220-4 (2002).
139. Jain, R. K. Normalization of tumor vasculature: an emerging concept in antiangiogenic therapy. *Science* 307, 58-62 (2005).
140. Glade Bender, J., Cooney, E. M., Kandel, J. J. & Yamashiro, D. J. Vascular remodeling and clinical resistance to antiangiogenic cancer therapy. *Drug Resist Updat* 7, 289-300 (2004).
141. Patan, S., Munn, L. L. & Jain, R. K. Intussusceptive microvascular growth in a human colon adenocarcinoma xenograft: a novel mechanism of tumor angiogenesis. *Microvasc Res* 51, 260-72 (1996).
142. Autiero, M. et al. Role of PlGF in the intra- and intermolecular cross talk between the VEGF receptors Flt1 and Flk1. *Nat Med* 9, 936-43 (2003).
143. Janmaat, M. L. & Giaccone, G. Small-molecule epidermal growth factor receptor tyrosine kinase inhibitors. *Oncologist* 8, 576-86 (2003).
144. Koshiji, M. et al. HIF-1 α induces genetic instability by transcriptionally downregulating MutS α expression. *Mol Cell* 17, 793-803 (2005).
145. Buttery, R. C., Rintoul, R. C. & Sethi, T. Small cell lung cancer: the importance of the extracellular matrix. *Int J Biochem Cell Biol* 36, 1154-60 (2004).
146. Miller, K. D., Sweeney, C. J. & Sledge, G. W., Jr. Can tumor angiogenesis be inhibited without resistance? *Exs*, 95-112 (2005).

147. Sweeney, C. J., Miller, K. D. & Sledge, G. W., Jr. Resistance in the anti-angiogenic era: nay-saying or a word of caution? *Trends Mol Med* 9, 24-9 (2003).
148. Gasparini, G., Longo, R., Fanelli, M. & Teicher, B. A. Combination of antiangiogenic therapy with other anticancer therapies: results, challenges, and open questions. *J Clin Oncol* 23, 1295-311 (2005).
149. Kerbel, R. S. et al. Possible mechanisms of acquired resistance to anti-angiogenic drugs: implications for the use of combination therapy approaches. *Cancer Metastasis Rev* 20, 79-86 (2001).
150. Ton, N. C. & Jayson, G. C. Resistance to anti-VEGF agents. *Curr Pharm Des* 10, 51-64 (2004).
151. Ferrara, N. & Kerbel, R. Angiogenesis as a therapeutic target. *Nature* (this issue) (2005).
152. Pepper, M. S., Rosnoble, C., Di Sanza, C. & Kruithof, E. K. Synergistic induction of t-PA by vascular endothelial growth factor and basic fibroblast growth factor and localization of t-PA to Weibel-Palade bodies in bovine microvascular endothelial cells. *Thromb Haemost* 86, 702-9 (2001).
153. Ma, L. et al. In vitro procoagulant activity induced in endothelial cells by chemotherapy and antiangiogenic drug combinations: modulation by lower-dose chemotherapy. *Cancer Res* 65, 5365-73 (2005).
154. Yang, R. et al. Effects of vascular endothelial growth factor on hemodynamics and cardiac performance. *J Cardiovasc Pharmacol* 27, 838-44 (1996).
155. Baffert, F. et al. Cellular changes in normal blood capillaries undergoing regression after inhibition of VEGF signaling. *Am J Physiol Heart Circ Physiol* (2005).
156. Gerber, H. P. et al. VEGF is required for growth and survival in neonatal mice. *Development* 126, 1149-59 (1999).
157. Kamba, T. et al. VEGF-dependent plasticity of fenestrated capillaries in the normal adult microvasculature. *Am J Physiol Heart Circ Physiol* (2005).
158. Tang, K., Breen, E. C., Gerber, H. P., Ferrara, N. M. & Wagner, P. D. Capillary regression in vascular endothelial growth factor-deficient skeletal muscle. *Physiol Genomics* 18, 63-9 (2004).
159. Eremina, V. & Quaggin, S. E. The role of VEGF-A in glomerular development and function. *Curr Opin Nephrol Hypertens* 13, 9-15 (2004).
160. Redman, C. W. & Sargent, I. L. Latest advances in understanding preeclampsia. *Science* 308, 1592-4 (2005).
161. Del Bo, R. et al. Vascular endothelial growth factor gene variability is associated with increased risk for AD. *Ann Neurol* 57, 373-80 (2005).
162. Isner, J. M., Ropper, A. & Hirst, K. VEGF gene transfer for diabetic neuropathy. *Hum Gene Ther* 12, 1593-4 (2001).
163. Kalaria, R. N. et al. Towards defining the neuropathological substrates of vascular dementia. *J Neurol Sci* 226, 75-80 (2004).
164. Cao, L. et al. VEGF links hippocampal activity with neurogenesis, learning and memory. *Nat Genet* 36, 827-35 (2004).
165. Zelzer, E. & Olsen, B. R. Multiple roles of vascular endothelial growth factor (VEGF) in skeletal development, growth, and repair. *Curr Top Dev Biol* 65, 169-87 (2005).
166. Ferrara, N. et al. Vascular endothelial growth factor is essential for corpus luteum angiogenesis. *Nat Med* 4, 336-40 (1998).
167. Hattori, K. et al. Vascular endothelial growth factor and angiopoietin-1 stimulate postnatal hematopoiesis by recruitment of vasculogenic and hematopoietic stem cells. *J Exp Med* 193, 1005-14 (2001).
168. Rafii, S. et al. Angiogenic factors reconstitute hematopoiesis by recruiting stem cells from bone marrow microenvironment. *Ann N Y Acad Sci* 996, 49-60 (2003).
169. Luttun, A. et al. Revascularization of ischemic tissues by PlGF treatment, and inhibition of tumor angiogenesis, arthritis and atherosclerosis by anti-Flt1. *Nat Med* 8, 831-40 (2002).
170. Germani, A. et al. Vascular endothelial growth factor modulates skeletal myoblast function. *Am J Pathol* 163, 1417-28 (2003).
171. Rottbauer, W. et al. VEGF-PLCgamma1 pathway controls cardiac contractility in the embryonic heart. *Genes Dev* 19, 1624-34 (2005).
172. Jain, R. K., Duda, D. G., Clark, J. W. & Loeffler, J. S. Lessons from phase III clinical trials on anti-

Appendix

VEGF therapy for cancer. Nat Clin Pract Oncol (in press) (2006).

